January 2018

Assessment Of Blood Pressure Regulatory Controls To Detect Hypovolemia And Orthostatic Intolerance

Ajay Kumar Verma

ASSESSMENT OF BLOOD PRESSURE REGULATORY CONTROLS TO DETECT HYPOVOLEMIA AND ORTHOSTATIC INTOLERANCE

by

Ajay Kumar Verma

Bachelor of Technology, Uttar Pradesh Technical University, 2011
Master of Science, The University of Texas at El Paso, 2014

A Dissertation

Submitted to the Graduate Faculty

of the

University of North Dakota

in partial fulfillment of the requirements

for the degree of

Doctor of Philosophy

Grand Forks, North Dakota
May
2018

This dissertation, submitted by Ajay Kumar Verma in partial fulfillment of the requirements for the Degree of Doctor of Philosophy from the University of North Dakota, has been read by the Faculty Advisory Committee under whom the work has been done and is hereby approved.

_____

Kouhyar Tavakolian, Chairperson

_____

Prakash Ranganathan, Committee Member

_____

Jau-Shin Lou, Committee Member

_____

Colin Combs, Committee Member

_____

Andrew Blaber, Committee Member

_____

Hassan Reza, Member at Large

This dissertation is being submitted by the appointed advisory committee as having met all of the requirements of the School of Graduate Studies at the University of North Dakota and is hereby approved.

_____

Dr. Grant McGimpsey

Dean of the School of Graduate Studies

_____

Date

PERMISSION

Title	Assessment of Blood Pressure Regulatory Controls to Detect Hypovolemia and Orthostatic Intolerance
Department	Electrical Engineering
Degree	Doctor of Philosophy

In presenting this dissertation in partial fulfillment of the requirements for a graduate degree from the University of North Dakota, I agree that the library of this University shall make it freely available for inspection. I further agree that permission for extensive copying for scholarly purposes may be granted by the professor who supervised my dissertation work or, in his absence, by the Chairperson of the department or the dean of the School of Graduate Studies. It is understood that any copying or publication or other use of this dissertation or part thereof for financial gain shall not be allowed without my written permission. It is also understood that due recognition shall be given to me and to the University of North Dakota in any scholarly use which may be made of any material in my dissertation.

Ajay Kumar Verma

3rd May 2018

Abstract

Regulation of blood pressure is vital for maintaining organ perfusion and homeostasis. A significant decline in arterial blood pressure could lead to fainting and hypovolemic shock. In contrast to young and healthy, people with impaired autonomic control due to aging or disease find regulating blood pressure rather demanding during orthostatic challenge. This thesis performed an assessment of blood pressure regulatory controls during orthostatic challenge via traditional as well as novel approaches with two distinct applications 1) to design a robust automated system for early identification of hypovolemia and 2) to assess orthostatic tolerance in humans. In chapter 3, moderate intensity hemorrhage was simulated via lower-body negative pressure (LBNP) with an aim to identify moderate intensity hemorrhage (-30 and -40 mmHg LBNP) from resting baseline. Utilizing features extracted from common vital sign monitors, a classification accuracy of 82% and 91% was achieved for differentiating -30 and -40 mmHg LBNP, respectively from baseline. In chapter 4, cause-and-effect relationship between the representative signals of the cardiovascular and postural systems to ascertain blood pressure homeostasis during standing was performed. The degree of causal interaction between the two systems, studied via convergent cross mapping (CCM), showcased the existence of a significant bi-directional interaction between the representative signals of two systems to regulate blood pressure. Therefore, the two systems should be accounted for jointly when addressing physiology behind fall. Further, in chapter 5, the potential of artificial gravity (2-g) induced via short-arm human centrifuge at feet towards evoking blood pressure regulatory controls analogous to standing was investigated. The observation of no difference in the blood pressure regulatory controls, during 2-g centrifugation compared to standing, strongly supported the hypothesis of artificial hypergravity for mitigating cardiovascular deconditioning, hence minimizing post-flight orthostatic intolerance.

Dedication

To my cousin Anita

You'll never be forgotten. Thank you for all the wonderful memories

Acknowledgments

The success of this dissertation is a result of contributions from many individuals. First of all, I would like to thank my advisor Dr. Kouhyar Tavakolian for providing me the opportunity and giving the freedom to conduct doctoral work in his laboratory. The skills that you have cultivated in me during the last four years will help me succeed in future endeavors. Thank you for investing your time in me. Special thanks to Dr. Andrew Blaber for his continuous guidance and for providing me an opportunity to work in Aerospace Physiology Laboratory, where the foundation of this doctoral work was laid and most of the data used in this dissertation were acquired. Thanks to Dr. Amanmeet Garg for his continuous support, guidance, and motivation along the way. I would not have been able to achieve what I have without your guidance and motivation. Thanks to Dr. Da Xu for his insightful feedback on my scholarly manuscripts. Thanks to my dissertation committee members Dr. Prakash Ranganathan, Dr. Colin Combs, Dr. Jau-Shin Lou, Dr. Andrew Blaber, and Dr. Hassan Reza for their constructive feedback. Thanks to department chair Dr. John Mehilich and program director Dr. Sima Noghanian for their key advice to ascertain timely completion. Thanks to electrical and biomedical engineering graduate programs for providing continuous financial support during the last four years. Thanks to my parents for their motivation and emotional support, my siblings Pooja Verma and Aman Verma, my uncle Radheshyam and aunt Vidya for always motivating me, my cousin Dr. Suresh Verma for always being there in full capacity. Thanks to my fiancée Aliza for unconditional love and support, thanks to Dawn, Bob, and Vlad for always making sure I am doing good. Last but not least thanks to my friends and colleagues from biomedical engineering research complex and other engineering lab for their continuous support and assistance.

Table of Contents

List of Tables

List of Figures

Chapter 1.

Introduction

1.1. Motivation

Regulation of blood pressure is complex and numerous variables play a vital role to ascertain its homeostasis under challenging physiological conditions(1). Dependent on the physiological conditions failure to maintain blood pressure homeostasis can result in hypovolemic shock or orthostatic intolerance leading to an unexpected fall(2,3). Mortality and financial burden associated with both hypovolemic shock and fall, respectively is significant and concerning(4,5). Hypovolemic shock accounts for approximately 5 million deaths annually and is the biggest cause of death in people under the age of 45(6), while over $31 billion is spent annually for treatment and management of injuries associated with unexpected fall(7).

Quantifying the blood pressure regulatory controls can provide key information regarding the mechanisms sustaining homeostasis and therefore can assist early identification of hypovolemia and fall proneness. However, the traditional methodologies for assessing blood pressure control fail to account for all mechanisms that play part in the regulation of blood pressure. For example, the autonomic control studied typically via heart rate and blood pressure variability and baroreflex sensitivity fail to account for the non-linearity of the signal under consideration and closed loop intersystem interaction to assure blood pressure homeostasis. Accordingly, this thesis supplemented the traditional methods with novel approaches to assess the regulation of blood pressure with application to early identification of 1) hypovolemia and 2) orthostatic intolerance.

1.2. Literature Review

1.2.1. Early Identification of Hypovolemia

Excessive loss of blood from circulation i.e. hemorrhage due to a traumatic injury remains one of the major cause of mortality in civilians as well as in soldiers on the battlefield(8–11). Over 29 million people in civilian settings are affected by traumatic events annually and 30-40 % of trauma deaths are associated with hemorrhage(4). Approximately 9-10 % of the deaths during the Vietnam War was postulated to be due to hemorrhage(12,13). Additionally, Post-partum hemorrhage is a perceived cause of maternal mortality, which accounts for over 125,000 deaths annually(10,14,15). In contrast to central nervous system injury, a leading cause of mortality, which has limited intervention to offer a hope for survival and recovery, hemorrhage is responsive to pertinent intervention(4,16). Therefore, early identification of the need to apply lifesaving intervention can greatly increase the survival rate both in civilians and on the battlefield(16–18). Due to complex physiological adaptation to hypovolemia, the greatest challenge caregivers experience is in the early and reliable identification of bleeding from the vital sign monitors, which are customarily utilized in a pre-hospital setting for monitoring physiological state(19–21).

Muscle sympathetic nerve activity, central venous pressure, and stroke volume can provide accurate insights regarding bleeding(22–24), however, measuring such parameters require sophisticated instrumentation and an expert operator, accordingly, such indicators of bleeding have limited application towards facilitating interventional strategies in a setting where the majority of traumatic events occur. Due to limited resources available in a pre-hospital setting to monitor the progression of hypovolemia, the arterial blood pressure is often relied on(25). However, due to the autonomic control of blood pressure, arterial blood pressure remains regulated during the early phase of

blood loss and until the point of autonomic collapse(26,27). Post autonomic collapse, the application of the interventional strategies have limited effect towards maintenance of tissue perfusion; making hemorrhagic shock inevitable(2,12,28).

Making a decision regarding resuscitation based on parameter specific based on statistical tests can be an inadequate indicator of hypovolemia due to high-inter subject variability and non-linearity of data distribution. Therefore, development of an automated trauma support system utilizing multiple indicators of hypovolemia can effectively underscore the need to apply interventional strategies. Machine learning in this context can be a promising tool given its potential to analyze the data and learn the information from the data. Although the application of machine learning in medicine has been exhaustive(29–31), its application towards design of an automatic system to detect hypovolemia has been limited(32–34). This thesis is an attempt in this direction which derives multiple indicators of hypovolemia from common vital sign monitors used in a pre-hospital setting.

1.2.2. Early Identification of Orthostatic Intolerance

Orthostatic intolerance, an inability of an individual to regulate arterial blood pressure during standing, is commonly observed in older people and in people with neurodegenerative diseases such as Parkinson's disease, stroke, and concussion, which can lead to unexpected fall(35–37). The prevalence of orthostatic intolerance ranges from 5% (people under the age of 50) to 30% (age greater than 70)(38). Since the elderly population is expected to grow in the future(39), the number of people affected by such diseases are also anticipated to grow. Elderly with neurological disorders experience fall more frequently than their healthy counterparts(35,40). Additionally, it has become a significant burden on the current healthcare system(7), as treatment of fall associated injuries often entails immediate medical attention. Over 31 billion dollars are spent

annually (in 2015) for treatment and management of fall-related incidents(7). Further falls can cause fear of another fall while conducting day-to-day activities leading to incapacitation, therefore, a severe degradation in the quality of life.

Regulation of blood pressure during standing depends on 1) the immediate compensatory efforts from the autonomic nervous system via neural pathways causing an elevation in heart rate and systemic vascular resistance and 2) the postural controls such as the skeletal muscle pump and postural sway to pump the pooled venous blood back to the heart in response to gravity-induced hypovolemia. Yet, the two systems have been studied independently in the literature when addressing the physiology associated with fall(3,41–45). Consequently, providing insufficient information regarding the underlying physiology. Therefore, the design of rehabilitation schemes to restore the postural stability based on the existing knowledge in people with a history of neurodegenerative disease is rendered inadequate.

In the recent years, the coupling between the representative signals of cardiovascular and postural systems during orthostatic challenge has been studied(46–48). These studies demonstrated the interdependency between the cardiovascular and postural controls of blood pressure, however, the degree and the direction of information flow (causality) between the representative signals of cardiovascular and postural controls of blood pressure remains to be generalized. This thesis attempts to address the existing limitation in the literature and studied the cause-and-effect relationship between the cardiovascular and postural controls of blood pressure during orthostatic challenge induced by standing. By studying a group of young and healthy participants, the thesis generalized the baseline behavior of the degree of causal information flow between the representative signals of the cardiovascular and postural systems facilitating blood pressure homeostasis, hence, stable upright stance.

1.2.3. Mitigation of Spaceflight Deconditioning

There is growing interest in NASA and European Space Agency (ESA) towards a manned mission to outer space(49–51). Spaceflight deconditioning is one of the several concerns hindering such aspiration(50). Exposure to microgravity causes a series of physiological changes due to redistribution of blood volume above thoracic(52). Although such changes account for microgravity environment, it can have a detrimental effect on the physiological performance when exposed back to natural gravity. Approximately 30% of astronaut experience orthostatic intolerance after short duration spaceflight, however, this number jumps to 80% following a long-duration spaceflight(53). Due to growing interest in the manned mission to outer space, long-duration spaceflight is anticipated in the future. Accordingly, there is a need for the development of a countermeasure system to minimize the deleterious effects of microgravity on the physiological performance and facilitate healthy life for astronauts on return to Earth.

Due to shift in central blood volume above thoracic in microgravity, the typical blood pressure regulatory controls remain under stimulated for the duration of spaceflight(54,55). Additionally, the posture muscle groups are left with nutritional scarcity due to lack blood flow resulting in muscle atrophy(52). Typical exercise routines currently employed to minimize the spaceflight deconditioning are limited in effect for their inability to challenge multiple physiological systems simultaneously analogous to standing in natural gravity(56,57).

Literature suggests intermittent exposure to artificial hypergravity can mitigate the adverse effect on physiological performance associated with microgravity(58,59). In this regards, Short-arm human centrifuge (SAHC), capable of creating artificial gravity of different g-load can be a promising training tool. This thesis compares the blood pressure regulatory

indices during 2-g created via centrifugation at feet with standing in a natural gravity to validate the hypothesis of SAHC towards evoking blood pressure regulatory controls analogous to standing.

1.3. Thesis Outline

Chapter 2 details the methodology considered for data analysis. Chapter 3 discusses the potential of non-invasive features derived from typical vital sign monitors for reliable detection of moderate category simulated hemorrhage (-40 mmHg). Chapter 4 establishes the degree of causal information flow in the novel model of blood pressure regulation during standing (cardio-postural control of blood pressure) with application to assessing fall proneness. In chapter 5, the comparison of blood pressure regulatory controls during 2-g centrifugation at feet with standing in natural gravity is performed. Chapter 6 outlines the major limitations of this thesis and proposes potential future work required to address such limitations.

1.4. Thesis Contribution

This thesis demonstrated the potential of quantification of blood pressure regulatory indices via robust methodology towards early identification of hypovolemia, orthostatic intolerance, and validation of training tool for minimizing post-flight orthostatic hypotension. The key contributions of the thesis are summarized below.

- Demonstrated the closed loop heart rate and blood pressure interaction as an early indicator of simulated hemorrhage *(Chapter 3, J.5.)*.
- Highlighted the possibility of early identification of hypovolemia based on features extracted from common pre-hospital vital sign monitors along with machine learning algorithms *(Chapter 3, J.3.)*.

- Generalized the degree of cause-and-effect relationship between the cardiovascular and postural controls of blood pressure during orthostatic challenge induced by standing *(Chapter 4, J.7, J.6, and C.3-C.7)*.
- Quantified further changes in the degree of causal relationship between the cardiovascular and the postural controls of blood pressure following exercise *(Chapter 4, J.6.)*.
- Demonstrated the role of individual leg muscles towards blood pressure regulation *(Chapter 4, J.2.)*.
- Validated the short-arm human centrifuge as a potential tool towards evoking blood pressure regulatory controls analogous to standing *(Chapter 5, J.4.)*.
- Proposed relevant future work to address the limitation of this thesis and outlined the potential strategy towards the development of a device with application in a remote setting *(Chapter 6, C.1, C.2, C.8, and C.9)*.
- The key limitation of the thesis was limited sample size and data from only young, healthy people.

1.5. Publications

A portion of the results presented in this thesis has been published in peer-reviewed journals and in the proceedings of the peer-reviewed international conferences. Other results are under review or in preparation for submission to peer-review journals. The work presented in chapter 3 resulted in article J.3 and J.4. The work presented in chapter 4 resulted in article J.1, J.2, J.6, and J.7, while the work presented in chapter 5 resulted in article J.4. The average impact factor of journals where the results of this thesis are published, under review, or will be submitted is 3.6. Additionally, the article J.6 was selected as a feature article in the September 2017 edition of the American Journal of

Physiology-Heart and Circulatory Physiology (http://ajpheart.podbean.com/mobile/e/cardio-postural-blood-pressure-control/)

Journal Articles

J.1. **A. K. Verma**, A. Garg, D. Xu, A. P. Blaber, and K. Tavakolian. Assessment of the Physiological Interdependence of Cardiovascular and Postural Systems using Joint Recurrence Quantification Analysis. *Annals of Biomedical Engineering*. 2018 *[Under Preparation] [IF 3.11]*

J.2. **A. K. Verma,** A. Garg, D. Xu, A. P. Blaber, and K. Tavakolian. Role of individual Calf Muscles towards Blood Pressure Regulation. *American Journal of Physiology-Regulatory Integrative and Comparative Physiology*. 2018 *[Under Preparation] [IF 2.98]*

J.3. **A.K. Verma**, A. Garg, C. Wang, D. Xu, A. P. Blaber, and K. Tavakolian. Automatic Classification of Moderate Category Simulated Hemorrhage. *Shock*. 2018 *[Internal review] [IF 3.01]*

J.4. **A. K. Verma**, D. Xu, M. Bruner, A. Garg, N. Goswami, A. P. Blaber, and K. Tavakolian. Blood Pressure during 2-g Centrifugation at Feet is Analogous to Standing. *Frontiers in Physiology*. 2018 *[Revision stage] [IF 4.13]*

J.5. **A. K. Verma**, D. Xu, A. Garg, A. T. Cote, N. Goswami, A. P. Blaber, and K. Tavakolian. Non-linear Heart Rate and Blood Pressure interaction in Response to Lower-Body Negative Pressure. *Frontiers in Physiology*. 2017 [IF 4.13]

J.6. D. Xu, **A. K. Verma**, A. Garg, M. Bruner, R. Fazel-Rezai, A. P. Blaber, and K. Tavakolian. Significant Role of Cardiopostural interaction towards Blood Pressure Regulation during Standing. *American Journal of Physiology-Heart and Circulatory Physiology*. 2018 [IF 3.35]

J.7. **A. K. Verma,** A. Garg, D. Xu, M. Bruner, R. Fazel-Rezai, A. P. Blaber and Kouhyar Tavakolian. Skeletal Muscle Pump Drives Control of Cardiovascular and Postural Systems. *Scientific Reports*. 2017 [IF 4.2]

Conference Proceedings

C.1. K. Sorenson, **A. K. Verma**, A. Blaber, J. Zanetti, S. E. Schmidt, J. J. Struijk, and K. Tavakolian. Challenges using Seismocardiography for Blood Pressure Monitoring. Computing in Cardiology. 2017

C.2. **A. K. Verma**, J. Zanetti, R. Fazel-Rezai, and K. Tavakolian. Pulse Transit Time Extraction from Xiphoid and Carotid Seismocardiogram. Proceedings of ASME Design of Medical Devices Conference. 2017

C.3. **A. K. Verma**, D. Xu, N. Goswami, A. Garg, F. Fazekas, A. Rossler, A. Blaber, R. Fazel-Rezai, and K. Tavakolian. Increased Systolic Blood Pressure Driven Skeletal Muscle Activation Following Stroke: A Causality Study. Computing in Cardiology. 2016

C.4. **A. K. Verma**, A. Garg, A. Blaber, R. Fazel-Rezai, K. Tavakolian. Analysis of Causal Cardio-Postural interaction using Convergent Cross Mapping. IEEE Emgineering in Medicine and Biology Society Conference. 2016

C.5. **A. K. Verma**, A. Garg, A. Blaber, R. Fazel-Rezai, and K. Tavakolian. Causality detection in Cardio-Postural interaction under Orthostatic Stress induced by Quiet Standing using Transfer Entropy. IEEE Electro-Information Technology Conference. 2016

C.6. **A. K. Verma**, A. Garg, A. Blaber, R. Fazel-Rezai, and K. Tavakolian. Causal Cardio-Postural interaction under orthostatic Stress. Journal of Medical Devices. 2016

C.7. **A. K. Verma**, A. Garg, A. Blaber, R. Fazel-Rezai, and K. Tavakolian. Causality in Cardio-Postural interactions during Quiet Stance. Computing in Cardiology. 2015

C.8. **A. K. Verma**, A. Blaber, R. Fazel-Rezai, and K. Tavakolian. Pulse Transit Time Extraction from Seismocardiogram and its Relationship with Pulse Pressure. Computing in Cardiology. 2015

C.9. **A. K. Verma**, R. Fazel-Rezai, J. Zanetti, and Kouhyar Tavakolian. Preliminary Results of Pulse Transit Time Extraction using Seismocardiogram. Journal of Mechanical Design. 2015

Chapter 2.

Methodology

2.1. Baroreflex Sensitivity

Baroreceptors, the stretch receptors localized in the aortic arch and the carotid sinus, sense the dynamics of beat-to-beat blood pressure and continuously relay the information pertaining to the pressure on the arterial wall to the brain stem(60). In the case of disturbance to hemodynamic homeostasis i.e. increase or decrease in arterial pressure, the baroreceptors increases or decreases, respectively the afferent traffic, making brain aware of the required reflex mechanisms to bring the blood pressure back to a preset value(1,61).

In the scenario of decreased arterial pressure, the reduced afferent traffic (baroreceptor unloading) results in withdrawal of vagal nerve activity and increased sympathetic activity via efferent pathways causing an increase in heart rate and systemic vascular resistance to regulate the arterial pressure to a preset value. Conversely, in case of increased arterial pressure sensed by the baroreceptors, the afferent traffic to the brain is increased resulting in sympathetic inhibition and increased vagal activity resulting in decreased heart rate and systemic vascular resistance. Thus, by controlling the heart rate and systemic vascular resistance via neural efferent pathways, the blood pressure is maintained during perturbed hemodynamic state.

The baroreflex sensitivity (BRS) is well-accepted norm to quantify the baroreflex activity(62). The BRS is defined as a change RR intervals (ms) with respect to per unit change in arterial blood pressure(62,63). For example, if arterial pressure rises by 10 mmHg and RR intervals increased by 200 ms, then BRS is $\frac{200}{10}$ = 20 ms/mmHg. The

baroreflex sensitivity is typically assessed in time and frequency domain. The time domain method requires calculation of slope of a sequence of beats during which RR intervals and arterial blood pressure increases or decreases(64,65). The frequency domain assessment of BRS requires calculation of arterial blood pressure to the RR intervals transfer function. The transfer function amplitude is analogous to the slope of the sequence method(62).

2.2. Spectral Analysis of Blood Pressure and RR intervals

The spectra of blood pressure and RR intervals is divided into three key frequency bands which are known to be associated with the key physiological phenomenon. These three frequency bands include; very-low frequency (VLF, 0-0.04 Hz), low-frequency (LF, 0.04-0.15), and high-frequency (HF, 0.15-0.4 Hz)(66). The VLF frequency band in the RR intervals is associated hormonal activity, the LF frequency is associated with the activity of sympathetic nerve activity, and HF band reflects the vagal or parasympathetic nerve activity and the ration of LF and HF power in normalized units reflect the sympatho-vagal balance(66–68). Similarly, the LF and HF frequency band of blood pressure are known to be associated with baroreflex and respiratory activity, respectively(69).

Prior to spectral analysis, the beat-to-beat time series for blood pressure and RR intervals are derived from continuous blood pressure waveform and electrocardiogram signal, respectively. The beat-to-beat time series interpolated to convert the beat-to-beat time series in the evenly sampled continuous signal. The mean of the evenly sampled signal is further removed before computation of Power Spectral Density (PSD) to stay in an alignment with the stationary assumption(66,67). Spectral analysis was computed using Welch PSD in MATLAB. The block diagram for step-by-step processing to calculate the spectral power distributed in the respective frequency bans is shown in Figure 2.1.

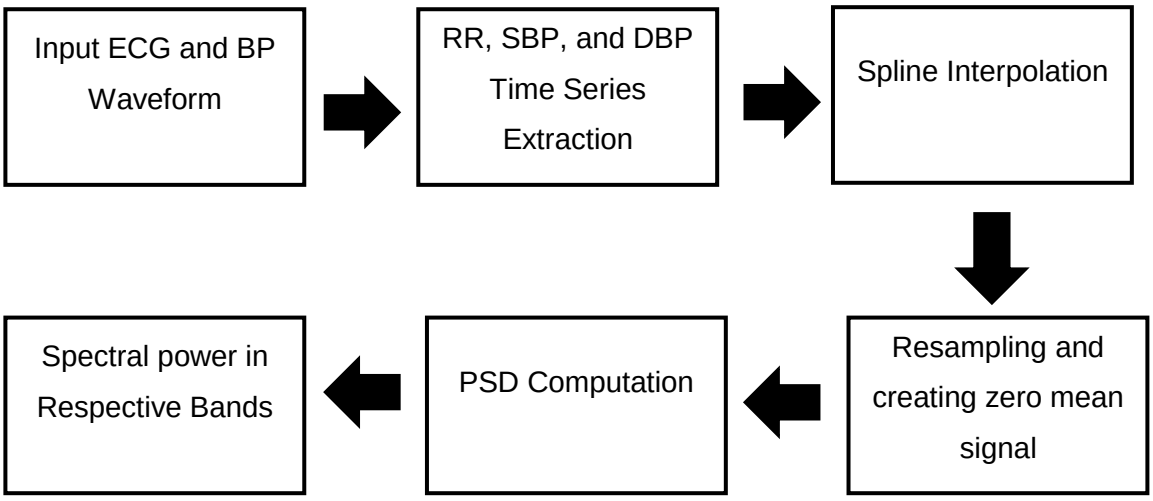

Figure 2.1. Step-by-step processing to calculate spectral power in RR, SBP, and DBP time series distributed in VLF (0-0.04 Hz), LF (0.04-0.15 Hz), and HF (0.15-0.4 Hz) frequency bands.

2.3. Convergent Cross Mapping

The cause-and-effect relationship between two inter-dependent systems provides key characteristic pertaining to their behavior. Deviation in such behavior from established baseline characteristic can serve as an indicator of system deterioration and accordingly can assist caregiver design idea intervention. To this end, the concept of Granger causality has been widely utilized(70,71), however, due to the assumption of linear and stationary signal behavior, it is limited in effect to unravel complex non-linear physiological interactions. Transfer entropy method is considered to address the limitation of linearity assumption of Granger causality(72), nevertheless, the stationary signal behavior and requirement to determine probability density function of a representative signal under consideration limits its wide application(73). Convergent cross mapping is a relatively new method to determine directional information flow in a non-linear system, has a potential infer causal information of weak to moderate strength.

Using CCM method, for X having a causal influence on Y, test for causality is conducted by quantifying the degree to which historical record of Y can be used to accurately estimate the states of X. In order to do so, first, the shadow manifold of Y (M_Y) and X (M_X) are constructed using lagged coordinates of variables Y and X, respectively(74,75). The lagged coordinates of X, say x(t) is formed as; X(t), X(t-τ), X(t-2τ)… X (t-(E-1)τ), where E and τ are embedding dimension and time lag used for constructing shadow manifold. The range of x (t) is from t=1+(E-1)τ to t=L, where L is data length. Similarly, the lagged coordinates of Y are formed. Next step is to find E+1 nearest neighbors, E+1 is the minimum number of points required in order bound a simplex in E-dimensional space, the time indices of E+1 nearest neighbors are denoted from closest to farthest. The nearest neighbors found on X manifold M_X is used to find the neighbors on Y manifold M_Y to estimate Y, the estimated Y denoted as $\hat{Y}|M_X = \sum w_i Y(t_i)$ i=1,2,3…….E+1 . Here, w_i is the weighting based on the distance between x (t) and its i^{th} nearest neighbor and Y (t_i) are concurrent values of Y(76). More detailed explanation of the choice of weighting is explained in(76). Once estimates of Y are determined, the strength of causality flowing from Y to X is quantified by calculating the Pearson correlation coefficient between the original (reconstructed Y) and estimated Y. Mathematically, $Y \rightarrow X = \rho(Y, \hat{Y}|M_x)$. Similarly, the test for causal information flowing X to Y can be conducted.

Using CCM method unidirectional and bidirectional causality can be detected. In case of a unidirectional causality (X →Y), the driver X can be estimated using a historical record from the manifold of Y (M_Y). However, Y cannot be estimated using the historical record from X manifold (M_X). The strength of causality varies between 0 and 1, where 0 represents the absence of causality and 1 represents maximum causality. Therefore, under an ideal case of unidirectional causality (X→Y) the value of correlation between X and estimated X will vary between 0 and 1, while this value for Y and estimated Y will be

zero. Mathematically, the case of X→Y could be represented as; $0<\rho(X, \hat{X}|M_Y)\leq 1$ and, $\rho(Y,\hat{Y}|M_X)=0$ where, ρ is Pearson correlation coefficient.

In case of bidirectional causality (X→Y and Y→X) the historical record from Y manifold (M_Y) can be used to estimate X, while historical record from X manifold (M_x) can be used to estimate Y. In this case both, the correlation of X and estimated X as well as the correlation of Y and estimated Y will vary between 0 and 1. Mathematically, $0<\rho(X, \hat{X}|M_Y)\leq 1$ and $0<\rho(Y,\hat{Y}|M_X)\leq 1$. However, for the variable having stronger effect on other variable, the correlation of that variable and its estimate will converge to a higher correlation coefficient value. For example, if X has a stronger effect on Y compared to vice-versa then mathematically, $\rho(X, \hat{X}|M_Y)-\rho(Y, \hat{Y}|M_X)>0$. The accuracy of the causality improves with increasing data length marked by increase in correlation between the original and estimated variables (convergence), also, the way CCM infers causality is contrary to the notion of causality proposed by Granger hence it's termed as cross mapping, as in CCM response is used to estimate driver(77–79). The mathematical details of the methodology can be found in the supplementary material of Sugihara et al and book on time series analysis(75,80). The MATLAB (Mathworks Inc., MA) implementation of CCM algorithm demonstrated in an application with non-linear signals in the study conducted by Krakovská et al. was considered for analysis(74).

2.4. Recurrence Quantification Analysis

The system behavior can be characterized via its fundamental property utilizing a set of meaningful features derived from the recurrence plots(81). The recurrence plot is a graphical representation of recurrences in dynamical systems. Based on the structure of recurrence plot a set of features can be derived to quantify the meaningful information

embedded in the recurrence plot, this quantification process is termed as recurrence quantification analysis (RQA)(81–83).

The recurrence quantification analysis has been used effectively in physiology to outline transitions in a dynamical pattern of a time series acquired from the human body under various physiological conditions(44,84,85). The construction of recurrence plot entails nonlinear phase space reconstruction of time series under investigation. The states of system change from time to time in a complex fashion, therefore, quantification of such changes provide pivotal information regarding the underlying systems behavior. The nonlinear state space reconstruction of a time series is performed according to Taken's theorem as $X(t)$, $X(t-\tau)$, $X(t-2\tau)\ldots X(t-(E-1)\tau)$.

Where E and τ are dimension of embedding and time delay, respectively. Appropriate choice of delay and embedding dimension is critical in accurately transferring time series information to phase space. Traditionally false nearest neighbor algorithm is employed to explore the minimization of false nearest neighbor as a function of embedding dimension for physiological signals under consideration and optimal dimension of reconstruction chosen accordingly. Since different signals may have different characteristics, the choice of parameters for respective signals will be detailed at relevant places throughout the thesis.

After multidimensional state space reconstruction, the distance between the individual points at i and j locations are calculated using a defined norm (such as Euclidean, Maximum norm, Minimum norm, and Levenshtein). The recurrence plot, therefore, describes the repetition of values of the signal in its phase space. When the distance at any given point is lower than the defined threshold than the coordinated at [i, j] then the recurrence point is plotted in the recurrence plot.

$$RP_{i,j} = \begin{cases} 1: x_i \approx x_j \\ 0: x_i \not\approx x_j \end{cases} \quad i, j = 1, \ldots, N$$

Where $RP_{i,j}$ is a recurrence matrix containing points 0 and 1. N is a number of states considered, $x_i \approx x_j$ means equality up to a defined threshold (or tolerance). The matrix holds the result of a system at times $i \; and \; j$, if the states are similar, the corresponding entry to the recurrence matrix is 1 otherwise the entry to the recurrence matrix is 0. The figure 2.2 is an example of recurrence of systolic blood pressure during standing for two participants belonging to different group i.e. healthy older person (A) and older person with a history of stroke (B).

The joint recurrence plot, an extension of recurrence plot, allows for an investigation of the relationship between multiple variables, utilizing a set of features derived from the joint-recurrence plot termed as joint recurrence quantification analysis(81). While the recurrence plot captures the correspondence between the two signals as the distance between the multi-dimension phase-space profiles, the joint recurrence plot outlines the correspondence between the individual recurrence plots of the two signals under consideration(81,86). Therefore, the first step to the joint recurrence analysis is the construction of individual recurrence plot of the systems under consideration. Secondly, the individual recurrence plots are joined together, as such, the common occurrences of the recurrence plot are kept, while the occurrences in the recurrence plot that are different (determined by threshold or tolerance) are disregarded. The RQA analysis was performed using freely available MATLAB based CRP toolbox(87).

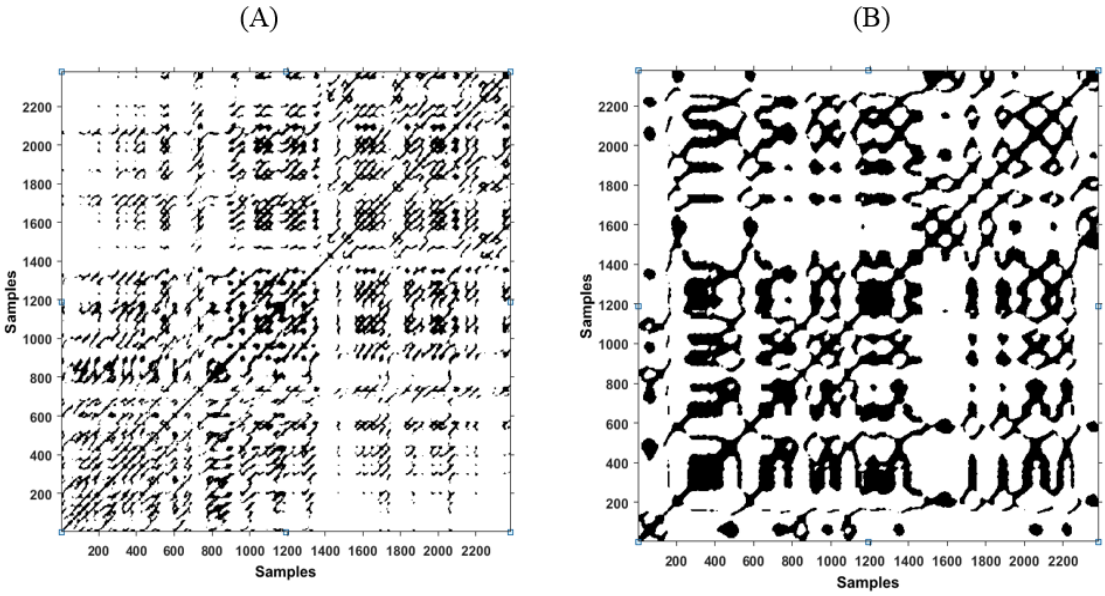

Figure 2.2. An example of the recurrence plot for systolic blood pressure during standing. As it can be seen visually that the recurrence plot for the healthy older person (A) is different from that of an older person with a history of stroke (B).

Chapter 3.

Early Identification of Moderate Category Simulated Hemorrhage

3.1. Summary

Background: Hemorrhage is one of the major cause of mortality in civilians and soldiers. Early identification of bleeding remains an open problem. In this regard, blood pressure has been an ineffective measure of blood loss due to numerous compensatory mechanisms sustaining arterial blood pressure homeostasis. Especially, in pre-hospital or remote settings where intervention decisions are dependent on the common vital sign monitors such as heart rate and blood pressure. This chapter investigated the feasibility of identification of moderate category bleeding by utilizing non-invasively extracted features from electrocardiogram and continuous blood pressure. **Methods:** The hemorrhage of variable degree was simulated via graded lower-body negative pressure (LBNP) of 0 mmHg, -20, -30, and -40 mmHg. Simultaneous electrocardiogram (ECG) and continuous blood pressure were acquired for 5-minutes of each LBNP stage from 27 young, healthy participants. Feature extraction was performed during the last 3 minutes of each LBNP stage to allow for effective blood pooling. **Results:** The findings showcased the feasibility of non-invasive features extracted from ECG and blood pressure with support vector machines (SVM) classifier algorithm towards classifying -30 mmHg and -40 mmHg LBNP with 82% and 91% accuracy, respectively. **Conclusion:** The outcome of the analysis leads to the conclusion that development of an automated decision support system to identify moderate intensity hemorrhage is possible from commonly employed vital sign monitors, which can facilitate pertinent intervention to impede hemorrhage progression.

3.2. Background

Trauma remains a major cause of mortality in civilians as well as in soldiers on the battlefield(8,9,18,88). According to World Health Organization, Trauma is associated with approximately 9% of the global annual mortality(4). Low and middle-income countries have witnessed overwhelming mortality pertaining to traumatic injury due to limited access to immediate medical care. Although most of the traumatic events have taken place in developing countries, industrialized nations are also severely affected by traumatic events, with over 29 million people suffering from traumatic events(4). Bleeding associated with traumatic events accounts for a considerable proportion of mortality(89). Post-partum hemorrhage accounts for approximately 125,000 deaths annually worldwide(14). Hypovolemic shock accounts for 80% of death within the first hour of injury, 33 to 56% of the death in a pre-hospital setting, and approximately 50% of death within a first 24-hour of trauma(4). Given that hemorrhage is responsive to appropriate intervention, early identification of hypovolemia can assist design of pertinent intervention.

Table 3.1. The relationship between lower-body negative pressure stages, degree of blood volume displaced, percent of total volume lost, and hemorrhage category(90).

LBNP (mmHg)	Hemorrhage (category)	Blood Loss (mL)	Blood Loss (%)
10-20	Mild	400-550	10
20-40	Moderate	500-1000	10-20
>40	Severe	>1000	>20

Hemorrhage is typically classified as mild, moderate, or severe depending on the amount of blood volume lost from the circulation. The approximate amount blood volume lost corresponding to the respective category of hemorrhage is summarized in Table 3.1. In most cases, due to numerous compensatory mechanisms, the traditional marker of blood loss i.e. blood pressure fails to provide information regarding the degree of blood loss. Baroreceptors are the stretch receptors localized in the carotid sinus and the aortic arch, these receptors keep firing impulses to the brain continuously; to relay information pertaining to the arterial blood pressure level.

In response to the early phase of blood loss, these pressure receptors sense the drop in pressure level and decrease the number of impulses relayed to the brain. The corresponding withdrawal of vagal nerve and activation of sympathetic nerve activity, causing an elevation in heart rate and systemic vascular resistance, is a typical autonomic mechanism to ascertain blood pressure is regulated. Nevertheless, with the progression of blood loss to a severe category, stroke volume drops significantly and the autonomic control of blood pressure fails to regulate arterial blood pressure (autonomic decompensation), after which blood pressure drops abruptly and hemorrhagic shock is imminent if stroke volume is not immediately somehow increased.

Table 3.2. List of traditional vital sign and hemodynamic parameters. Table highlights the changes in such parameters in response to central hypovolemia.

Vital Signs	**Changes**	**Reference**
Heart Rate	Not Specific	(21,26,91)
Systolic Blood Pressure	Late	(27,92,93)

Diastolic Blood Pressure	Late	(27,93,94)
Mean Arterial Pressure	Late	(26,27,92,93,95)
Pulse Pressure	Not specific	(92,93)
Shock Index	Late	(93)
Respiratory Rate	Late	(93)
Compensatory Reserves	Early	(93,94,96)

Since it is rather impracticable, due to ethical reasons, to have humans go through severe blood loss, typically the research conducted for algorithm development and validation are performed during simulated hemorrhage. The lower-body negative pressure (LBNP) is an acclaimed tool for simulating hemorrhage. The application of LBNP translocate the central blood volume below the heart level in peripheral regions (mostly in pelvis and leg region)(90,97). The response of the cardiovascular system to LBNP has been shown to be analogous to blood loss, therefore, it provides safe and reproducible experimental setup for studying and developing algorithms impede hemorrhage(24). The continuous application of LBNP increases the blood volume displaced in the lower periphery, which reduces central venous pressure, therefore, preload and stroke volume. Compensatory increase in heart rate and systemic vascular resistance strives to maintain blood pressure by pumping out quickly the blood in the pulmonary artery. However, with a continuous decline in preload due to increased lower-body suction the pulmonary reservoir drains and autonomic collapse occurs resulting in an abrupt decline in blood pressure. The LBNP stage of -30 to -40 mmHg simulates a moderate category hemorrhage, therefore,

successful differentiation of -30 and -40 mmHg LBNP from resting state can assist surgical triage to impede hemorrhage progression.

Considerable research have been conducted in the last two decades focused on the development of automatic algorithms for early detection of blood loss. However, limited success have been achieved in this regards. The more sophisticated way of tracking the compensatory response such as invasive stroke volume, central venous pressure, or muscle sympathetic nerve activity have shown potential towards accurately outlining the degree of blood loss(22,23,98,99). Nonetheless, due to their invasive nature and sophisticated instrumentation requirement, these approached have limited application in settings where the majority of hemorrhagic shock occurs (in the battlefield, rural, low-income countries, and home monitoring). Table 3.2 summarizes the list of physiological features those are commonly employed and their potential as an early or late marker of blood loss.

In recent years, interest has emerged towards quantifying compensatory mechanisms as an early indicator of hemorrhage progression(93,94,96). Autonomic control of blood pressure quantified via spectral analysis of heart rate and blood pressure and spontaneous baroreflex sensitivity (BRS) is long known to provide information regarding sympathetic, vagal, and baroreflex activity in response to an external perturbation to the cardiovascular homeostasis(66,100). However, due to the assumption of linear system behavior for spectral analysis and the inability of BRS to separate the feedforward and feedback control of blood pressure, these traditional methods are considered insufficient regarding underlying physiology when aimed to get accurate information pertaining to blood pressure regulation(101,102).

Arterial blood pressure and heart rate interaction, a closed loop control systems, is shown to be a pivotal inter-system interaction for regulating arterial blood pressure during orthostatic challenge(102,103). Therefore, quantified knowledge of causal heart rate and blood pressure interaction can provide key information pertaining to hemorrhage progression. The closed-loop heart rate and blood pressure interaction have a feedforward or non-baroreflex arm, governed by Frank-Starling and Weindkessel mechanisms and a feedback or baroreflex arm which signifies the strength of baroreceptors activity towards regulation of arterial blood pressure(104). In literature, the concept such bidirectional interaction is well studied and demonstrated for its ability to track central hypovolemia induced by head-up tilt or stand the test (Table 3.3).

However, its potential towards tracking the degree of blood loss has not yet been validated. Additionally, a pertinent literature indicates a difference in physiological behavior in response to orthostatic challenge evoked via head-up tilt and LBNP. Such observations further warrant comprehensive investigation of heart rate and blood pressure directional interaction in response to LBNP to validate its potential as an early indicator of hypovolemia. Table 3.3 summarizes the studies which assessed heart rate and blood pressure interaction in response to orthostatic challenge. In this chapter we combine the traditional and novel features extracted from the ECG and blood pressure waveform and assess their potential to classify moderate intensity (-30 and -40 mmHg LBNP) simulated hemorrhage. An automated system that can classify hemorrhage at an early stage from common vital sign monitors will be of great clinical significance towards making interventional decisions to impede hemorrhage progression to a severe category.

Table 3.3. List of research assessing heart rate and blood pressure interaction in response to orthostatic challenge.

Research	Signals	Method
Javorka et al(105)	SBP and RR	Tilt test
Javorka et al(104)	SBP and RR	Tilt test
Porta et al(106)	SBP and RR	Tilt test
Silvani et al(69)	SBP and RR	Tilt test and Phlebotomy
Faes et al(107)	SBP and RR	Tilt Test
Faes et al(108)	SBP and RR	Tilt Test
Nollo et al(109)	SBP and RR	Tilt Test
Porta et al(103)	SBP and RR	Tilt test

3.3. Methods

3.3.1. Experimental protocol and Instrumentation

The participants for the study were recruited via an oral advertisement on the Simon Fraser University (SFU) campus. The approval for experimentation was obtained from the research ethics board of SFU, which approved the experimental protocols as a minimum risk protocol. Any participants over the age of 18 and without any cardiovascular disease were eligible to participate in the study. The experimental protocols were conducted in the Aerospace Physiology Laboratory in the Department of Biomedical Physiology and Kinesiology. Written informed consent for participation was obtained from each participant

prior to experimentation. A registered nurse was present during the experimentation for the safety of participants.

The lower body of each participant was placed in the LBNP chamber and sealed at the level of the iliac crest. The participants lay supine inside the chamber for 5 minutes of baseline recording after which, the pressure inside the chamber was gradually reduced to -20 mmHg, from this point the chamber pressure was reduced in steps of 10 mmHg up to -40mmHg. Five minutes of negative pressure was applied at each LBNP stage. A straddling bicycle seat inside the chamber prevented participants from getting further pulled inside the chamber. The chamber pressure was immediately terminated if a participant exhibited 1) pre-syncopal symptoms 2) sudden drop in blood pressure and/or heart rate 3) any discomfort or 4) upon request.

Simultaneous electrocardiogram (ECG) and blood pressure were acquired from 27 young, healthy participants (15 males and 12 females, age: 27±1 years, weight: 66±2 kg, height: 169±2 cms, mean±SE) who underwent graded LBNP. The detailed demographic information is summarized in Table 3.4. The ECG signal was acquired in a lead II configuration using LifePak8 (Medtronic Inc., MN, USA) and the blood pressure signal was acquired using a finger photoplethysmograph cuff (FMS, Amsterdam, The Netherlands) applied on the mid phalanx of the middle finger (left hand). Five minutes of data were acquired during baseline resting and each LBNP stages using an NI 9205 analog input module (National Instruments Inc., TX, USA) at a sampling rate of 1000 Hz. Figure 3.1 shows the experimental setup for data acquisition during LBNP protocol.

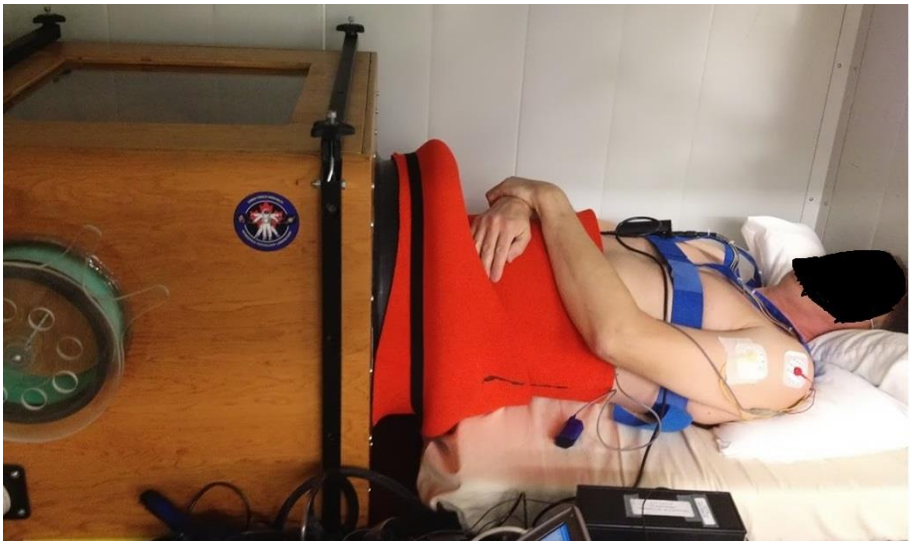

Figure 3.1. Experimental set up of lower-body negative pressure protocol. Lower body is placed in the chamber where suction is applied to translocate central blood volume in the lower periphery.

Table 3.4. Detailed demographic information of the 27 participants. The table lists each participant's age, height, weight, and gender.

Subject No.	Age	Height (cms)	Weight (Kgs)	Gender
1	34	174	70	Male
2	27	179	90	Male
3	29	168	54	Female
4	24	162	61	Male
5	24	165	56	Female
6	26	162	57	Female

7	39	165	85	Male
8	28	169	59	Female
9	25	171	67	Female
10	25	175	77	Male
11	25	169	64	Female
12	30	164	58	Female
13	29	178	70	Male
14	31	169	65	Male
15	18	158	60	Female
16	39	170	85	Female
17	24	177	77	Male
18	22	180	68	Male
19	26	183	71	Male
20	25	156	44	Female
21	25	168	62	Male
22	24	150	53	Female

23	23	151	45	Female
24	23	169	67	Male
25	26	175	72	Male
26	28	167	74	Male
27	23	177	71	Male

3.3.2. Data Processing

From the acquired signals RR intervals, beat-to-beat systolic blood pressure (SBP) and diastolic blood pressure (DBP) was obtained using the beatscope software (Finapres, FMS, The Netherlands), mean arterial pressure (MAP) was derived from SBP and DBP as; $MAP=\frac{2}{3}\times DBP+\frac{1}{3}\times SBP$. An evenly sampled signal was created from beat-to-beat signals using spline interpolation and was resampled to 10 Hz prior to assessing heart rate and blood pressure causality and spectral analysis of blood pressure and RR intervals. The appropriate parameter for causality analysis was determined using false nearest neighbor (FNN) algorithm at a delay of 10 samples using CRP toolbox in MATLAB. The FNN minimization was achieved at M=3. Therefore, the heart rate and blood pressure causality was computed at M=3 and τ=10 unless mentioned otherwise.

The spectral analysis was performed using Welch power spectral density (PSD) using a Hamming window of size 128 sampled and 50% overlap. The normalized power distributed in the VLF, LF, and HF band of blood pressure and RR intervals during each LBNP stage was calculated. The causality and spectral analysis were performed only

during the last 3 minutes of each LBNP stages to allow for effective blood pooling achieved by LBNP and its effect on the cardiovascular parameters. Pulse pressure was obtained as a difference between the SBP and DBP for each LBNP stage.

3.3.3. Statistical Analysis

The group mean of RR, SBP, DBP, MAP, pulse pressure (PP = SBP-DBP), the non-baroreflex i.e., feedforward (RR→SBP and RR→MAP), the baroreflex i.e., feedback (SBP→RR and MAP→RR) causality values, normalized spectral power distribution in respective bands of blood pressure and RR intervals, and gain value and % significant time interaction in respective frequency bands for the last 3min of each LBNP stage was obtained. Test for normality of the data was conducted using the Shapiro-Wilk test at $\alpha = 0.05$. A one-way test of ANOVA (normally distributed data) or Kruskal-Wallis test (data failed the normality test) was conducted to test the significance of the difference. The group mean of baroreflex causality (SBP→RR and MAP→RR) was compared with the group mean of non- baroreflex causality (RR→SBP and RR→MAP) under baseline using one-way ANOVA. A multiple comparison test, to account for the significance of the difference in the cardiovascular parameters and on the blood pressure regulatory indices, inflicted by different LBNP stages, was conducted using appropriate statistical test followed by post-hoc analysis using the Tukey-HSD method. All tests for significance were conducted using a statistical toolbox of MATLAB (Mathworks Inc., MA, USA). The test result at $\alpha = 0.05$ was considered as significant. All tabular results are presented as mean ± SD while all graphical results are presented as mean±SE unless mentioned otherwise.

3.4. Results

The cardiovascular parameters and the blood pressure regulatory indices passed the test of normality, therefore, a one-way test of ANOVA was conducted followed by post-hoc analysis using the Tukey-HSD method. Figure 3.2 summarizes the behavior of cardiovascular parameters in response to different LBNP stages. No change was observed in the SBP ($p=0.50$), DBP ($p=0.79$), or MAP ($p=0.99$) as a consequence of LBNP application. Pulse pressure decreased significantly ($p<0.05$) at -40 mmHg LBNP compared to baseline. Additionally, pulse pressure was observed to be significantly ($p<0.05$) different at -40 mmHg LBNP compared to -20 mmHg LBNP. RR intervals and heart rate decreased and increased, respectively at -30 and -40 mmHg compared to baseline. Furthermore, both parameters changed significantly ($p<0.05$) at -40 mmHg compared to -20 mmHg.

The response of baroreflex and non-baroreflex causalities are summarized in Figure 3.3. In response to LBNP stages no change ($p>0.05$) was observed in the non-baroreflex arm, while the baroreflex arm showed a significant increase ($p<0.05$) at -30 mmHg LBNP and at -40 mmHg LBNP compared to baseline. Moreover, a significant difference ($p<0.05$) was observed in the baroreflex causality between -20 mmHg LBNP and -40 mmHg LBNP. During resting stage the non-baroreflex arm of the interaction was observed to be dominant compared to the baroreflex arm, as higher ($p<0.05$) causal information flow in the direction RR→SBP or RR→MAP was noted compared to the causal information flow in reverse direction i.e. SBP→RR or MAP→RR (Figure 3.4).

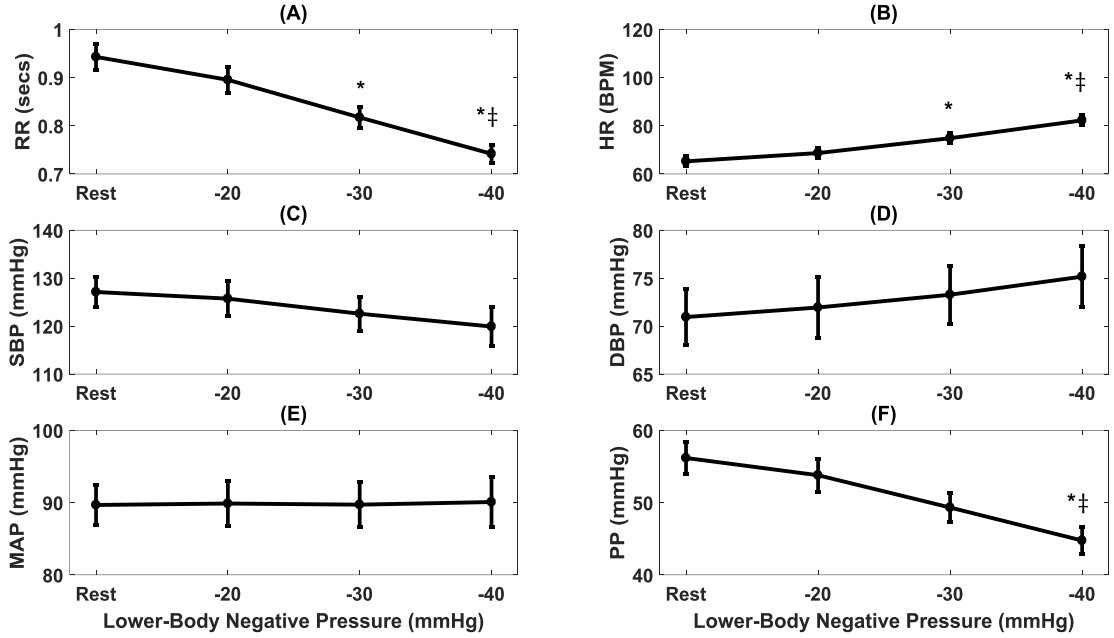

Figure 3.2. The response of cardiovascular parameters to graded lower-body negative pressure. R-R intervals (A) reduced significantly both at −30 (p=0.001) and −40 (p<0.001) mmHg LBNP compared to rest. Heart Rate (B) increased significantly at -30 mmHg and -40 mmHg compared to baseline. Pulse pressure (F) changes significantly at -40 mmHg compared to baseline. Additionally, R-R intervals (p<0.001), heart rate (p<0.001), and pulse pressure (p=0.02) reduced significantly at −40mmHg LBNP compared to −20mmHg LBNP. The systolic blood pressure (C), diastolic blood pressure (D), and the mean arterial pressure (E) did not change (p=0.50, p=0.79, and p=0.99, respectively) in response to graded lower-body negative pressure, * and ‡ represents significant change (p<0.05, post-hoc result) compared to rest and −20mmHg, respectively.

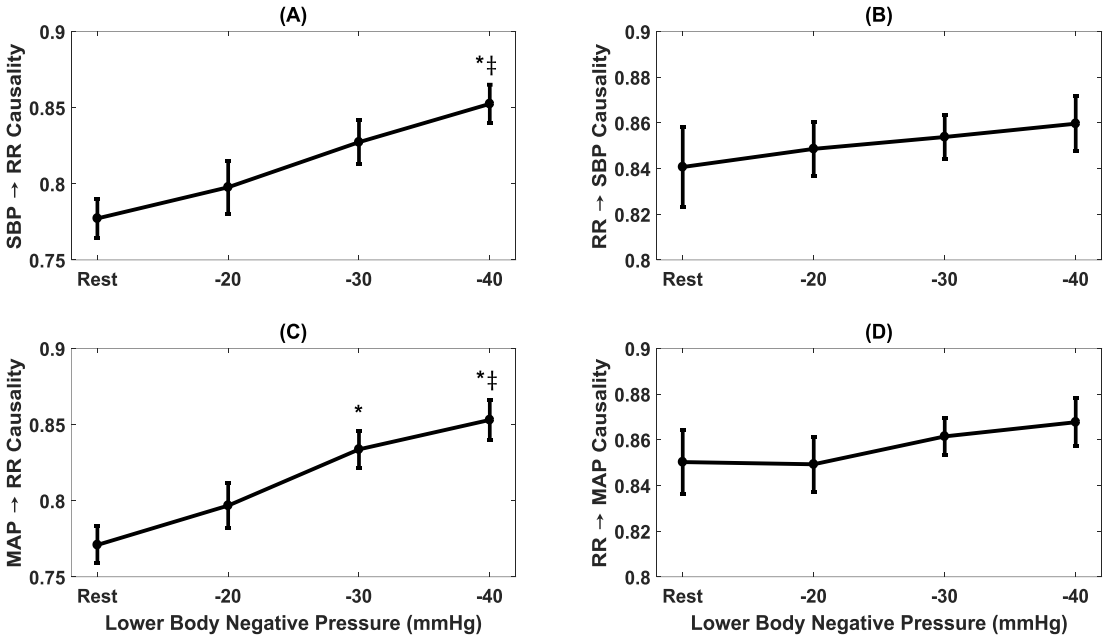

Figure 3.3. The response of baroreflex (A, C) and non-baroreflex (B, D) causalities to graded lower-body negative pressure. In response to LBNP, MAP→RR ($p=0.004$) causality increased significantly at −30mmHg compared to rest, SBP→RR ($p=0.001$) causality increased significantly at −40mmHg compared to rest. Compared to −20mmHg the SBP→RR ($p=0.04$) and MAP→RR ($p=0.01$) causality increased significantly at −40mmHg LBNP. No change in RR→SBP ($p=0.76$) and RR→MAP ($p=0.60$) causality was observed in response to LBNP. *Represents significant difference ($p<0.05$, post-hoc result) from rest while ‡represents significant difference from −20mmHg.

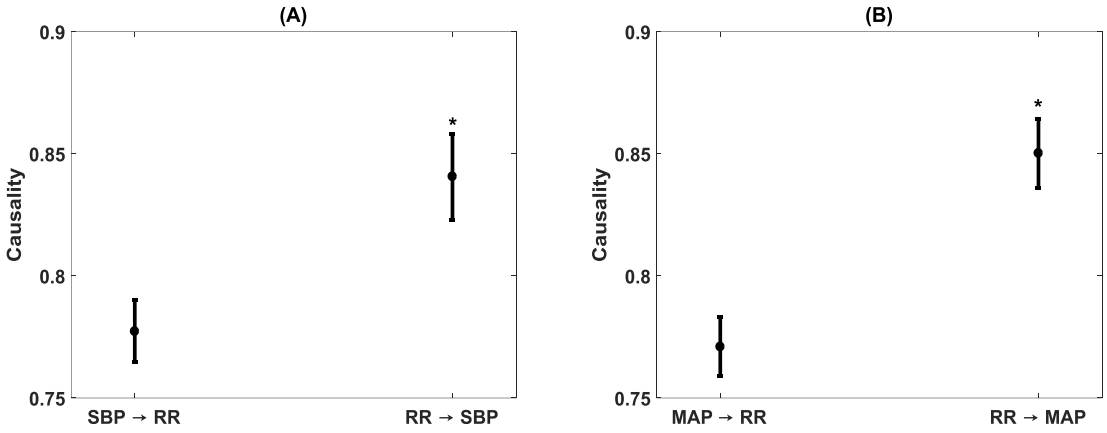

Figure 3.4. Comparison of non-baroreflex or feedforward (RR→SBP and RR→MAP) and baroreflex or feedback (SBP→RR and MAP→RR) causalities during supine baseline. The feedforward causality was significantly stronger ($p<0.001$) than the feedback causality for both RR↔SBP (A) and RR↔MAP (B) interactions. *Represents significantly ($p<0.05$, one-way ANOVA) stronger causality.

The behavior of autonomic control of blood pressure assessed via spectral analysis of RR, SBP, and DBP is summarized in Figure 3.5. A significant decline RR_{HF} at -30 and -40 mmHg compared to baseline was observed. $RR_{LF/HF}$ increased significantly at -30 and -40 mmHg compared to baseline. The DBP_{LF} increased significantly only at only -40 mmHg compared to baseline while no change was observed spectral distribution in the SBP. Shock index, modified shock index, and PP/HR all changed significantly at -30 and -40 mmHg compared to resting baseline (Figure 3.6). A 5-fold cross-validation was performed to test the potential of different classifier towards classifying moderate category hemorrhage (-30 and -40 mmHg LBNP) from baseline. Highest accuracy of 82% was achieved for classifying -30 mmHg LBNP from baseline, while an accuracy of 91% was observed for classifying -40 mmHg from baseline. The results for different classifier are summarized in Table 3.5 and 3.6 for -30 mmHg and -40 mmHg LBNP, respectively. Values of spectral power distributed in each frequency band is summarized in Table 3.7.

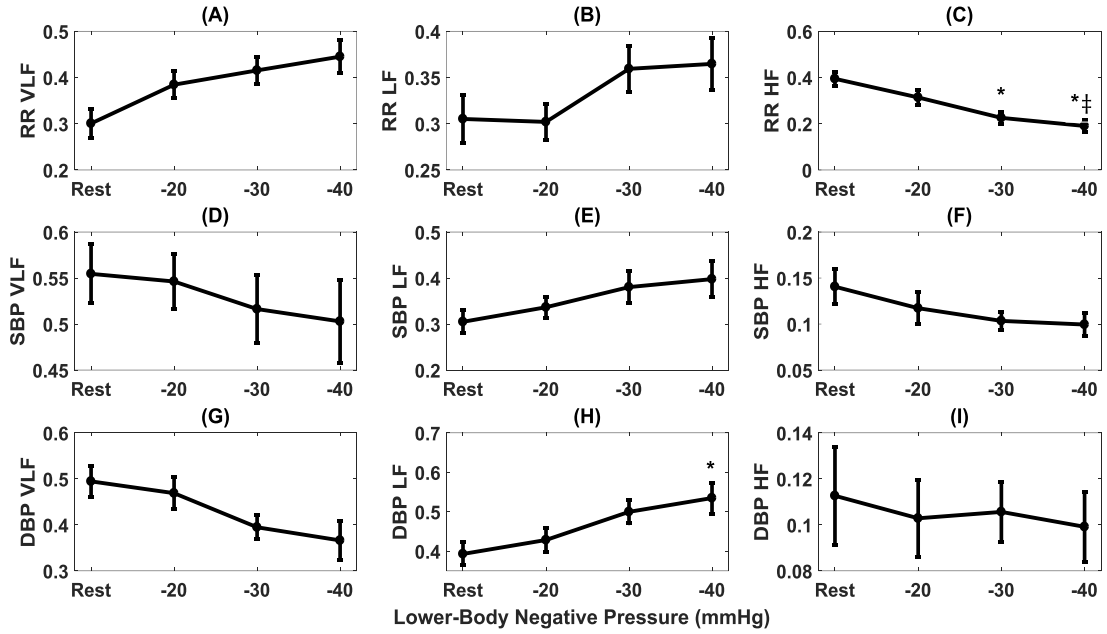

Figure 3.5. Spectral power distribution in SBP (A-C), DBP (D-F), and MAP (G-I) in respective frequency bands. No change ($p>0.05$) was observed in the spectral power distribution except for LF power in DBP, which increased significantly ($p<0.05$) at -40 mmHg compared to baseline.

3.5. Interpretation

This chapter investigated the feasibility of differentiating moderate intensity hemorrhage by utilizing non-invasive feature derived from commonly employed indicators of hemodynamic state i.e. ECG and continuous blood pressure signals. To this end, the findings of the research highlighted the capability of machine learning application towards differentiating the dynamics of moderate category hemorrhage (-40 mmHg) simulated via lower-body negative pressure utilizing a set of meaningful features derived from common vital sign monitors.

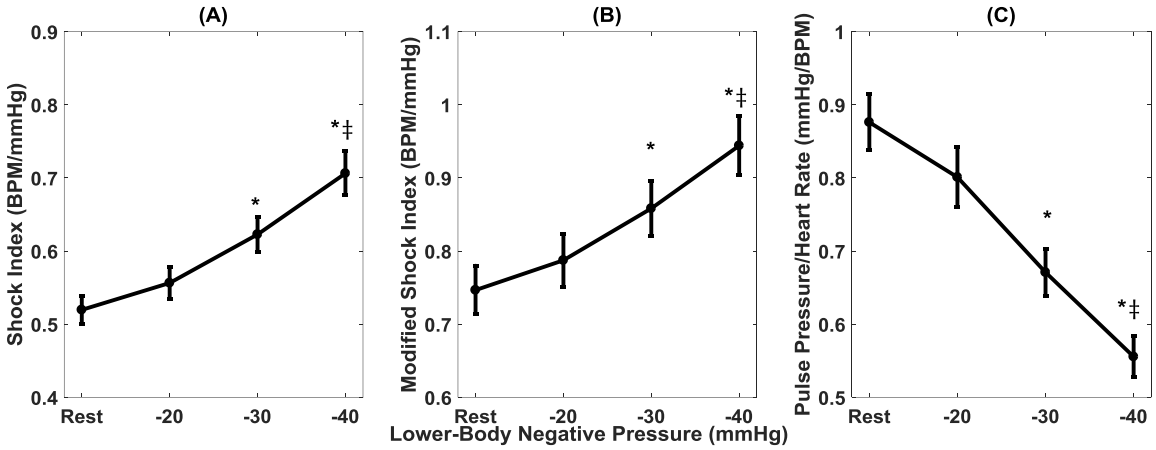

Figure 3.6. The behavior of Shock index (A), modified Shock index (B), and pulse pressure/heart rate (C) in response to lower-body negative pressure. All indices changed significantly at -30 and -40 mmHg compared to baseline. Moreover, they changed significantly at -40 mmHg compared to -20 mmHg. * Represents significant difference from baseline while ‡ represents a significant difference from -20 mmHg.

3.5.1. Cardiovascular Parameters in response to LBNP

Owing to convoluted physiological mechanisms regulating arterial blood pressure until autonomic collapse has rendered arterial blood pressure as an ineffective marker of early stage bleeding. Following autonomic collapse, blood pressure falls abruptly, however, at this point the interventional steps may be limited in effect towards maintenance organ perfusion. Therefore, early diagnosis of blood loss can assist the design of appropriate interventional strategies. The LBNP stage of -30 to -40 mmHg simulates a spectrum of moderate category simulated hemorrhage, and accurate classification moderate category simulated hemorrhage on the basis of non-invasive features derived from commonly employed vital sign monitors for hemodynamic monitoring can be a great asset.

Reduction in stroke volume is observed in response to central hypovolemia(26,95,110), nevertheless, accurate measurement of stroke volume is invasive and often entails

sophisticated instrumentation and expert operator, and thus, limiting its application to the environment where the majority of hemorrhagic shock occurs. Consequently, caregivers have to rely on systolic, diastolic, or mean arterial pressures to get insights regarding the dynamics of bleeding. Nevertheless, numerous physiological mechanisms responsible for arterial blood pressure regulation have limited the efficacy of blood pressure from exhibiting early symptoms of blood loss from the circulation, which often remain regulated until the hemorrhage has progressed to severe category. Pulse pressure as an alternative to stroke volume has been explored as an early indicator of progressive hypovolemia, although it showed potential to track hypovolemia, its clinical application is hindered due to high inter-subject variability(92,111,112).

Accordingly, noninvasive detection of stroke volume can have a clinical significance towards monitoring central hypovolemia, in this regard, attempts have been made to derive stroke volume from continuous arterial blood pressure waveform. Scherhag et al(113) and Tavakolian et al(110) have shown the possibility of such metric towards tracking hypovolemia by performing a comparison with non-invasively derived stroke volume with accurately measured stroke volume via echocardiography.

Additionally, the ratio of pulse pressure and heart rate has also been demonstrated to be correlated with stroke volume in an animal model, however, its application to humans towards tracking hypovolemia has not yet been demonstrated. Pulse pressure in response to simulated hemorrhage changed only at -40 mmHg compared to resting baseline while heart rate changed both at -30 mmHg and -40 mmHg compared to resting baseline. While heart rate showed an early change in its dynamics, making a triage decision based on heart rate alone controversial due its variable behavior and dependence numerous factors such as pain, hormones, vagal and sympathetic tone.

Figure 3.6 (C) highlights the dynamics of PP/HR ratio in response to LBNP stages. The ratio significantly declined at -30 mmHg and -40 mmHg compared to baseline, additionally

the ratio successfully differentiated -40 mmHg from -20 mmHg underscoring its capability to continuously monitor the severity of bleeding. The Figure 3.7 details the distribution of such index for individual participants for resting baseline and moderate category hemorrhage (-40 mmHg). The ratio declined significantly in the majority of the participants suggesting its application towards monitoring the intensity of progressing central hypovolemia.

3.5.2. Shock Index in Response to LBNP

Shock index, a ratio of heart rate and systolic blood pressure, is also a commonly utilized feature for tracking the degree of blood loss(114,115). However, changes in such index are not specific, some research have found it an early indicator of hypovolemia, while in others no change in shock index was observed during moderate category hemorrhage which further highlights great degree of variance in the behavior of heart rate in the literature(93). In our data, with the application of moderate category LBNP (-30 and -40 mmHg), we observed a significant increase in the heart rate in response to a reduction in stroke volume to maintain cardiac output and arterial blood pressure, consequently, inflicting significant change in shock index. The behavior of shock index in response to LBNP is shown in Figure 3.6, significant difference compared to resting baseline was observed as early as -30 mmHg compared to resting baseline.

Majority of studies utilize systolic blood pressure for calculation of shock index, however, DBP can also be of particular importance given its potential to provides information pertaining to the systemic vascular resistance, and thus incorporation of mean arterial pressure for calculating shock index i.e. modified shock index can have wider application towards tracking hypovolemia(116). The behavior of modified shock index in response LBNP is summarized in Figure 3.6, a significant change was observed in the modified shock index at -30 and -40 mmHg compared to resting baseline. In addition, both indexes

were observed to be significantly different at -40 mmHg compared to -20 mmHg further validating its potential to track the degree of blood loss.

3.5.3. Spectral Analysis in Response to LBNP

Furthermore, we studied the autonomic control of blood pressure during simulated hemorrhage via spectral analysis of heart rate and blood pressure in the normalized units. The spectral power distributed in the high-frequency region of the RR intervals reduced significantly with the application of LBNP suggesting vagal withdrawal, while no change was observed in the VLF and LF frequency bands of the RR intervals. Additionally, the $RR_{LF/HF}$ ratio increased significantly at -30 and -40 mmHg compared to resting baseline. This behavior is summarized in Table 3.7. The increased $RR_{LF/HF}$ ratio was more so due to a sudden decline in vagal behavior as opposed to an increase in sympathetic behavior in response to LBNP. This observation suggests during hypovolemia in supine posture, the autonomic control of blood pressure is achieved via sudden vagal withdrawal leading to shift in sympatho-vagal balance more towards sympathetic activity causing an increase in heart rate and systemic vascular resistance for regulating cardiac output and blood pressure.

The spectral power distributed in the low-frequency and high-frequency band of blood pressure is shown to reflect baroreflex and respiratory activity, respectively. When SBP was used as a blood pressure marker, we observed no change ($p>0.05$) in the spectral power distributed in any frequency bands. However, when DBP was used as a blood pressure marker, we observed a significant change in the DBP_{LF} at -40 mmHg compared to resting baseline suggesting activation of baroreflex response (Figure 3.5). This discrepancy can be associated with the postural effect on the translocation of blood volume. Application of LBNP translocate the blood volume in the lower extremities while standing or head-up tilt translocate the blood volume in the splanchnic bed(117).

Table 3.5. Different classifier performance towards classifying moderate category hemorrhage (-30 mmHg) from resting baseline. Table lists the highest values for each classifier category.

Classifier	Sensitivity	Specificity	Accuracy
SVM	85%	78%	82%
kNN	89%	70%	80%
DA	67%	78%	72%
LR	74%	70%	72%
Ensemble	85%	81%	83%
DT	70%	70%	70%

Table 3.6. Different classifier performance towards classifying moderate category hemorrhage (-40 mmHg) from resting baseline. Table lists the highest values for each classifier category.

Classifier	Sensitivity	Specificity	Accuracy
SVM	89%	93%	91%
kNN	89%	85%	87%

DA	89%	89%	89%
LR	74%	74%	74%
Ensemble	89%	89%	89%
DT	74%	74%	74%

While the spectral analysis is well-accepted norm to study the autonomic control of blood pressure in response to the orthostatic challenge, the same is also criticized for its ability to not account for non-linearity of signals under investigation.

3.5.4. Non-linear Heart Rate and Blood Pressure Interaction

The thesis substantiated the analysis by incorporating non-linear heart rate and blood pressure interaction in response to LBNP. To impede progressing hemorrhage, it is central to quantify the compensatory mechanisms regulating arterial blood pressure. To this end, the current research investigated the sensitivity of causal heart rate and blood pressure interaction for monitoring simulated central hypovolemia which is known to act in a closed loop to regulate arterial blood pressure during orthostatic challenge. Furthermore, owing to the robustness of the nonlinear methodology, we successfully highlighted the contribution of the non-baroreflex (RR→SBP and RR→MAP) and the baroreflex (SBP→RR and MAP→RR) mechanisms responsible for blood pressure regulation under a variable degree of LBNP induced physiological stressor (Figure 3.3). The directional information flow, mediated by both baroreflex and non-baroreflex arms of the interaction was observed, with the non-baroreflex (RR→SBP and RR→MAP) arm being dominant

($p<0.001$) during the resting stage compared to the baroreflex arm (SBP→RR and MAP→RR), Figure 3.4.

With the application of external perturbation to the hemodynamic homeostasis in the form of lower body negative pressure, an elevation in the causal activity, in the direction of blood pressure to heart rate (SBP→RR and MAP→RR) was observed, representing activation of baroreflex mediated control of heart rate towards the maintenance of arterial blood pressure homeostasis. Progression of central hypovolemia to moderate intensity (-30 mmHg) was accompanied by no significant elevation in the SBP→RR ($p=0.07$) causality but significant elevation in the causal drive from MAP→RR ($p=0.004$) while no change was observed in the strength of reverse drive, which is a representative of heart rate mediated blood pressure changes i.e. RR→SBP ($p=0.76$) and RR→MAP ($p=0.60$).

This observation indicated that under resting condition blood pressure is primarily maintained through blood pressure changes mediated by heart rate, contrarily, under physiologically perturbed cardiovascular system due to a decline in venous return, the baroreflex mediated heart rate control acts as a compensatory mechanism leading to arterial blood pressure homeostasis. Thus, the two blood pressure regulatory mechanisms interact in closed loop at any given time in order to maintain blood pressure homeostasis. Furthermore, the baroreflex causality (SBP→RR and MAP→RR) was able to differentiate -40 mmHg from -20 mmHg, therefore highlighting its capability to track and differentiate varying intensity of hemorrhage (Table 3.7).

This behavior of closed loop heart rate and blood pressure interaction under varying physiological conditions ascertained the contribution of either arm of the blood pressure regulation mechanism. The findings of the current research corroborated with the previous findings regarding heart rate and blood pressure interaction highlighted under head-up tilt

and the stand test, which demonstrated an elevation in the baroreflex activity during orthostatic challenge compared to baseline with SBP being an indicator of blood pressure functioning(69,104,105). However, the literature is limited in terms of comprehensive quantified knowledge of such nonlinear behavior with respect to progressing blood loss simulated by LBNP.

The report by Dorantes-Mendez et al and Silvani et al(69,118) investigated heart rate and blood pressure coupling with respect to LBNP and actual blood loss, respectively. However, a linear methodological approach was considered for such quantification. Moreover, the heart rate and blood pressure interaction is known to be of nonlinear nature, therefore, a more robust approach would be a prerequisite, for accurately underpinning the continuous dynamics of the non-baroreflex and the baroreflex arms of such interaction. With the application of nonlinear methodology and higher sample size compared to previous two works, in the current research, we systematically demonstrated the degree of statistical alteration in both the non-baroreflex and the baroreflex mechanisms of blood pressure regulation in response to the simulated progressing hemorrhage (LBNP). Our study, therefore, provided comprehensive insights regarding the feasibility of compensatory directional interaction for monitoring progression of hemorrhage and for surgical triage.

Additionally, we compared the use of SBP and MAP as a marker of baroreflex mediated heart rate control (baroreflex causality) in response to LBNP. As such, we found MAP to be a more sensitive marker of baroreflex mediated heart rate control in response to moderate category (-30 mmHg) LBNP compared to SBP (Figure 3.3). The MAP→RR causality achieved statistical significance at -30 mmHg LBNP compared to baseline while the SBP→RR causality did not show a significant change in its dynamics until -40 mmHg LBNP. However, SBP→RR and MAP→RR both showed a significant change in their

dynamics at -40 mmHg compared to baseline and -20 mmHg (Figure 3.3). This observation leads us to conclude that MAP→RR causality is more sensitive to the early phase of central blood loss simulated by LBNP, thus, a better marker of baroreflex activity when aimed to gain early information regarding progressing blood loss from the circulation. Mean arterial pressure perhaps is a better indicator of early phase of central blood pooling in the lower limbs compared to SBP due to its relationship with cardiac output (CO), systemic vascular resistance (SVR), and central venous pressure (CVP); MAP=(CO×SVR)+CVP(61), validation of this hypothesis under gravity-induced orthostatic stress (head-up tilt or stand test) requires future work.

The behavior of nonlinear causal heart rate and blood pressure interaction in response to simulated hemorrhage via LBNP is not extensively explored in the literature. The references that exist regarding such behavior have been outlined under orthostatic challenge induced via head-up tilt and stand test, which have considered systolic blood pressure as a marker of arterial blood pressure. The lower-body negative pressure is hypothesized to exert orthostatic challenge on the human body analogous to head-up tilt(117,119). Therefore, the physiological response to LBNP is expected to be analogous to that of head-up tilt and quiet standing. Nevertheless, the outcomes of some studies have highlighted the differences in the cardiovascular, cerebrovascular, and the hormonal responses when using LBNP to evoke orthostatic challenge compared to head-up tilt(117,120–122).

The absence of gravity induced hydrostatic gradient during lower-body negative suction is shown to be the major contributor towards the existence of such difference. The application of LBNP empties splanchnic blood volume (analogous to hemorrhage) while the gravity induced orthostatic stress (such as head-up tilt) increases the blood volume in the splanchnic bed(117). Recent work by Silvani et el(69) further highlighted such

discrepancy, where a significant change in baroreflex response (using SBP) during head-up tilt but not during 1000 ml of blood loss was observed, similarly, the baroreflex response (SBP→RR) in our analysis failed to differentiate -30 mmHg LBNP (equivalent to approximately 1000 ml of blood loss) from baseline. These observations, besides highlighting the fact that baroreflex response differs between head-up tilt and central blood loss, raise concern regarding SBP as baroreflex marker when aimed to gain early insights regarding blood loss.

The discrepancies that might exist in the blood pressure regulation via causal heart rate and blood pressure interaction during orthostatic challenge induced by the application of LBNP compared to head-up tilt or stand test is not the scope of this thesis, and future work shall follow to address such concerns to further our understanding regarding underlying physiology. The current thesis aimed at investigating the capability of causal heart rate and blood pressure interaction in tracking progressing simulated hemorrhage. In such context, the findings of the study are promising and underscored capability of MAP→RR causality to differentiate moderate category hemorrhage (-30 mmHg LBNP) from resting baseline.

Although the parameters extracted from the blood pressure waveform and electrocardiogram show statistical capability to differentiate moderate category hemorrhage from resting baseline, it is pivotal also consider the behavior on an individual basis, high inter subject variability can limit the potential of such predictor to accurately classify progressing hemorrhage. Figure 3.7 shows the behavior of individual participants during baseline and -40 mmHg LBNP.

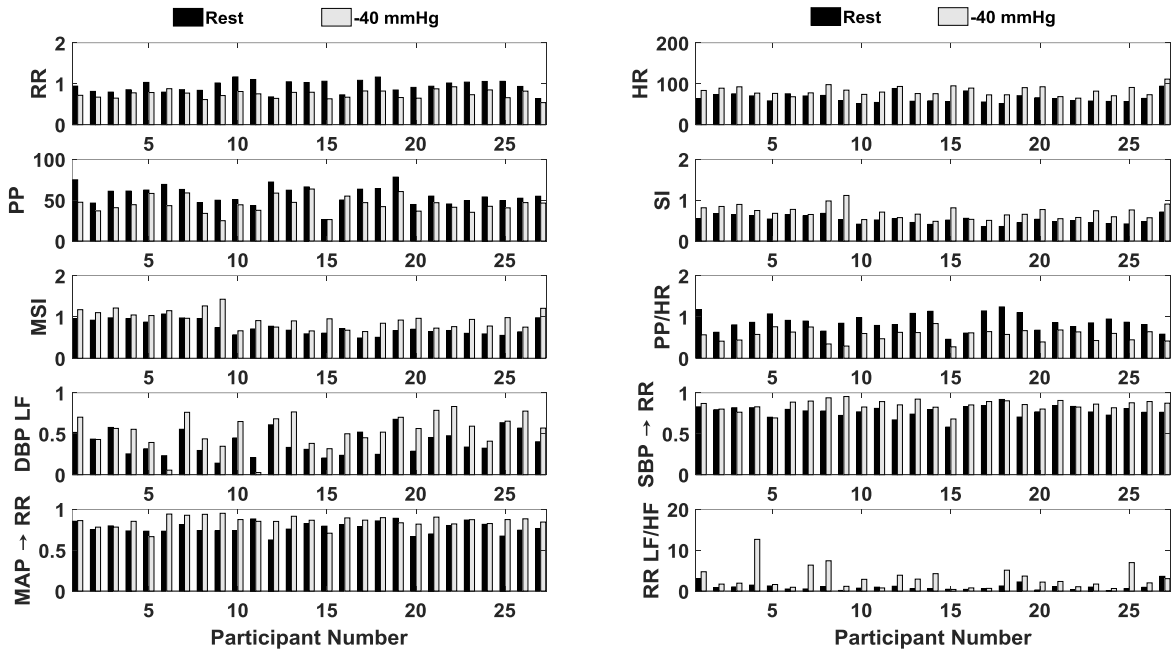

Figure 3.7. Comparing rest vs -40 mmHg of different parameters which showed a significant change in response to lower-body negative pressure.

Table 3.7. Values of different parameters studied in this research in reponse to lower-body negative pressure. * Represent significant difference from rest while ‡ represents a significant difference from -20 mmHg.

Variables	Rest	-20 mmHg	-30 mmHg	-40 mmHg
RR (ms)	0.94±0.14	0.90±0.14	0.82±0.11*	0.74±0.10*‡
HR (BPM)	65±11	69±12	75±11*	82±11*‡
SBP (mmHg)	127±16	126±19	123±19	120±21
DBP (mmHg)	71±15	71±17	73±16	75±17
MAP (mmHg)	90±15	90±16	90±16	90±18

SBP_{VLF} (n.u.)	0.55±0.17	0.55±0.16	0.52±0.19	0.50±0.24
SBP_{LF} (n.u.)	0.30±0.13	0.34±0.12	0.38±0.18	0.40±0.20
SBP_{HF} (n.u.)	0.14±0.10	0.12±0.09	0.10±0.05	0.10±0.07
DBP_{VLF} (n.u.)	0.49±0.18	0.50±0.18	0.39±0.13	0.37±0.22
DBP_{LF} (n.u.)	0.39±0.15	0.43±0.15	0.50±0.15	0.53±0.20*
DBP_{HF} (n.u.)	0.11±0.11	0.10±0.09	0.11±0.07	0.10±0.08
RR_{VLF} (n.u.)	0.30±0.16	0.38±0.15	0.42±0.15	0.45±0.18
RR_{LF} (n.u.)	0.31±0.13	0.30±0.10	0.36±0.13	0.36±0.15
RR_{HF} (n.u.)	0.39±0.15	0.31±0.17	0.23±0.13*	0.19±0.14*‡
SI (BPM/mmHg)	0.52±0.10	0.56±0.11	0.62±0.13*	0.71±0.16*‡
MSI (BPM/mmHg)	0.75±0.17	0.79±0.19	0.88±0.19*	0.94±0.21*‡
PP/HR (mmHg/BPM)	0.88±0.20	0.80±0.21	0.67±0.17*	0.56±0.14*‡
RR→SBP	0.84±0.09	0.85±0.06	0.85±0.05	0.86±0.06
SBP→RR	0.78±0.07	0.80±0.09	0.83±0.07	0.85±0.07*‡
RR→MAP	0.85±0.07	0.85±0.06	0.86±0.04	0.87±0.05
MAP→RR	0.77±0.06	0.80±0.07	0.83±0.06*	0.85±0.07*‡

3.5.5. Classification of Moderate Category Hemorrhage from Baseline

Although numerous parameters have been explored in the literature to accurately differentiate hypovolemic state compared to the normovolemic state, limited success has been obtained due to the existence of high inter-subject variability. These observations evidently hint towards the need of a more robust system for accurately and reliably monitoring hypovolemia progression. Such system would require decision making based on numerous parameters accentuating respective physiological information. In this context, the concept of machine learning can play a pivotal role. Even though machine learning is frequently utilized in literature for performing multi-level classification, its application towards the automatic classification of trauma is limited(32–34,123). The concept of the compensatory reserve is promising in this context which utilized advanced machine learning scheme to monitor hypovolemic state(93,96). The work by Bennis et al utilized neural network with noninvasive features to differentiate -50 mmHg from resting baseline(33). From limited research conducted in this area, it can be concluded that machine learning can overcome the limitations such as high inter-subject variability and reliance on specific parameter to make a decision on intensity of hemorrhage.

The extracted features for machine learning classification in this research shown in Figure 3.7 were fed to different classifiers to test its potential to accurately classify moderate category hemorrhage (-30 ad -40 mmHg LBNP) from resting baseline. Table 3.5 and 3.6 lists the performance of classifier using different kernels towards the classification of -30 and -40 mmHg LBNP compared to baseline. Even though numerous study parameters showed significant change at -30 mmHg compared to resting baseline, the classification accuracy of only 82% was achieved, this further emphasized insufficiency of decision making based on the group mean behavior of specific parameter due to the existence of inter-subject variability, thus, decision support system utilizing information via multiple

predictors of blood loss can be more reliable and accurate. Utilizing same features classification accuracy for -40 mmHg LBNP was 91% suggesting the set features discussed in this manuscript may assist automatic detection of blood loss at an early stage, accordingly assist surgical triage to impede hemorrhage progression to a severe stage.

3.6. Conclusion

In conclusion, the thesis showed strong evidence towards classifying moderate intensity hemorrhage with reasonable accuracy (82% for -30 mmHg and 91% for -40 mmHg) based on features derived from non-invasively acquired common vital sign monitors. Further validation is warranted with a bigger cohort to gain potential application towards design of automated decision support system for caregivers to facilitate surgical triage.

Chapter 4.

Cardio-Postural Control of Blood Pressure: Validation of a Novel Model to Assess Orthostatic Tolerance

4.1. Summary

Background: Blood pressure during standing is regulated in part by autonomic activity and partly via skeletal muscle activation by pumping the pooled venous blood back to the heart. Despite such knowledge, the physiology of the postural instability is studied independently as cardiovascular and postural problems. In recent years, significant coupling between the cardiovascular and postural controls of blood pressure during standing has been demonstrated, however, the cause-and-effect relationship between the respective signals of cardiovascular and postural controls of blood pressure remains to be established. **Methods:** In this chapter, we extended the previous work and explored the existence of a degree of cause-and-effect relationship between the representative signals of cardiovascular and postural systems during last 4-minutes of standing via non-linear convergent cross mapping (CCM). Systolic blood pressure was considered as a marker of cardiovascular performance, while calf-electromyography (EMG) and postural sway (COPr) were considered as representative of postural systems. Causality was studied between EMG↔SBP, COPr↔SBP, and EMG↔COPr signal pairs. **Results:** The bi-directional causal information flow confirmed the previously conceived notion of interdependency between the cardiovascular and postural systems towards blood pressure regulation during orthostatic challenge. Further, this chapter observed a significant change in such behavior following a 12-minute bout of submaximal exercise. **Conclusions:** The findings of this chapter underscored the existence of a significant

interaction between cardiovascular and postural towards regulation of blood pressure and therefore, stresses upon considering cardiovascular as well as postural controls of blood pressure when addressing physiology behind orthostatic intolerance or postural instability.

4.2. Background

Maintaining postural instability remains a major concern in people with neurodegenerative diseases such as stroke, concussion, and Parkinson's disease (PD)(35,124–127). Unexpected falls are associated with postural instability and are one of the leading cause of injury in such population group(5). Older people with a history of neurodegenerative disease have a higher chance of falling compared to their healthy counterparts(35,40). Given that neurodegenerative diseases are predominantly prevalent in older people and with elderly population is anticipated to grow in the future(39), the prevalence of neurodegenerative diseases and associated fall is expected to increase in the near future. Injuries due to falling entail immediate medical attention and are a major cause of a visit to the emergency department of the hospital. With over $31 billion spent annually for treatment and management, the fall and associated injuries have become a significant financial burden on the current healthcare system(7). Additionally, such events are debilitating; limiting individual's mobility leading to severe degradation in the quality of life.

On assuming upright stance, the central blood volume is translocated below the heart level as a consequence of gravity induced hydrostatic gradient. Given the compliant nature of the venous system, pooling of blood takes place; in the veins of the lower periphery. Excessive venous pooling can result in a decline in preload and therefore, drop in blood pressure, which if not compensated for can initiate symptoms of syncope. On standing, the immediate translocation of blood volume is compensated via the baroreceptor unloading leading to vagal withdrawal and sympathetic nerve activation causing increased

heart rate and systemic vascular resistance. However, prolonged standing can cause continuous displacement of blood in the lower periphery, under such circumstances blood pressure regulation is dependent on the calf musculature to pump the pooled venous blood back to the heart (skeletal muscle pump).

Additionally, the postural control system integrates the information via the visual, vestibular, and the somatosensory systems, the absence of such information can lead to postural instability(128,129). Therefore, maintaining stable upright stance is an intricate process and dependent on the autonomic and postural controls of blood pressure. This thesis aims to investigate the physiology of fall either due to the deterioration of postural mechanisms or the impairment of the cardiovascular performance. However, only limited research have considered both systems jointly when addressing the physiology of postural instability(48,130). Figure 4.1 details the hypothesized link between the cardiovascular and postural controls of arterial blood pressure during orthostatic challenge.

Research has demonstrated individuals with poor orthostatic tolerance relied on increased postural sway for the maintenance of preload, where postural sway is believed to contribute to greater activation of calf skeletal muscles, therefore, facilitating a venous return to the heart to facilitate blood pressure homeostasis(3). The cardio-locomotor model proposed by Novak et al hypothesized that forces generated during locomotion by increased contraction of skeletal muscles can act as a pump, consequently, propelling the pooled venous blood back to the heart(131). The cardio-locomotor model was further modified by Blaber et al as a cardio-postural model to assess orthostatic tolerance(130). Of late, bidirectional coupling was shown to exist between the respective signals of the cardiovascular and postural systems during orthostatic challenge evoked via standing utilizing an advanced wavelet transform coherence, further validating the applicability of the cardio-postural model for assessing orthostatic tolerance(46,48). However, the causal

information flow between the respective variables of the cardiovascular and postural systems remains to be understood(132–135).

Causality describes the directional relationship between cause and its effect. The human body as a highly integrated group of dynamic and adaptive systems often shows cause and effect relationships, such relationship has been studied in neural(71,136,137), cardiovascular(103,107), cardio-respiratory(70,138), and cardio-neural systems(139,140). The established knowledge of causality between dynamical systems could be exploited for physiological system performance monitoring, as; a significant deviation in the behavior of causally linked systems from the established norm could be symptomatic of system impairment. For example, the directional interaction between heart rate and blood pressure has been extensively studied in the literature, and the behavior has been generalized, therefore, deviation in such generalized behavior can serve as an early indicator system deterioration.

To this end, the commonly applied Granger causality method measures the ability of one signal to predict the future of other to establish causal behavior. However, assumptions of linear statistical inference, stationary signal behavior, and determination of appropriate model order limit the application of Granger causality methods to linear and stationary systems(71,136). Transfer entropy, a nonlinear model free methodology is often considered for addressing limitations of Granger causality(72,108,141). Nevertheless, the assumption of stationary signal behavior and the requirement to estimate probability density function of signals under consideration limit its application(73). Physiological signals are inherently nonlinear in nature, thus, a nonlinear approach would be necessary to obtain accurate inference with respect to the dynamics of the complex causal interplay between physiological systems.

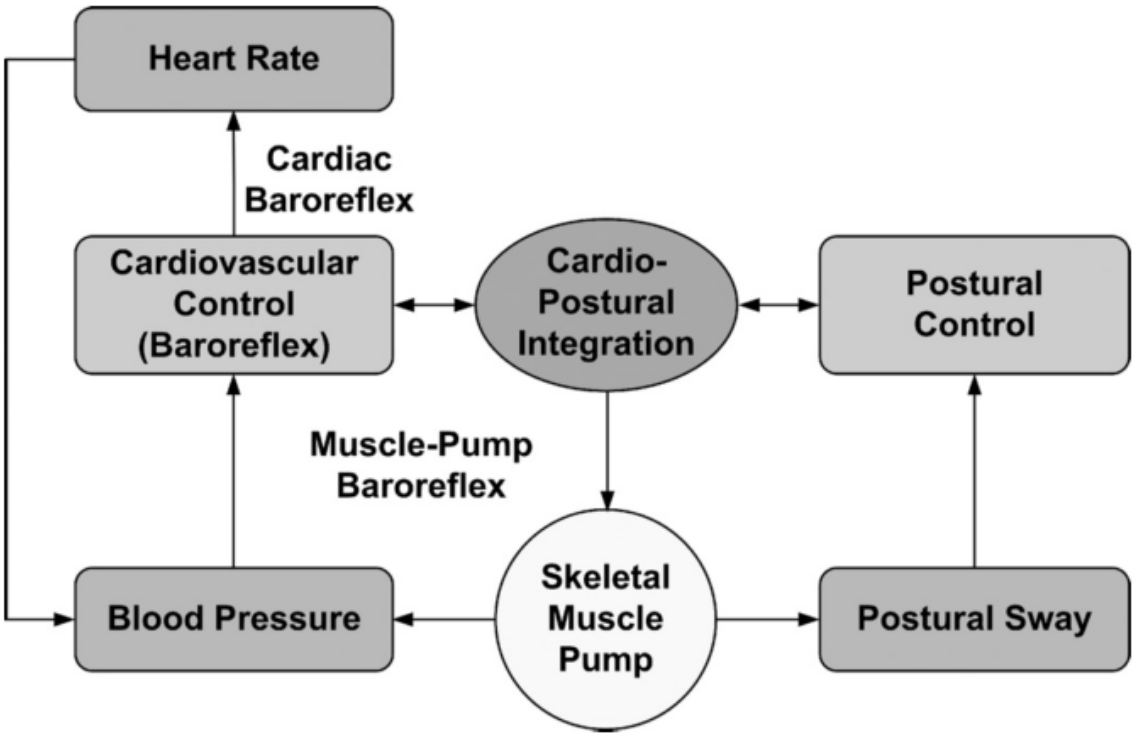

Figure 4.1. The hypothesized cardio-postural model for regulation of arterial blood pressure during orthostatic challenge induced by upright stance(142).

Convergent cross mapping (CCM), a nonlinear approach for estimating causality between two time series is based on the state space reconstruction of a time series called 'shadow-manifold'(75). Causality is estimated by quantifying the correspondence between two manifolds. State space reconstruction of variables is dependent on the selection of time delay (τ) and embedding dimension of reconstruction (E) (74,143). Under optimal choice of two parameters, CCM is expected to uncover accurate underlying nonlinear directional physiological interaction. Moreover, in contrast to Granger causality, the CCM method is capable of inferring causality in systems with weak to moderate coupling, while the performance of Granger causality is contingent on data separability(78,143). Causality analysis using Granger-based approaches is often subject to statistical hypothesis testing,

whereby, causality inference is based on acceptance/rejection of the null hypothesis while the physiological systems are interacting continuously with variable intensity.

On the other hand, CCM infers causality in terms of strength of coupling, thus, revealing vital information regarding the degree to which the interacting variables are coupled. The quantified knowledge of the strength of directional interaction can have a clinical relevance; as aging or pathology may cause an alteration in the strength of such interaction. The strength of the CCM method has been demonstrated in physiological applications to understand blood pressure and cerebral blood flow velocity interaction(144) and in the interaction between heart rate variability and the electroencephalographic signals(79). Additionally, the performance of CCM method has been shown to be superior to the Granger causality with signals of nonlinear nature(79). With evidence of success in the literature, CCM is expected to accurately unearth dynamics of underlying physiological interactions between cardio-postural-musculoskeletal systems (cardio-postural control loop), a pivotal intersystem interaction required for maintaining stable upright posture. In addition to studying the cause-and-effect relationship between the cardiovascular and postural systems, this chapter also studied the interdependency between the cardiovascular and controls of blood pressure using joint recurrence quantification analysis. Although the concept of recurrence quantification analysis is abundantly studied in literature to address physiological problems, the concept of joint recurrence quantification analysis which would highlight the interdependency between the systems is not well explored in the literature.

This chapter investigates the existence of a degree of directional information flow between the respective signals of cardiovascular and postural systems account for the cardio-postural control loop to ascertain blood pressure homeostasis during orthostatic challenge. Also, this chapter investigates the coupling between the cardiovascular and

postural controls of blood pressure using novel joint recurrence quantification analysis. We hypothesize following closed-loop interaction 1) cardio-postural (SBP↔COPr), 2) muscle pump-baroreflex (SBP↔EMG), and 3) muscle pump-postural (EMG↔COPr). The hemodynamic homeostasis was perturbed via stand test, further stress was applied via 12 minutes of submaximal exercise to increase blood pooling. The response of cardio-postural control of blood pressure was studied before and after exercise to highlight the underlying physiology regulating blood pressure during standing. The goal behind the choice of adding a short bout of exercise was the known concept of post-exercise hypotension typically observed; even in young, healthy population(145). Altered physiology post-exercise can result in excessive pooling of central blood volume in the venous system due to vasodilation. Thus, under such physiological state, the alteration in a cardio-postural model of blood pressure can be more evident, therefore, furthering our understanding of the cardio-postural control of blood pressure under challenging physiological state.

4.3. Methods

4.3.1. Experimental Protocol

Data were collected from 21 participants with no history of the cardiovascular, respiratory, or neurological disease, major musculoskeletal injuries, or hormone imbalance. The details regarding experimental protocol and signals acquisition can be found here(142). Detailed demographic information is summarized in Table 4.1. The use of prescription medications and naturopathic remedies were reported. Participants taking any substance that could alter cardiovascular regulation or postural stability were excluded. Prior to the experiments, participants' height, weight, general medical history, and present medications were recorded. Female participants were asked to report the use of

prescription contraceptives and the number of days since their last menstruation to determine the phase of the menstrual cycle at the time of testing. All participants were instructed to refrain from exercise and caffeine consumption for 24 hours prior to the experiment. The experiment protocol was approved to be of minimal risk by Simon Fraser University's Research Ethics Board. Written informed consent was obtained from each participant before the experiment.

After all the physiological monitoring sensors were in place, participants were seated and the measurement authenticity was then verified for necessary adjustments prior to data collection. The experiment protocol consisted of three parts: pre-exercise sit-to-stand test, sub-maximal cycle ergometer exercise, and post-exercise stand test. All tests were conducted in a sensory-minimized environment – a dark room with black drapes in front of the participants with minimal ambient noise. During the sit-to-stand test, participants were seated quietly with arms relaxed by their sides for 5 minutes, after which assistance was provided to transition into an upright stance on a force platform for an additional 5 minutes to induce orthostatic stress. Participants' feet were placed parallel and 5 cm apart on the center of the force platform. They were instructed to keep their eyes closed, maintain imaginary eye-level gaze, and not to alter foot placement.

After the sit-to-stand test, participants were seated comfortably on a cycle ergometer to carry out a 12-minute sub-maximal exercise protocol. The exercise protocol consisted of a 2-minute warm-up at 25W, followed by 10 minutes at 80W or 100W for female and male participants, respectively. Participants were instructed to maintain 70 RPM throughout the duration of the exercise protocol. This protocol was designed to induce mild stress on the cardiovascular system without crossing the aerobic threshold and limited the risk of musculoskeletal fatigue. No data were collected during the exercise period. Immediately upon cessation of exercise, a 6-minute stand test was conducted with eyes closed (forward gaze), and identical pre-test foot placement on the force platform. Approximately

30 seconds elapsed in the transition from the cycle ergometer to the force platform and initiate data acquisition.

4.3.2. Data Acquisition

After careful review, data from 18 participants (age: 25±2 years, height: 174±8cm, weight: 68±11 Kg, 8 females) were found appropriate for analysis. During the pre-exercise sit-to-stand test and post-exercise stand test, electrocardiography (ECG) was acquired with custom equipment from LifePak 8 (Medtronic Inc, MN, USA) in a standard Lead II electrode configuration. Continuous blood pressure was monitored through a non-invasive photoplethysmography finger cuff from Finometer Model 1 (FMS, Amsterdam, The Netherlands). Surface EMG signals were measured from four bilateral lower leg muscles: tibialis anterior, lateral soleus, and medial and lateral gastrocnemius. Transdermal differential recording of the signals was performed using the Bagnoli-8 (Delsys Inc, MA, USA) EMG system. The sites for surface EMG sensor placement were chosen based on recommendations from the SENIAM project. Postural sway data, in the form of COP coordinates (medial-lateral sway COPx and antero-posterior sway COPy) were derived from force and moment data obtained with an Accusway Plus force platform (AMTI, MA, USA). The exercise protocol was performed on a digital Jaeger ER 800 cycle ergometer (Wuerzburg, Germany). Data were acquired at a sampling rate of 1000 Hz using National Instruments PCI-6229 16-bit data acquisition platform and Labview 8.2 software (National Instruments Inc, TX, USA). Figure 4.2 demonstrated an example of experimental setup for acquisition of data pertaining to cardiovascular and postural systems.

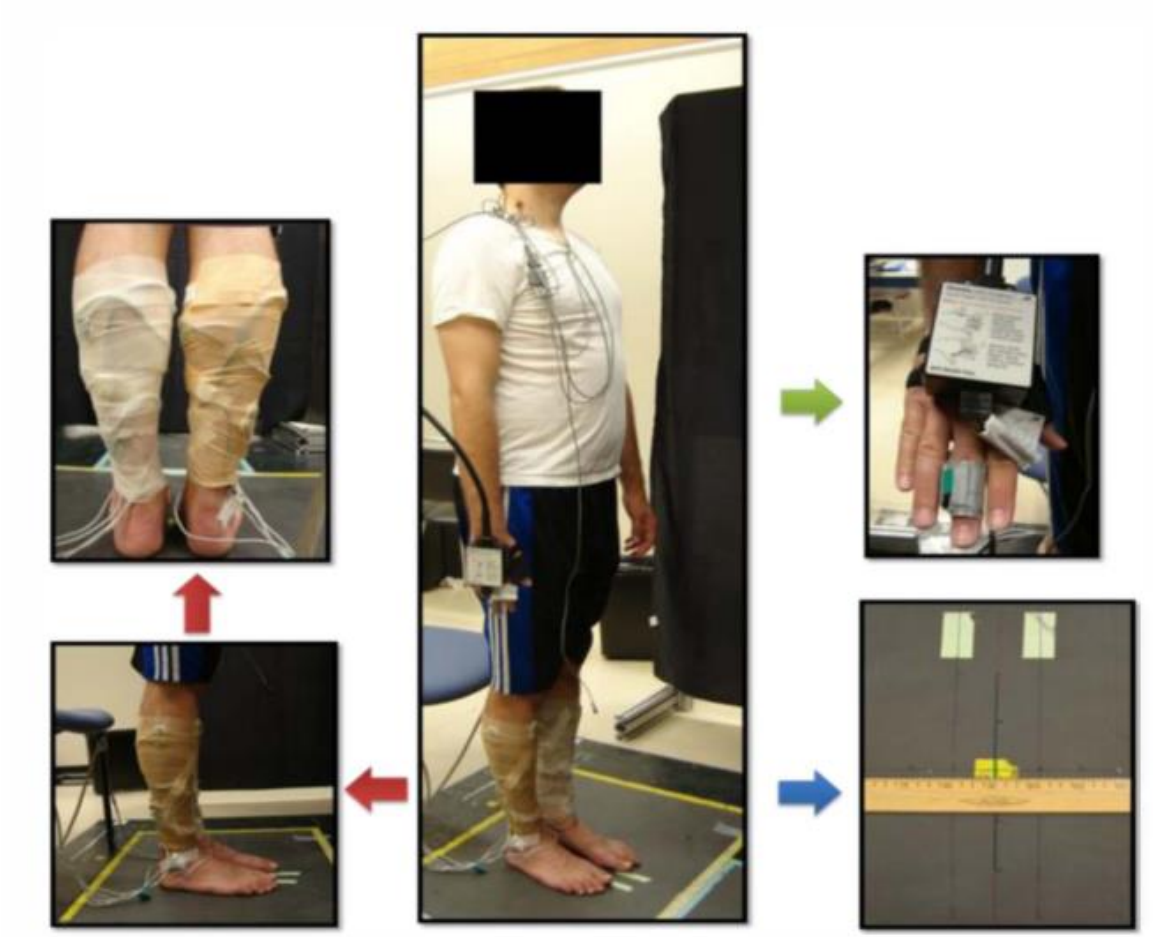

Figure 4.2. An example of experimental setup for acquisition of simultaneous blood pressure, calf electromyography, and postural sway (Centre). Calf electromyography acquired from four different leg muscles (left). Force platform right (bottom), and finger plethysmography (top right)(146).

4.3.3. Data Processing

Data analyses were implemented in MATLAB (MathWorks, MA, USA). The last five minutes of the quiet stance phase were used for analysis. The QRS complex was first detected from ECG based on a Pan-Tompkins algorithm, which yielded the time series of heartbeat period (i.e., RR-interval). Beat-by-beat time series of SBP were then obtained from the maximum pressure values of the blood pressure waveform within each RR-

interval while the diastolic blood pressure (DBP) time series was constructed by identifying the minimum blood pressure values prior to the SBP peak of the following beat. The beat-by-beat mean arterial pressure (MAP) was then calculated by averaging the blood pressure waveform between two adjacent DBP valleys.

Aggregate EMG was obtained by addition of rectified EMG signals from all individual leg muscles to represent the overall muscle activities. The EMG envelope was then captured by a moving average filter whose cutoff frequency was recommended by the SENIAM project to be within 5-20 Hz. Considering the low frequency response of cardio-postural control (<0.5 Hz), a cutoff frequency of 5 Hz was used for the filter in EMG envelope extraction to minimize the estimation uncertainty. Finally, analogous to the impulse of force, the area under the EMG envelope within each heartbeat (i.e., EMG impulse, EMG) was calculated to represent the muscle contraction strength on a beat-by-beat basis. The concept of impulse was employed because, in a beat-by-beat perspective, the strength of muscle contraction over a heartbeat would be related to the time period of that beat. That is, a brief strong contraction can be considered to be equivalent to weaker contractions over a longer period and the same contraction level would produce higher overall strength over a longer heartbeat. The resultant COP was obtained from COPx and COPy (i.e., $COPr=\sqrt{COPx^2+COPy^2}$) and the change rate of resultant COP was calculated as the first derivative of resultant COP and averaged within each beat (COPr). The resulted COPr time series represent the beat-by-beat postural sway velocity. All beat-by-beat time series were resampled to 10 Hz using spline interpolation prior to the causality and joint recurrence quantification analysis.

4.3.4. Statistical Analysis

Shapiro-Wilk test was employed to test the normality of data (SPSS, IBM Corporation, Armonk, NY). One-way test of ANOVA for normally distributed data otherwise Kruskal-Wallis test was employed to test the behavior of cardiovascular parameters strength of EMG↔COPr (EMG→COPr and COPr→EMG), EMG↔SBP (EMG→SBP and SBP→EMG), and COPr↔SBP (COPr→SBP and SBP→COPr), and joint recurrence quantification indices for cardio-postural coupling (EMG↔SBP, SBP↔COPr, and EMG↔COPr). Additionally, the effect of exercise on the behavior of cardiovascular parameters and each of the six causal events and three coupling pairs was studied using one-way test of ANOVA or Kruskal-Wallis test. Furthermore, whenever necessary the post-hoc analysis was performed via the Tukey-HSD method. All tabular data are presented as mean±SD while graphical data are presented as mean±SE.

Table 4.1. Detailed demographic information of study participants.

Participant #	Age	Weight	Height	Gender
1	25	57	165	Female
2	24	85	177	Male
3	25	63	177	Male
4	28	62	167	Female
5	27	67	181	Female
6	22	61	172	Female
7	27	74	177	Male
8	24	87	181	Male
9	23	66	172	Female

10	25	57	167	Female
11	28	63	179	Male
12	28	70	180	Male
13	23	52	168	Male
14	23	81	191	Male
15	24	61	157	Female
16	27	78	180	Male
17	27	69	178	Male
18	30	55	165	Female
19	22	58	162	Female
20	28	54	163	Female
21	28	86	177	Male

4.4. Results

The appropriate dimension of embedding for state space reconstruction was conducted using a false nearest neighbor algorithm (FNN) at a delay of 10 samples to account for changes within a heartbeat range. False nearest neighbor minimization of greater than 95% was achieved at the dimension of 4 for the last 4 minutes of data. Therefore, all strength of causality discussed in this chapter is reported at $\mathrm{E}=4 \text{ and } \tau=4$. Same parameters were chosen to perform joint recurrence quantification analysis, an additional parameter, the threshold was required which was chosen to be 1 based on distribution of % determinism. However, to ascertain behavior of embedding dimension of respective

cardio-postural signals the behavior was calculated at other values of delay for investigatory purposes, this is summarized in Figure 4. 3.

The CCM causality analysis resulted in the existence of a bidirectional interaction between baroreflex and muscle-pump baroreflex (EMG↔SBP), muscle pump and postural sway (EMG↔COPr), and baroreflex-postural sway (SBP↔COPr). The baroreflex causal events (SBP→EMG and SBP→COPr) were found to be significantly lower in strength compared to non-baroreflex events (EMG→SBP and COPr→SBP), Figure 4.4.

After establishing the baseline cardio-postural control of blood pressure, such behavior was studied after the application external perturbation to the system via mild exercise. The comparison of changes in the cardiovascular behavior before and after the exercise is summarized in Table 4.2, while the behavior of cardio-postural control of blood pressure is summarized in Table 4.3. Heart rate increased significantly ($p<0.05$) post exercise, SBP and EMG activity decreased significantly ($p<0.05$) post-exercise, while no change ($p>0.05$) in DBP, MAP, and COPr was observed. Spontaneous BRS changed significantly ($p<0.05$) post exercise.

A significant reduction ($p<0.05$) in baroreflex causality (SBP→EMG and SBP→COPr) was observed post-exercise. No change ($p>0.05$) in causal information flow in the non-baroreflex direction (EMG→SBP and COPr→SBP) was observed post exercise. Additionally, the strength of postural sway driven muscle pump activation (COPr→EMG) and muscle pump driven postural sway (EMG→COPr) reduced significantly ($p<0.05$) post exercise.

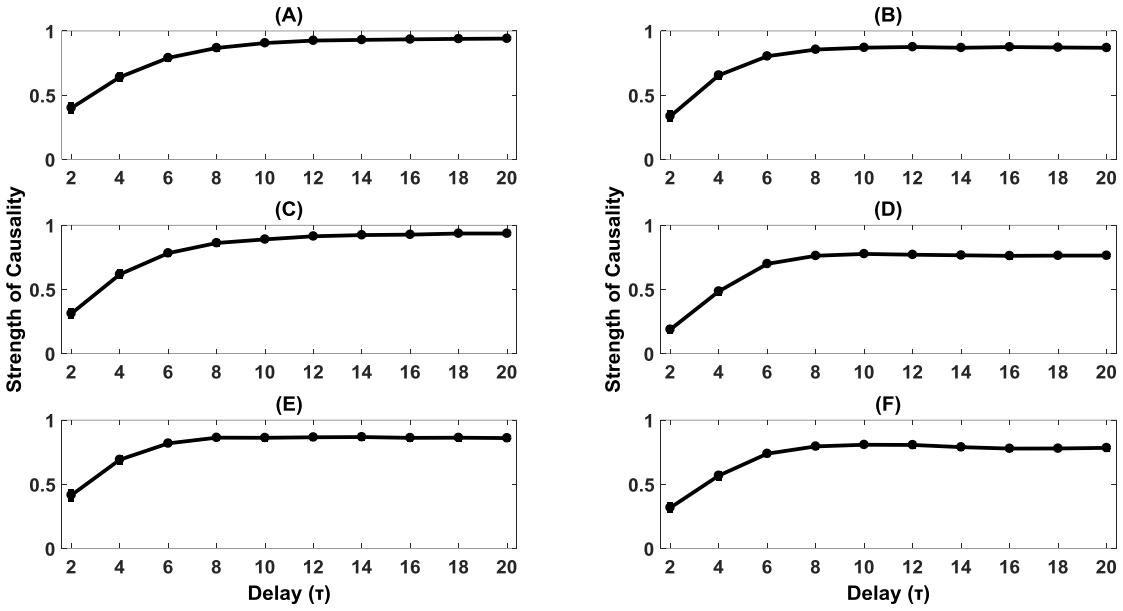

Figure 4.3. The behavior of different cardio-postural causality at different delay (τ) at chosen dimension of reconstruction (E=4). The causal events EMG→SBP (A), SBP→EMG (B), COPr→SBP (C), SBP→COPr (D), EMG→COPr (E), COPr→EMG (F). It can be observed that the strength of different causal events started to saturate at τ=10.

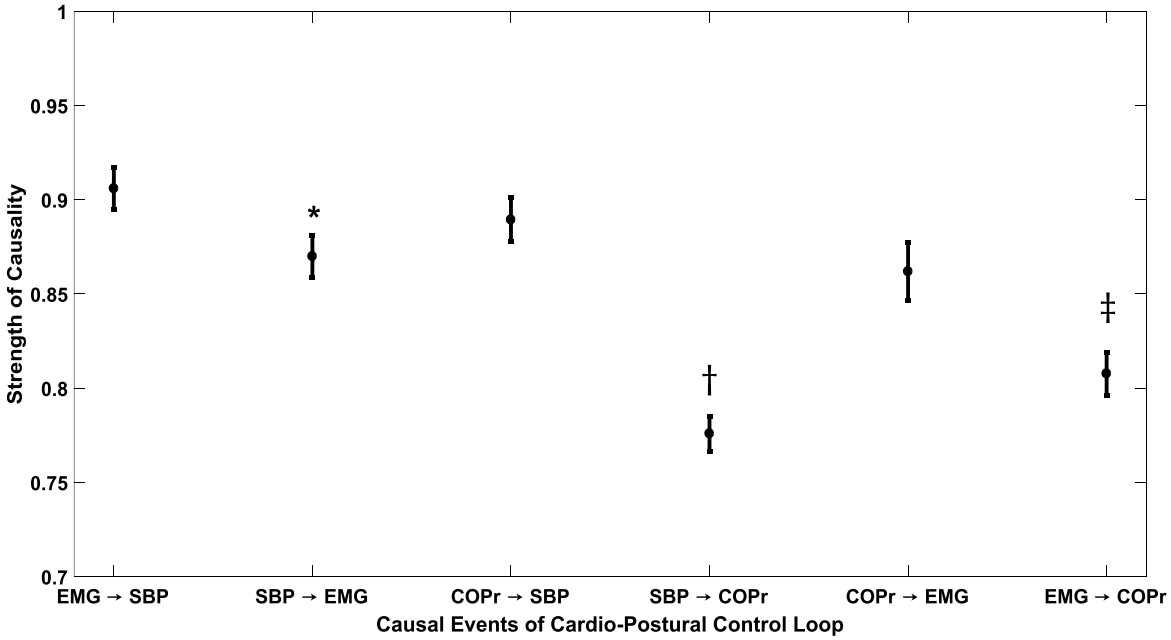

Figure 4.4. Representation of baseline behavior of different causal events during last 4-minutes of quiet standing. The non-baroreflex arm (EMG→SBP and COPr→SBP) of the interaction were significantly higher ($p<0.05$) than the baroreflex arm (SBP→EMG and SBP→COPr). The COPr→EMG causality was higher than the EMG→COPr. * Represents significant difference from EMG→SBP, † represents a significant difference from COPr→SBP, and ‡ represents a significant difference from COPr→EMG.

The effect of exercise on cardio-postural coupling is summarized in Table 4.3. The non-baroreflex events (EMG→SBP and COPr→SBP) remain statistically unchanged ($p>0.05$) post-exercise standing, while the baroreflex events (SBP→EMG and SBP→COPr) decreased significantly ($p<0.05$) post-exercise standing. Additionally, both COPr→EMG and EMG→COPr decreased significantly post-exercise (Table 4.3).

Table 4.2. Comparison of the behavior of different cardiovascular and postural control variables before and after exercise during standing. Results are considered significant at $\alpha=0.05$.

VARIABLES	Exercise	
	Pre	Post
HR (BPM)	77±10	86±15*
SBP (mmHg)	106±10	103±9*
DBP (mmHg)	67±5	66±7
MAP (mmHg)	82±7	80±7
BRS (ms/mmHg)	13±13	8±7*
EMG_{imp} (uV.s)	40±24	28±19*
$COPr_v$ (mm/s)	9±5	8±4

Table 4.3. Comparison of different cardio-poatural causal events before and after exercise during standing. * Represents significant difference at α=0.05.

Causal Events	Exercise	
	Pre	Post
EMG→SBP	0.92±0.04	0.91±0.04
SBP→EMG	0.88±0.05	0.82±0.09*
COPr→SBP	0.91±0.04	0.90±0.05
SBP→COPr	0.78±0.04	0.73±0.10*
EMG→COPr	0.81±0.05	0.73±0.12*

COPr→EMG	0.87±0.06	0.81±0.10*

The EMG signal used so far were aggregate of 4 different leg muscles, we also aim to study the role of individual leg muscles towards regulation of postural sway and blood pressure. Table 4.4. Summarizes the causal strength between respective muscle group and SBP and postural sway. A significant difference between the feedforward and feedback causalities were observed when medial-gastrocnemius and tibialis anterior muscle group were used as muscle pump marker. No difference was observed between the feedback and feedforward causality when other muscle groups (lateral soleus and lateral-gastrocnemius) were used a marker of muscle pump. Multiple comparison tests resulted in no difference ($p=0.71$) in the strength of directional information flow from respective muscle group towards SBP (feedforward causality). However, the causal information flow in the reverse direction i.e. SBP to respective muscle group was significantly different (Figure 4.5). The strength of $SBP \rightarrow EMG_{LG}$ and $SBP \rightarrow EMG_{MG}$ were significantly different, additionally, a significant difference was observed between $SBP \rightarrow EMG_{MG}$ and $SBP \rightarrow EMG_{TA}$. The causality between individual leg muscles and COPr signal was also studied, no difference was observed in such relationship, the results are summarized in Table 4.4.

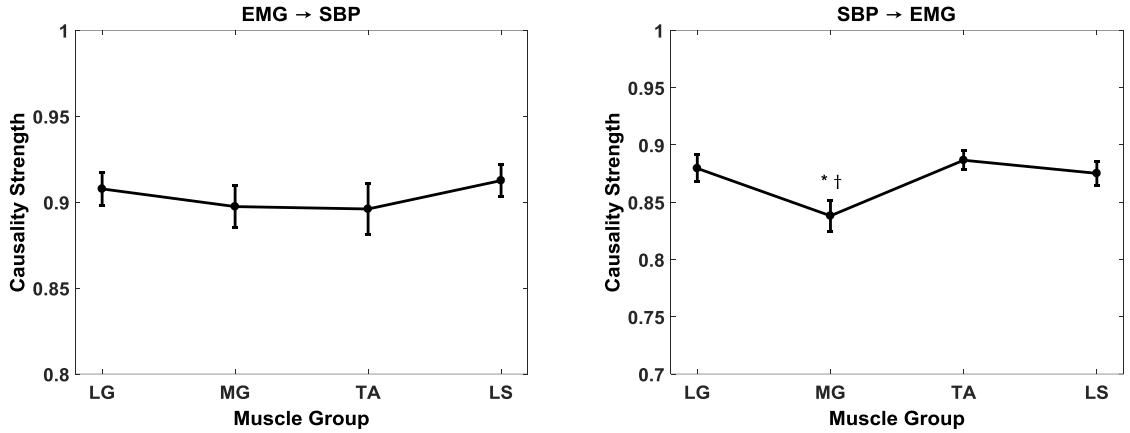

Figure 4.5. The role of individual leg muscles towards blood pressure regulation highlighted via EMG↔SBP causality. No difference ($p>0.05$) was observed between the causality from individual leg muscles towards SBP. The reverse causality SBP→EMG_{MG} was significantly different from SBP→EMG_{LG} and SBP→EMG_{TA}, marked by * and † respectively.

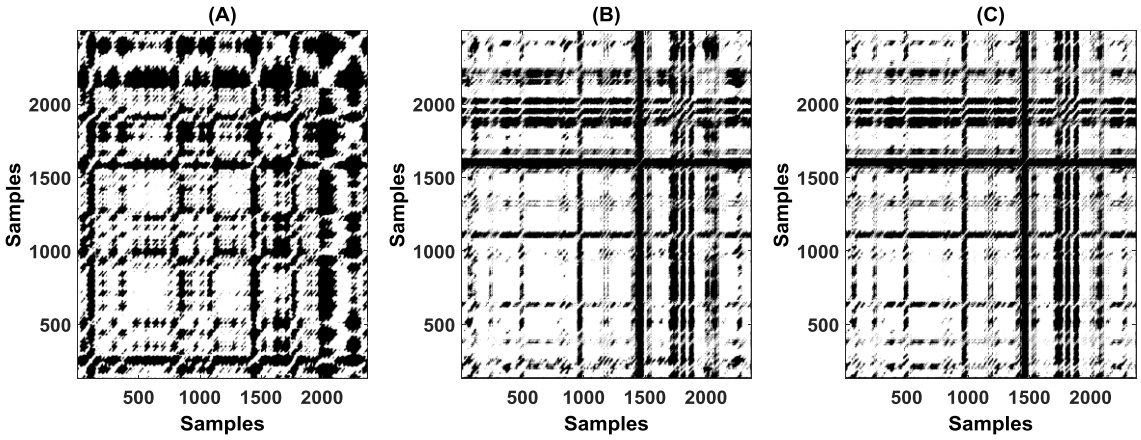

Figure 4.6. An example of joint recurrence plot for EMG↔SBP (A), COPr↔SBP (B), and EMG↔COPr (C) signal pairs during the last 4 minutes of standing from one participant (age: 25 years, height: 165, weight: 65, Female).

In additional to cause-and-effect relationship, the novel concept of joint-recurrence quantification analysis was also explored to further validate the inter-dependency between the cardiovascular and postural controls of blood pressure, The results, both for pre and

post exercise conditions are summarized in Table 4.5. It can be observed that strong coupling between the cardio-postural controls of blood pressure was observed. An example of joint recurrence plot for EMG↔SBP, SBP↔COPr, and EMG↔COPr is illustrated in Figure 4.6. Further, the effect of exercise had non-significant ($p>0.05$) impact on the recurrence behavior of the cardiovascular and postural controls of blood pressure.

4.5. Interpretation

4.5.1. Parameters Choice and Cardio-Postural Behavior

Accurate information regarding the degree of causal information flow from one system to the other via CCM method entails appropriate choice of embedding dimension and delay. For respective signals of the cardio-postural system, we empirically determined the input parameters of choice. The embedding dimension was first determined by varying the delay from 2 to 20 in a step of two, it was observed that for respective signals the false nearest neighbor was minimized around 4. Additionally, the ideal time delay was determined by analyzing different causal events at the choice of embedding dimension and different delays, these observation is summarized in Figure 4.3 for different signal pairs. After determining the overall behavior of signal pairs, the causality in this chapter is reported at $E=4$ and delay of 10 samples to account for changes within a heartbeat range.

A quantified knowledge of existence directional information flow between the signals representing the cardiovascular and postural systems can provide key information pertaining to individual's ability to maintain the prolonged stable stance. The key finding of the current research was the validation of the previous hypothesis of the existence of bi-directional or closed loop relationship between the variables representing cardio-postural control loop. Additionally, the current research highlighted alteration in the strength of such relationship post perturbation to the system induced by mild exercise.

The causal information flow from one variable to another was of variable degree indicating one system to be the dominant drive of other under given physiological condition. In case of muscle pump and muscle pump baroreflex (EMG↔SBP) interaction, the mechanical muscle pump mediated blood pressure changes (EMG→SBP) was of significantly higher strength compared to reverse causality (SBP→EMG), which is hypothesized to be muscle pump activation in response to blood pressure changes. This observation indicated muscle pump to be a dominant driver of the facilitating venous return to the heart, contrarily, muscle pump baroreflex although lower in strength was observed to activate skeletal muscles. Similarly, for postural sway and baroreflex (COPr↔SBP) interaction, the postural sway mediated blood pressure changes was significantly higher than reverse causality of baroreflex mediated postural sway (SBP→COPr), suggesting postural sway can lead to blood pressure fluctuation and further sway as a feedback result to maintain blood pressure equilibrium. For muscle pump-postural sway (EMG↔COPr) interaction, the causal information flow in the direction of postural sway to the muscle pump (COPr→EMG) was significantly higher than the causal information flow in the reverse direction (EMG→COPr). This observation is indicative of activation of calf skeletal muscle in response to postural sway and further sway of posture as a result of such activation, hence a closed loop interaction between the two signals to ascertain postural stability.

The causal behavior in the cardio-postural control loop highlighted the twofold role of postural sway; 1) activation of calf skeletal muscle facilitating control postural sway and simultaneously increasing venous return to the heart and 2) driving control of blood pressure in response to postural sway and further control of sway in response to fluctuations in blood pressure. There were two primary pathways of causal information flow were observed 1) the dominant non-baroreflex driven control of blood pressure via skeletal muscle activation and 2) weaker baroreflex driven control of postural sway via skeletal muscle activation. This bidirectional pathway to ascertain postural stability by

control of blood pressure and body sway is outlined in Figure 4.7. The dominant pathway is highlighted in black, while the non-dominant behavior is shown in red. These two pathways of cardio-postural control loop demonstrated the bidirectional transitive behavior (X↔Y and Y↔Z, then X↔Z, i.e. if there is a bidirectional causal behavior between X (COPr) and Y (EMG) and between Y and Z (SBP), then there should a bidirectional causal behavior between X and Z) towards regulation of blood pressure.

4.5.2. Effect of Exercise on Cardio-Postural Causality

To further assess the changes in the behavior of cardio-postural causality as a consequence of disturbance to hemodynamic homeostasis, a concept of mild cycling exercise was adopted. A short bout of exercise resulted in a significant reduction in RR intervals and SBP suggesting mild exercise was able to disturb the hemodynamic homeostasis. However, no change in DBP and MAP was observed. Our observation of reduced RR intervals (or increased heart rate) and SBP is in accordance with the existing findings in the literature. Moreover, spontaneous baroreflex sensitivity declined significantly post exercise, suggesting vagal withdrawal leading to increased heart rate to ascertain arterial blood pressure equilibrium (Table 4.2). Furthermore, no change in COPr but significant decline in EMG activity was observed post exercise (Table 4.3).

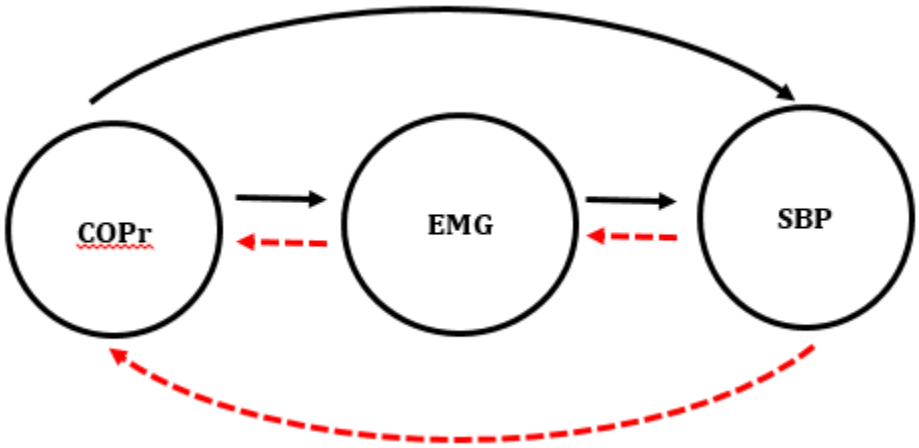

Figure 4.7. Two primary pathways of causal information flow in the cardio-postural control loop to assure stable upright stance. Dominant causality (black) represents feedforward control SBP via skeletal muscle activation and non-dominant baroreflex mediated correction of postural sway as a feedback control (red).

Orthostatic intolerance is a result of the failure of cardiac as well as postural controls of blood pressure, however, often the two controls governing blood pressure are looked independently. We have shown in this chapter a significant role of muscle pump baroreflex towards activation of calf skeletal muscles to pump the pooled venous blood back to the heart in addition to well-known mechanical feedforward muscle pump. Therefore, the cardio-postural control of blood pressure should always be considered when addressing orthostatic intolerance. As per our hypothesis, we expected greater pooling of central blood volume in the compliant venous system, which would evoke a greater degree of muscle pump baroreflex (SBP→EMG) to facilitate pooled venous blood back to the heart. In contrary to our hypothesis, we observed a significant decline in the strength of muscle pump baroreflex, which was further accompanied by a decline skeletal muscle activation.

Despite significant drop in the muscle pump baroreflex, the strength of non-baroreflex mechanical muscle pump remain unchanged, this observation along with no change in the

mean arterial pressure and DBP suggesting system was less stressed post-exercise lead us to speculate a less stressed system post exercise which could result in resetting of skeletal muscle activation post-exercise evident from a significant decline in skeletal muscle activity post exercise. A further decline in the strength of COPr→EMG causality and EMG→COPr causality with the dominant causality i.e. COPr→EMG remain unchanged post-exercise highlights the systemic disassociation of postural control loop, which could have resulted from increased postural sway via sources other than skeletal muscle contraction such as respiration.

4.5.3. Effect of Individual Calf Muscles on Cardio-Postural Causality

The role of individual leg muscles towards blood pressure regulation and postural sway was also investigated. The knowledge of such behavior can assist the design of appropriate therapy regime or exercise to target specific muscle group during rehabilitation or to prevent muscle atrophy during long-duration spaceflight. We observed no change in the behavior of causal information flowing from postural sway to individual muscle group ($p=0.71$), similarly, no change ($p=0.32$) was observed in the reverse causal information flow i.e. causal information flow from individual leg muscles towards postural sway (Table 4.4). These findings suggest that activation of all four calf leg muscles are equally important and shall be considered altogether when addressing an issue related to balance.

For directional interaction between individual leg muscles and blood pressure, we observed no change in the strength of causal information flow from individual leg muscles towards SBP (Figure 4.5), suggesting well-activated calf muscles to propel the venous blood back to the heart. The strength of reverse causality i.e. muscle pump baroreflex was significantly different in the direction of lateral-gastrocnemius and tibialis anterior compared to medial-gastrocnemius. While no change was observed in EMG_{MG}→SBP

compared to other muscle groups, a significant decline in reverse causality i.e. SBP→EMG_{MG} leads us to speculate the reliance of medial-gastrocnemius muscle group on other factors such as postural sway and respiration, further highlighting a strong intersystem interaction between cardio-postural control loop towards facilitating blood pressure regulation and upright stance.

Table 4.4. Causality of individual leg muscles with SBP and COPr.

Causal Events	**Causality Strength**
EMG_{LG}→SBP	0.90±0.04
EMG_{MG}→SBP	0.89±0.07
EMG_{TA}→SBP	0.89±0.06
EMG_{LS}→SBP	0.91±0.04
SBP→EMG_{LG}	0.87±0.05
SBP→EMG_{MG}	0.83±0.05
SBP→EMG_{TA}	0.88±0.03
SBP→EMG_{LS}	0.87±0.04
EMG_{LG}→COPr	0.79±0.05
EMG_{MG}→COPr	0.80±0.05
EMG_{TA}→COPr	0.82±0.08
EMG_{LS}→COPr	0.79±0.05
COPr→EMG_{LG}	0.86±0.05

$COPr \rightarrow EMG_{MG}$	0.86±0.06
$COPr \rightarrow EMG_{TA}$	0.87±0.05
$COPr \rightarrow EMG_{LS}$	0.87±0.06

4.5.4. Interdependency between Cardiovascular and Postural Controls using Joint Recurrence Quantification Analysis

Recurrence quantification has been widely studied in the literature to address physiological problems, however, the extension of recurrence quantification analysis i.e. joint recurrence quantification to address existing physiological problem is limited in the literature. The interplay between the physiological systems is expected under given physiological condition to maintain homeostasis, therefore, not accounting for existing coupling between the systems can lead to inadequate information regarding the underlying physiology. In this chapter, we quantified the coupling between the EMG↔SBP, COPr↔SBP, and EMG↔COPr signal pairs. The joint recurrence features i.e. recurrence rate (RR), the average length of adjacent recurrence points (Mean L), Shannon entropy of the distribution of the diagonal lines (Entropy L), the average length of diagonally adjacent recurrence points (Mean V), and Shannon entropy distribution of vertical lines (Entropy V).

An example of joint recurrence plot for EMG↔SBP, COPr↔SBP, and EMG↔COPr is illustrated in Figure 4.6, while the results for each pair under the pre and post exercise conditions are summarized in Table 4.5. No change ($p>0.05$) was observed in the dynamics of any of signal pairs following a short bout of exercise (Table 4.5). This observation was indicative of system homeostasis was not disturbed following a short bout

of exercise. The behavior of different JRQA features was compared for the three interactions (EMG↔SBP, COPr↔SBP, and EMG↔COPr) to highlight the baseline behavior of this coupling, this comparison resulted in significant change between the three pairs, and the post-hoc comparison p-value is summarized in Table 4.6 for pre-exercise and 4.7 for post-exercise. For pre-exercise comparison, a significant difference was observed for the three comparisons except for the recurrence rate (EMG↔SBP vs COPr↔SBP, p=0.77) and the average length of diagonally adjacent recurrent points (EMG↔SBP vs SBP↔COPr, p=0.08 and COPr↔SBP vs EMG↔COPr, p=0.07). For post-exercise comparison, no change (p>0.05) was observed for any comparison in recurrence rate. No change was observed in the average length of recurrent points (Mean L) for COPr↔SBP and EMG↔COPr comparison. In case of diagonally adjacent recurrence points (Mean V), no change was observed for EMG↔SBP vs SBP↔COPr (p=0.05) and COPr↔SBP vs EMG↔COPr comparison.

Table 4.5. Joint Recurrence Quantification Analysis of Cardio-Postural Variables during pre and post exercise. * Represents significant difference from pre-exercise.

JRQA Features	**Pre-Exercise**			**Post-Exercise**		
	EMG↔SBP	COPr↔SBP	EMG↔COPr	EMG↔SBP	COPr↔SBP	EMG↔COPr
% REC	57.44±1.59	58.36±4.82	61.86±4.57	58.48±2.65	58.62±3.39	61.25±6.01
Mean L	75.73±21.33	52.91±24.10	35.66±15.02	77.60±25.23	49.45±26.82	29.59±23.43
Entropy L	7.43±0.52	6.59±0.82	5.77±0.65	7.41±0.56	6.35±0.95	5.33±0.85
Mean V	90.71±33.35	69.5±31.90	47.40±19.34	93.01±38.12	65.18±35.08	40.59±28.73

Entropy V	7.54±0.51	7.05±0.63	6.37±0.39	7.51±0.52	6.86±0.73	6.06±0.63

Table 4.6. Comparison of different JRQA features for EMG↔SBP, COPr↔SBP, and EMG↔COPr signal pairs during pre-exercise experimental protocol. Table list post-hoc comparison p-values. * Represents significant difference.

JRQA Features	**EMG↔SBP Vs SBP↔COPr**	**EMG↔SBP Vs EMG↔COPr**	**COPr↔SBP Vs EMG↔COPr**
% REC	0.77	0.004*	0.03*
Mean L	0.004*	<0.001*	0.04*
Entropy L	0.004*	<0.001*	0.001*
Mean V	0.08	<0.001*	0.07
Entropy V	0.02*	<0.001*	<0.001*

Table 4.7. Comparison of different JRQA features for EMG↔SBP, COPr↔SBP, and EMG↔COPr signal pairs during post-exercise experimental protocol. Table list post-hoc comparison p-values. * Represents significant difference.

JRQA Features	**EMG↔SBP Vs**	**EMG↔SBP Vs**	**COPr↔SBP Vs**

	SBP↔COPr	EMG↔COPr	EMG↔COPr
% REC	0.99	0.14	0.16
Mean L	0.004*	<0.001*	0.06
Entropy L	<0.001*	<0.001*	0.001*
Mean V	0.05	<0.001*	0.09
Entropy V	0.009*	<0.001*	0.001*

4.5.5. Limitations

The major limitation of the study was availability of data from only young and healthy population, in which post-exercise vasodilation leading to excessive pooling of blood was not as effective as hypothesized. Consequently, our initial hypothesis of achieving greater pooling in the compliant venous system post-exercise was rendered inadequate. Therefore, the role of muscle-pump baroreflex (SBP→EMG) as a dominant driver of EMG↔SBP was not validated in this research as blood pressure was well regulated; suggesting blood pooling post-exercise was not significant compared to pre-exercise. In the future study, a concept of near-infrared spectroscopy shall be adopted to accurately measure the degree of blood pooling achieved during orthostatic stress. The investigation of causal behavior in relation to the degree of blood pooling achieved will extend our knowledge regarding the cardio-postural control of blood pressure. Moreover, potential JRQA to gain insights regarding the impairment of cardiovascular and postural controls needs to be studied in relation to challenging experimental protocol which can disturb the homeostasis of the system. Furthermore, involving other signals such as respiration known to affect both venous return and postural sway will further our understanding

pertaining to underlying mechanisms of blood pressure regulation during standing and validation of a model for early detection of fall proneness.

Chapter 5.

Validation of Short-arm Human Centrifuge as a Tool for Mitigating Post-Flight Orthostatic Intolerance in Astronauts

5.1. Summary

Background: Autonomic control of blood pressure is essential towards maintenance of cerebral perfusion during standing, failure of which could lead to fainting. Long-term exposure to microgravity deteriorates autonomic control of blood pressure. Consequently, astronauts experience orthostatic intolerance on their return to the gravitational environment. Ground-based studies suggest sporadic training in artificial hypergravity can mitigate spaceflight deconditioning. In this regard, short-arm human centrifuge (SAHC), capable of creating artificial hypergravity of different g-loads, provides an auspicious training tool. Here, we compare autonomic control of blood pressure during 2-g centrifugation at feet with standing in natural gravity. **Methods:** Continuous electrocardiography and blood pressure were acquired simultaneously from 13 healthy participants during supine, standing, and 2-g centrifugation, from which heart rate (RR) and systolic blood pressure (SBP) were derived. The autonomic blood pressure regulation was assessed during supine, standing, and 2-g centrifugation via spectral analysis of SBP and RR, spontaneous baroreflex sensitivity, and non-linear heart rate and blood pressure causality. **Results:** While these blood pressure regulatory indices were significantly different during standing and 2-g centrifugation compared to supine, a non-significant difference was observed in the same indices during 2-g centrifugation compared to standing. **Conclusions:** Outcome of the analysis conducted in this chapter highlighted the

capability of SAHC towards evoking blood pressure regulatory controls analogous to standing, therefore, a potential utility towards mitigating post-flight orthostatic intolerance.

5.2. Background

Right from birth, humans experience gravity, which pulls the human body towards the earth with a force equivalent to the product of the body mass and the gravitational acceleration i.e. 9.8 m/s^2(147). Therefore, quintessential physiological performance is highly dependent on gravity(52,148). Physiological adaptation, a result of long-term microgravity exposure, can cause changes in physiological functions(128,149–152). Of such, cardiovascular adaptation to microgravity can have detrimental effects on the autonomic control of blood pressure upon return to the gravitational environment(52,153). Orthostatic intolerance, an inability to regulate blood pressure on assuming upright stance(154,155), is commonly experienced by astronauts on their return to Earth after long-duration spaceflight(156,157). Typically, one in four astronauts fails to maintain 10-minutes of quiet stance on the landing day(158). The success of envisioned Mars exploration would entail frequent long-duration spaceflight in the future(159–161). To this end, profound investigation of potential countermeasures is warranted to mitigate the adverse effects of microgravity on physiological performance to facilitate healthy life for astronauts on their return to Earth(161).

The transition of posture, from supine to standing, reduces the blood pressure at the brain level (~ 70 mmHg) and increases the blood pressure at the feet level (~ 200 mmHg), as a consequence of gravity(55,153). Central blood volume, owing to gravity induced hydrostatic pressure gradient, is displaced below heart level and venous return and preload are reduced challenging blood pressure equilibrium, see Figure 5.1. Regulating blood pressure is imperative for the sustainability of prolonged and stable upright stance,

otherwise, cerebral perfusion will be challenged resulting in a feeling of dizziness and eventually syncope. During a physiological state of standing, blood pressure is regulated via reduced afferent discharge of the baroreceptor impulses localized in the carotid sinus and the aortic arch, leading to increased heart rate and systemic vascular resistance via neural efferent pathways resulting in vagal withdrawal and sympathetic nerve activation(60,162).

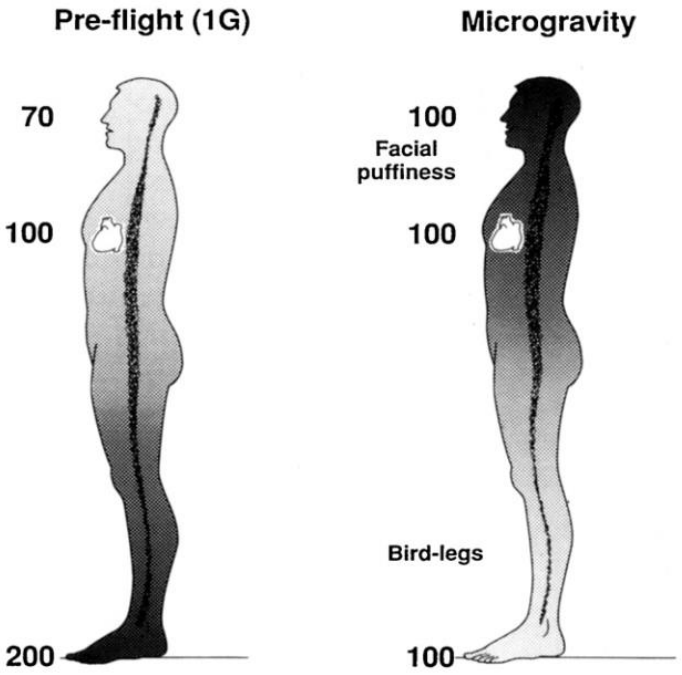

Figure 5.1. Comparison of the distribution of central blood volume during standing at Earth (1-G) and in microgravity. Blood is translocated above heart level due to increased mean arterial pressure at the brain level in a microgravity environment(55).

Therefore, to cope with the effects of an orthostatic challenge on physiological performance, autonomic, baroreceptor, and vasomotor controls play a consequential role to various degrees. Enfeebled or impaired blood pressure regulatory controls owing to long-term microgravity exposure could lead to an abrupt decline in arterial blood pressure on assuming upright stance resulting in reduced cerebral perfusion(3,129,163). Thus,

impaired autonomic control has an ominous effect on the individual's ability to maintain standing(52,147,153).

Ground-based experiments, performed to comprehend physiological response to microgravity simulated via bed rest immobilization(164–166) and potential countermeasures such as exercise training, lower-body negative pressure, and artificial gravity(119,153,167), have concluded an intermittent exposure to artificial hypergravity as an important factor towards improving orthostatic tolerance(58,59,153,168). The short-arm human centrifuge (SAHC), in this regard, can serve as a promising training tool(59,169,170). The feasibility of short-arm centrifuge to be a part of a long duration spaceflight, owing to compact modern design, has opened new avenues towards minimizing the severity of microgravity-induced systemic deconditioning(169,171–173). Figure 5.2 shows the concept of artificial gravity created via short-arm human centrifuge.

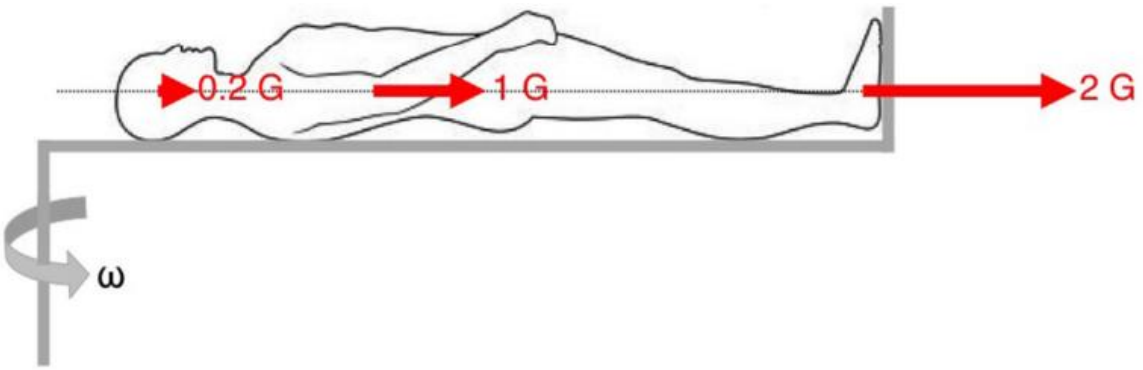

Figure 5.2. The concept of short-arm human centrifuge to create artificial gravity at feet. The magnitude of the artificial gravity created at feet depends on the rotating speed (ω) of the short-arm human centrifuge(170).

In the previous work from our group(174), we demonstrated the response of cardiovascular and the cerebrovascular system during 2-g centrifugation at feet to be analogous to orthostatic challenge exerted by standing in a natural gravity. However, the

response of blood pressure regulatory indices to 2-g centrifugation at feet in relation to standing in a natural gravity remains to be generalized. In the current analysis, we extend our previous work to a comparison of the response of autonomic control of blood pressure during 2-g centrifugation in relation to standing. The autonomic control of blood pressure was assessed via causal heart rate-blood pressure interaction, spontaneous baroreflex sensitivity, and spectral analysis of SBP and RR time series.

5.3. Method

5.3.1. Experimental Protocol and Data Acquisition

The detailed experimental protocol has been explained in the previous work from our group(174). Here, we briefly outline the experimental protocol with respect to the current research. All participants were pre-screened for physical and medical status. None of the participants had a prior history of cardiovascular, neurological, and musculoskeletal diseases or vasovagal syncope. Twelve hours prior to experimentation, all participants were required to refrain from alcohol, caffeine, and any medication.

In the centrifuge, the participant was strapped with their head near the center of 2.8-meter radius centrifuge and feet outwards. In this orientation, the g-load at the feet is hypothesized to be proportional to the rotational speed of the centrifuge, while at the head the g-load is approximately zero, therefore simulating the typical hydrostatic difference created by standing in a natural gravity(57). The participant remained supine in the centrifuge for 20 minutes of baseline recording. After completion of baseline, the participant was transitioned into the standing position for 5 minutes of stand test. After stand test, participant lay supine in the centrifuge for another 15 minutes, after which the centrifuge was ramped up to a rate that applied 2-g at feet (0.44g at Middle Cerebral Artery and 0.75g at the heart). The participant was kept at 2-g for 5 minutes. Following 5 minutes

of centrifugation at 2-g the centrifuge rotation was slowed and halted in 30 seconds. The centrifuge facility at MEDES, France was used in this research.

Data were acquired simultaneously from 13 participants (age: 28.08±8.4 year, height: 172±6.9 cm, weight: 67.6±10.5 kg, 6 females). Detailed demographic information is listed in Table 5.1. Electrocardiogram was acquired with a standard lead II configuration using LifePak8 (Medtronic Inc, MN, USA) and continuous blood pressure from non-invasive finger photoplethysmography cuff (Portapress, FMS, The Netherlands) using NI data acquisition (National Instruments Inc., TX, USA) system at a sampling rate of 1000 Hz.
Ethics approval for experimentation was obtained from the University of Toulouse. Experimentation complied with rules and regulations set forth by the research ethics board of the University of Toulouse. Written and informed consent form for participation was obtained from each participant prior to any experimentation.

5.3.2. Data Processing

The QRS complex was detected using Pan-Tompkins algorithm(175), from which, R-R time series was obtained. Systolic blood pressure (SBP) and diastolic blood pressure (DBP) were obtained from continuous blood pressure waveform as the maximum and minimum values between adjacent R peaks, respectively. Mean arterial pressure (MAP) was derived from SBP and DBP as; $MAP=\frac{2}{3}\times DBP+\frac{1}{3}\times SBP$.

RR interval and SBP time series were interpolated using spline interpolation to generate an evenly sampled signal and resampled to 2 Hz with zero mean before conducting the spectral analysis. The Welch power spectral density (PSD) of RR and SBP was calculated in very low frequency (VLF, 0-0.04 Hz), low frequency (LF, 0.04-0.15), and high frequency (HF, 0.15-0.4 Hz) bands. There upon, the RR and SBP power distributed (P) in the

respective bands were normalized as VLF_{nu}= P_{VLF} ÷Total Power, LF_{nu}=P_{LF} ÷Total Power, and HF_{nu}=P_{HF} ÷Total Power, where Total Power=P_{VLF}+P_{LF}+P_{HF}. The PSD was computed with a Hamming window of size 128 samples and 50% overlap.

The arterial baroreflex sensitivity was calculated using sequence method(176,177) by using CardioSeries computer software V2.4 (http://www.danielpenteado.com) similar to other research in the literature(178,179). Beat-to-beat RR intervals and SBP were input to the software, search for a sequence of at least three consecutive beats in which increase in SBP was followed by an increase in RR intervals (upslope) and decrease in SBP followed by a decrease in RR intervals (downslope) with a correlation greater than 0.8 was considered. The slope of linear regression between SBP and RR intervals was considered as a marker of spontaneous BRS. In addition to BRS, the number of baroreflex and non-baroreflex sequences were also calculated.

The strength of closed loop heart rate-blood pressure interaction (RR↔SBP), signifying the feedforward(non-baroreflex) and feedback (baroreflex) controls of blood pressure was obtained using convergent cross mapping (CCM) similar to our previous work(27,142). Prior to causality analysis, the evenly sampled continuous RR and SBP signals were resampled to 10 Hz. Mathematical details of the methodology are provided in the supplementary material of Sugihara et al(75) and in a book on time series analysis by McCracken et al(80).

Table 5.1. Detailed demographic information of study participants.

Participant #	Age	Height	Weight	Gender
1	23	172	73	Male
2	31	165	55	Female

3	24	164	56	Female
4	25	169	62	Female
5	25	176	75	Male
6	35	175	76	Male
7	23	165	53	Female
8	29	175	79	Male
9	24	174	55	Female
10	35	189	84	Male
11	39	178	73	Male
12	37	166	72	Male
13	32	169	68	Female

5.3.3. Statistical Analysis

Test for normality of the data was conducted using Shapiro-Wilk test (SPSS, IBM Corporation, Armonk, NY). A multiple comparison test was conducted using one-way test of ANOVA (for normally distributed data) or Kruskal-Wallis test (data failed normality) followed by post-hoc analysis using the Tukey-HSD method to account for the significance of changes in the cardiovascular parameters and blood pressure regulatory indices during different experimental conditions. The test of significance was conducted using a statistical toolbox of MATLAB (Mathworks Inc., MA, USA). The test results at $\alpha=0.05$ were considered significant. All tabular data in the article are presented as mean±SD unless mentioned otherwise.

5.4. Results

Test of normality resulted in data exhibiting mixed behavior given the limited sample size, therefore, Kruskal-Wallis test followed by post-hoc analysis using Tukey-HSD method was conducted to account for difference exerted by different experimental conditions on the cardiovascular parameters as well as on the blood pressure regulatory indices. Table 5.2 summarizes the behavior of cardiovascular parameters during supine rest, standing, and 2-g centrifugation. Stand test or application of 2-g centrifugation inflicted no change in SBP ($p=0.25$), DBP ($p=0.58$), or MAP ($p=0.44$). RR intervals reduced significantly during standing ($p=0.01$) and 2-g ($p<0.001$) compared to supine. No change ($p=0.38$) in RR intervals was observed between standing and 2-g.

Table 5.2. Values (mean±SD) of cardiovascular parameters during supine, standing, and 2-g. * Represents significant difference from supine.

Parameters	Supine	Stand	2-g
R-R (ms)	967±177	755±135*	669±115*
SBP (mmHg)	110±15	122±21	114±20
DBP (mmHg)	58±9	65±17	61±16
MAP (mmHg)	75±10	84±17	79±17

Figure 5.3 summarizes the normalized spectral power distribution in the VLF, LF, and HF bands of SBP and RR intervals. Table 5.3 lists the post-hoc comparison p-value between experimental conditions for respective frequency bands. Significant change ($p<0.05$) was observed in SBP_{VLF}, SBP_{LF}, and $RR_{LF/HF}$ during stand and 2-g compared to supine. SBP_{HF}

and RR_{HF} showed significant change ($p<0.05$) only at 2-g compared to supine. No change ($p>0.05$) was observed in the spectral power distribution in any frequency bands of SBP and RR at 2-g compared to standing (Table 5.3).

Baroreflex sensitivity decreased (both up and down slope) significantly during standing (up slope, $p=0.01$ and down slope, $p=0.003$) and 2-g (up slope, $p<0.001$ and down slope, $p<0.001$) compared to supine. No change (up slope, $p=0.50$ and down slope, $p=0.31$) in BRS was observed at 2-g compared to standing. The number of baroreflex sequence decreased only at 2-g ($p<0.001$) compared to supine, Table 5.3. No change ($p>0.05$) in a number of non-baroreflex sequence was observed as a consequence of different experimental conditions (Table 5.3). The distribution of BRS for the study group is detailed in Figure 5.4.

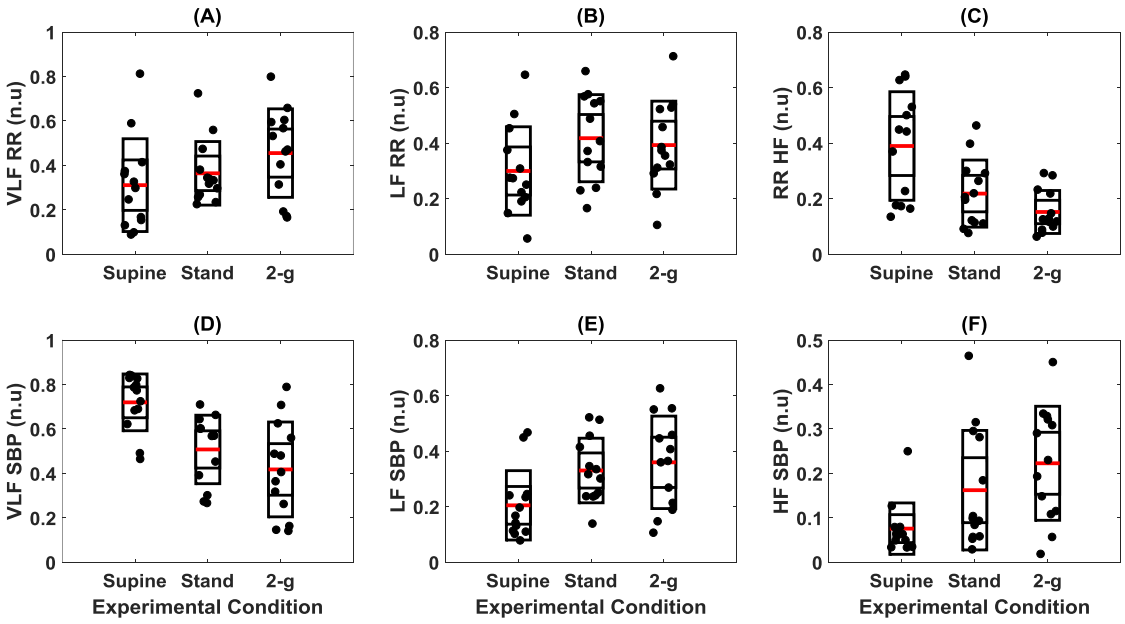

Figure 5.3. Distribution of systolic blood pressure and RR intervals spectral power (n.u). The figure details RR (A-C) and SBP (D-F) spectral power distribution in the VLF (0-0.04

Hz), LF (0.04-0.15 Hz, and HF (0.15-0.4 Hz) bands during supine, stand, and 2-g experimental protocol.

The optimal embedding dimension to perform non-linear state space reconstruction in CCM was determined via false nearest neighbor algorithm at a delay of 10 samples to account for changes within a heartbeat range. The optimal dimension of reconstruction was determined to be 4 for SBP and RR based on the minimization of the false nearest neighbor using CRP toolbox in MATLAB(180,87). Therefore, the RR↔SBP causality was computed at an embedding dimension of 4 and delay of 10 samples unless mentioned otherwise. The causal behavior between RR and SBP is detailed in Figure 5.5.

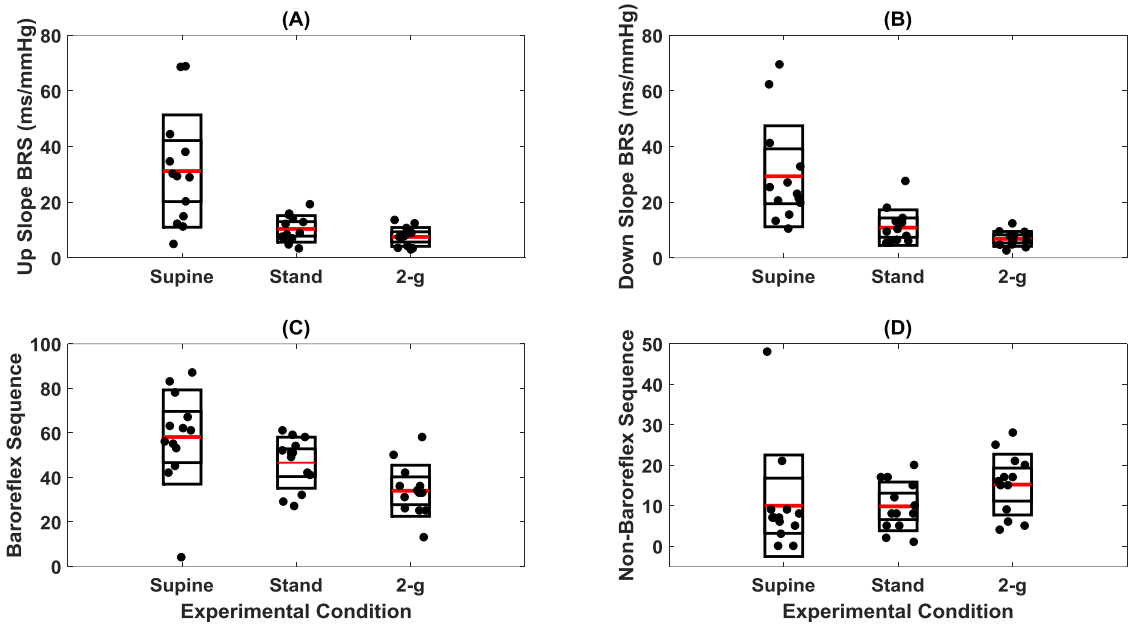

Figure 5.4. Spontaneous baroreflex sensitivity determined via sequence method. Figure details the distribution of up slope BRS (A), down slope BRS (B), number of baroreflex sequences (C), and number of non-baroreflex sequences (D) during supine, stand, and 2-g.

At supine rest, the non-baroreflex arm of the heart rate and blood pressure interaction was significantly higher than the baroreflex arm. During standing (p=0.009) and 2-g centrifugation (p=0.03), a significant increase in baroreflex arm of the interaction compared to supine was observed, while no change (p>0.05) in the non-baroreflex arm of the interaction was observed. Additionally, no difference between the standing and 2-g centrifugation was observed in either arm (RR→SBP, p=0.80 and SBP→RR, p=0.88) of the heart rate and blood pressure interaction (Table 5.3). Table 5.4 lists the values (mean±SD) of all blood pressure regulatory indices during supine, standing, and 2-g.

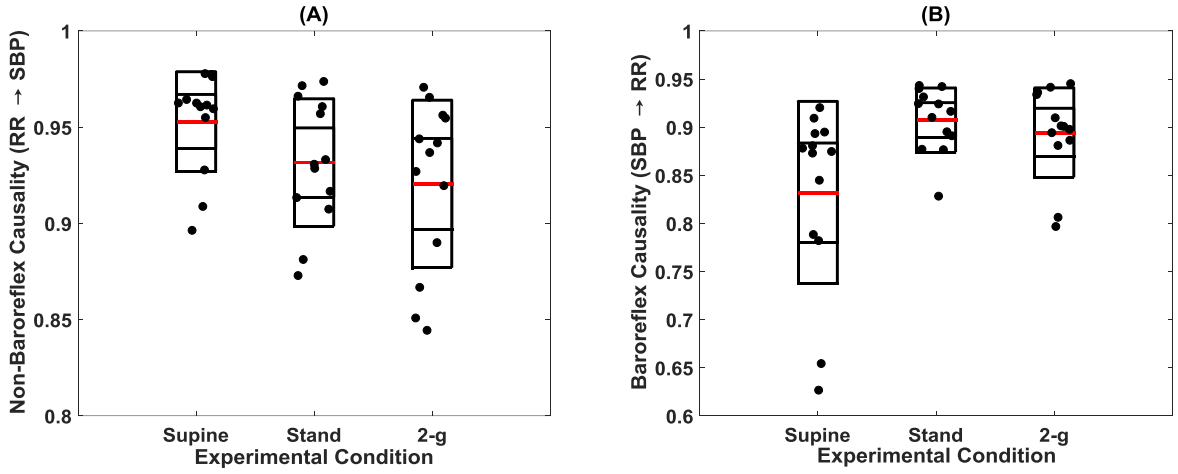

Figure 5.5. Boxplot representation of non-baroreflex (feedforward) and baroreflex (feedback) causalities in response to supine, stand, and 2-g.

5.5. Interpretation

The current research investigated the capability of 2-g centrifugation at feet to evoke autonomic control of blood pressure analogous to standing. The autonomic blood pressure control via causal heart rate-blood pressure interaction, spontaneous baroreflex sensitivity, and spectral analysis of SBP and RR were studied. The analysis results ascertained previously contemplated yet undocumented potential of the short-arm human

centrifuge to evoke autonomic blood pressure control analogous to standing in natural gravity, therefore, a potential utility towards minimizing the adverse effects of long-term microgravity exposure on the cardiovascular performance, hence, minimizing orthostatic intolerance in astronauts upon return to Earth.

Table 5.3. Comparison of changes in blood pressure regulatory indices inflicted by different experimental conditions. Table lists post-hoc comparison p-values. Significant results ($p<0.05$) are marked with *.

Variables and Conditions To Compare	**Supine Vs Stand**	**Supine Vs 2-g**	**Stand Vs 2-g**
SBP_{VLF}	0.01*	<0.001*	0.66
SBP_{LF}	0.04*	0.02*	0.97
SBP_{HF}	0.16	0.005*	0.40
RR_{VLF}	0.63	0.10	0.50
RR_{LF}	0.09	0.24	0.88
RR_{HF}	0.07	0.002*	0.47
$RR_{LF/HF}$	0.04*	0.003*	0.65
$BRS_{up\ slope}$	0.01*	<0.001*	0.50
$BRS_{down\ slope}$	0.003*	<0.001*	0.31
Non-Baroreflex Sequence	0.76	0.07	0.28
Baroreflex Sequence	0.15	<0.001*	0.12
RR→SBP	0.23	0.06	0.80

SBP→RR	0.009*	0.03*	0.88

The success of future inter-planetary missions to Mars depends on the design of pertinent countermeasures to mitigate the adverse effects of spaceflight deconditioning. The shift of central blood volume above thoracic leading to increased ventricular filling, stroke volume, and cerebral blood flow is an immediate consequence of physiological adaptation to microgravity. Accordingly, baroreceptor unloading, autonomic sympathetic nerve activity, and the vasomotor control remain vastly inhibited for the duration of spaceflight(55,158,181). The prolong inhibition of such blood pressure regulatory controls can have an adverse effect on individual's orthostatic tolerance level, which can be analogous to aging and/or pathology(53,182). Additionally, the microgravity-induced cephalic fluid shift could lead to increased intracranial pressure which may cause an alteration in vision and anatomy of the eye(183,184) and could further challenge postural stability on return to the gravitational environment.

Furthermore, decreased blood flow to the peripheral regions, especially to the calf skeletal muscles, render posture muscle group with nutritional scarcity, and is a major contributor towards skeletal muscle atrophy, bone remodeling, and decline in the calf circumference(152,164,185). While assuming upright stance on a return to the gravitational environment, the blood pressure regulatory controls such as autonomic blood pressure controls and skeletal muscle pump remains vastly ineffective. Such change in physiological function can lead to excessive pooling of central blood volume in the lower periphery, resulting in cerebral perfusion reduction leading to a feeling of dizziness and potentially syncope.

Thus, an external system capable of evoking autonomic control of blood pressure (baroreceptor unloading leading to increased sympathetic, decreased vagal activity, and increased systemic vascular resistance) and simultaneously increasing blood flow to the calf musculature to assure adequate nutritional and metabolic supply can mitigate the deterioration of cardiovascular performance associated with long-term exposure to microgravity.

Table 5.4. Values (mean±SD) of blood pressure regulatory indices in response to different experimental conditions. * Represents significant difference (Tukey-HSD post-hoc analysis) from supine.

Blood Pressure Regulatory Indices	**Supine**	**Stand**	**2-g**
SBP_{VLF}	0.72±0.13	0.51±0.15*	0.42±0.21*
SBP_{LF}	0.20±0.12	0.33±0.12*	0.36±0.17*
SBP_{HF}	0.08±0.06	0.16±0.13	0.22±0.13*
RR_{VLF}	0.31±0.21	0.36±0.14	0.46±0.20
RR_{LF}	0.30±0.16	0.42±0.16	0.39±0.16
RR_{HF}	0.39±0.20	0.22±0.12	0.15±0.08*
$RR_{LF/HF}$	1.10±1.02	2.89±2.54*	3.10±1.90*
$BRS_{up\ slope}$	31.18±20.19	10.40±4.78*	7.52±3.38*
$BRS_{down\ slope}$	29.31±18.15	10.85±6.39*	6.80±2.67*

Non-Baroreflex Sequence	10±12.54	9.84±6.01	15.23±7.50
Baroreflex Sequence	58.15±21.16	46.61±11.47	34±11.48*
RR→SBP	0.95±0.03	0.93±0.03	0.92±0.04
SBP→RR	0.83±0.09	0.91±0.03*	0.89±0.05*

Exercise training and lower-body negative pressurization have been utilized as a potential countermeasure to spaceflight deconditioning. However, traditionally used aerobic exercise, resistance training, and lower-body suction has been limited in effect due to their inability to challenge multiple physiological systems that are associated with standing(170,173,186). Consequently, interest has shifted towards short-arm human centrifuge as a training tool to minimize microgravity-induced physiological deconditioning(57). Short-arm human centrifuge, given its capability to create artificial gravity at feet, has a potential to produce hydrostatic gradient analogous to standing and evoke multiple physiological systems simultaneously(171,172). Achieving desired performance from SAHC, however, is contingent on an ideal choice of g-load. High g-load could initiate early syncopal symptoms, while low g-load could be insufficient to inflict strenuous perturbation to hemodynamic homeostasis, therefore, fails to evoke desired autonomic control of blood pressure. The choice of the 2-g at feet was based on the outcomes of previous studies, which have demonstrated such g-load to be under the safe limit in addition to being strenuous enough to evoke physiological responses analogous to standing(174,187).

The autonomic control of blood pressure via the conventional approach of arterial baroreflex sensitivity and heart rate variability have been shown to exhibit microgravity or

hypergravity induced an alteration in the autonomic performance(188,189). However, the effect of orthostatic challenge induced via centrifugation artificial gravity in relation to quiet standing on the autonomic behavior has not been reported in the literature. The low frequency (0.04-0.15 Hz) and the high frequency (0.15-0.4 Hz) spectral power of RR intervals in normalized units are associated with the response of the sympathetic and the vagal nerve, respectively and the ratio of the two is widely recognized indicator of sympatho-vagal balance(66). The SBP power distributed in the low-frequency band (0.04-0.15 Hz) has been reported to be associated with the baroreflex response(69). Thus, the spectral analysis of RR and SBP provides insights regarding the autonomic control of blood pressure under a given physiological state.

In the current research, we applied external perturbation to the hemodynamic homeostasis via stand test and 2-g centrifugation at feet. No change ($p>0.05$) was observed in SBP, DBP, or mean arterial pressure due to standing or 2-g compared to supine (Table 5.2). This observation suggests that blood pressure was well regulated during orthostatic challenge evoked via standing and 2-g centrifugation by active autonomic control of blood pressure. A significant increase was observed in the $RR_{LF/HF}$ during standing ($p=0.04$) and 2-g ($p=0.003$) compared to baseline (Table 5.4), suggesting a shift of sympatho-vagal balance towards sympathetic activity. Also, increase in low frequency SBP power was observed during standing ($p=0.04$) and 2-g ($p=0.02$) compared to supine. Additionally, baroreflex sensitivity (both upslope and downslope) declined during standing and 2-g compared to supine (Table 5.3), which is the result of decreased vagal activity (Table 5.3) and increased heart rate or reduced RR intervals (Table 5.2) contributing towards the maintenance of blood pressure equilibrium. No change ($p>0.05$) in the autonomic blood pressure control between standing and 2-g was observed (Table 5.3).

While the spectral analysis of SBP and RR time series and baroreflex sensitivity are well-accepted norm to account for the autonomic control of blood pressure, criticism of such approaches in the literature is also prevalent for the inability of the spectral method to account for the non-linearity of underlying physiology and BRS for not able to address the closed loop heart rate and blood pressure interaction(101,190). As such, in addition to traditional measures, the current article studied the non-linear causal heart rate and blood pressure interaction, a closed loop control system. Where the feedforward control signifies the Frank-Starling effect on blood pressure while the feedback control accentuates the baroreflex control of blood pressure. We studied the strength of feedforward (non-baroreflex, RR→SBP) and feedback (baroreflex, SBP→RR) controls of blood pressure during supine, standing, and 2-g centrifugation.

The results of closed loop heart rate and blood pressure interaction are detailed in Figure 5.5. No change ($p>0.05$) was observed in the dynamics of non-baroreflex (RR→SBP) causality during standing or 2-g compared to supine. However, a significant increase was observed in the baroreflex (SBP→RR) causality; both during standing ($p=0.009$) and 2-g ($p=0.03$), Table 5.4. Additionally, no change was observed in the non-baroreflex ($p=0.80$) or baroreflex ($p=0.88$) causal events during 2-g compared to standing. The findings of this chapter corroborate with existing literature regarding the behavior of closed loop heart rate and blood pressure interaction during orthostatic challenge(69,104,107). Therefore, the observations of current study confirmed our hypothesis of 2-g centrifugation at feet is capable of evoking autonomic control of blood pressure analogous to standing.

5.6. Limitations and Future Directions

The limitation of the present study was the unavailability of the respiration signal, as such, the role of hypergravity towards the dynamics of respiration could not be studied.

Respiration is known to affect both heart rate (RR) as well as blood pressure(108,138). Additionally, it may also play a role towards facilitating venous return via the physiology of respiration pump(191). Therefore, the role of respiration towards facilitating blood pressure homeostasis in response to orthostatic challenge shall be investigated in the future. Moreover, the blood volume redistribution in the splanchnic bed and the lower periphery due to standing and 2-g centrifugation shall also be measured and compared in the future. Orthostatic challenges evoked via a source that eliminates the effect of gravity such as lower-body negative pressure is observed to be different from that due to natural gravity (such as head-up tilt)(117). Certain blood pressure regulatory controls such as SBP_{HF}, RR_{HF}, and a number of baroreflex sequence changed only at 2-g compared to supine (Table 5.3), which indicate 2-g was more stressful than standing. Accurate information regarding the degree of blood pooling achieved during each experimental condition will shed further light pertaining to the vigor of 2-g in relation to standing.

Moreover, additional mechanisms that account for blood pressure regulation such as skeletal muscle pump (cardio-postural blood pressure regulation) shall also be investigated and compared in the future(48,142,192). Furthermore, due to small sample size, the gender effect on blood pressure regulation and alteration in the dynamics of such behavior under artificial hypergravity remains to be understood. Female astronauts account for approximately 22% of total astronaut population(193), and studies have demonstrated significant gender difference in autonomic mechanisms leading to stable stance and in response to countermeasures designed to mitigate deleterious effect of spaceflight deconditioning(194–197). Therefore, a generalization of gender effect would further improve our understanding regarding the potential of the short-arm human centrifuge as a training tool towards evoking blood pressure regulatory controls analogous to standing.

5.7. Conclusion

Cardiovascular adaptation to microgravity impairs autonomic control of blood pressure, consequently, astronauts are susceptible to orthostatic intolerance on return to the gravitational environment. Sporadic training in artificial hypergravity is proposed to mitigate the effects of spaceflight deconditioning. A short-arm human centrifuge is a promising tool for simulating artificial gravity of different g-loads. The response of blood pressure regulatory controls to simulated hypergravity in relation to standing is not well established in the literature. This thesis investigated the response of autonomic control of blood pressure during 2-g centrifugation in relation to standing. While no difference was observed in the autonomic control of blood pressure between standing and 2-g, the blood pressure regulatory indices during standing and 2-g centrifugation were significantly different from supine (Table 5.4). The findings of the current study lead us to conclude that 2-g centrifugation at feet via short-arm human centrifuge has potential to evoke autonomic control of blood pressure analogous to standing, therefore, a potential training tool towards reducing orthostatic intolerance in astronauts on their return to Earth.

Chapter 6.

Conclusions and Future Directions

6.1. Conclusions

Hemorrhage associated with a traumatic event is one of the leading cause of mortality affecting over 29 million people in the US. Post-partum hemorrhage is a recognized cause of maternal mortality accounting for approximately 125,000 deaths per year. The prime reason for mortality associated with the hemorrhage is the inability to recognize hemorrhage at an early stage due to complex physiological mechanisms maintaining homeostasis. Additionally, fall associated with orthostatic intolerance (failure to sustain blood pressure during standing) is prevalent in people with neurodegenerative diseases such as Parkinson's disease, stroke, and concussion. Over 31 billion dollars are spent annually for the treatment and management of fall-related (fatal and non-fatal) incidents. Physiology pertaining to fall is not adequately studied in the literature, accounting for integration of mechanisms associated with postural stability can assist early identification of fall proneness. Furthermore, astronauts experience orthostatic intolerance on a landing day following a long duration spaceflight due to physiological adaptation to microgravity. This thesis was aimed towards addressing above issues linked together via a common variable i.e. blood pressure regulation. The major conclusions of the thesis are outlined below.

6.1.1. Early Detection of Hemorrhage

Early identification of hemorrhage is vital for the design of trauma support system. On the battlefield and in a setting lacking sophisticated instrumentation, early identification of hemorrhage relies on arterial blood pressure. However, owing to compensatory

physiological mechanisms, blood pressure is proven to be an ineffectual marker of blood loss. This thesis investigated the potential of features extracted from electrocardiogram and continuous blood pressure waveform to classify moderate intensity hemorrhage from resting baseline. In this regard, our studies find convincing evidence regarding the potential of such features towards classification of moderate category hemorrhage (-40 mmHg). In future, bigger cohort needs to be studied to further confirm its feasibility towards the development of decision support system to assist surgical triage in a pre-hospital setting.

6.1.2. Cardio-Postural Blood Pressure Regulation Model

Regulating arterial blood pressure is essential for maintaining stable and prolonged upright stance. During standing blood pressure regulation is achieved via autonomic activity, which causes an elevation in heart rate and systemic vascular resistance and skeletal muscle activation, which pumps the venous blood back to the heart. Therefore, the independent model of cardiovascular and postural systems to assess orthostatic intolerance is inadequate to explain the underlying physiology. This thesis, aimed at investigating the dependency between the two systems by quantifying the degree of directional information flow between the cardiovascular and postural controls of blood pressure via representative signals, found strong statistical evidence of bidirectional information flow between the cardiovascular and the postural controls of blood pressure. Further, this thesis found statistical alteration in the strength of cardio-postural relationship following 12-minutes of submaximal exercise. Accordingly, a significant deviation in the strength of such interaction can be symptomatic of system impairment and further study extending beyond young, healthy group is warranted to validate its potential towards assessment of orthostatic intolerance.

6.1.3. Artificial Gravity for Minimizing Spaceflight Deconditioning

Exposure to microgravity can cause a series of physiological adaptation resulting in prolonged inhibition of autonomic controls of blood pressure, which can lead to cardiovascular deconditioning analogous to aging and/or pathology. Accordingly, astronauts commonly experience post-flight orthostatic intolerance. Intermittent exposure to artificial hyper gravity is hypothesized to mitigate spaceflight deconditioning. This thesis investigated the potential of artificial gravity created via 2-g centrifugation at feet to evoke autonomic control of blood pressure in relation to standing in natural gravity. The thesis found a strong statistical difference in the autonomic controls of blood pressure between supine and standing as well as between supine and 2-g. However, the difference in autonomic controls of blood pressure between standing and 2-g centrifugation was statistically insignificant. The findings of the analysis strongly support the hypothesis of artificial gravity (2-g centrifugation) towards minimizing spaceflight induced physiological deconditioning. Therefore, a potential towards minimizing post-flight orthostatic intolerance in astronauts.

6.2. Future Directions

6.2.1. Extension of the Assessment of Cardio-Postural Blood Pressure Regulation Model beyond Young, Healthy Population

The major limitation of this thesis was the unavailability of the data from patients. As such, the behavior of a cardio-postural model of blood pressure regulation during the orthostatic challenge was solely limited to young, healthy participants. In a group of young, healthy participants the experimental protocol was rendered insufficient to evoke symptoms of orthostatic hypotension in the study participants. The arterial blood pressure was well-regulated throughout the experimentation and the blood volume accumulated in the calf

musculature was not measured, therefore, the validation of the role of muscle pump baroreflex (SBP→EMG) towards the activation of calf skeletal muscle would require future work.

In future, adding a group of people with history of neurodegenerative disease can further highlight the effectiveness of the cardio-postural model as an assessment tool for early detection of fall proneness, as people with a history of stroke and concussion and those affected by Parkinson's disease have impaired autonomic and neural control(37,127,198–201), which may lead to excessive pooling of blood in the lower extremities immediately upon maintaining upright stance; acutely challenging the blood pressure equilibrium. Additionally, such population groups are observed to have poor postural stability(124,202,203). Accordingly, the cardio-postural model stressed upon in this thesis can provide key information regarding the interaction between cardiovascular and postural controls associated with regulation of blood pressure during orthostatic challenge.

Furthermore, a more intense experimental protocol such as head-up tilt or bed rest immobilization can be considered in the future work to disturb the hemodynamic homeostasis of the system and study the behavior of cardio-postural control loop in relation to such physiological state. Therefore, the results presented in this thesis shall be considered as a baseline and future analysis needs to be performed on the data acquired from patients or its analog to further validate the model prior to any clinical application towards early detection of fall proneness.

6.2.2. Accurate Measurement of Degree of Blood Pooling during Orthostatic Challenge

In this research, the degree of blood pooling as a consequence of orthostatic challenge induced via standing was not measured, therefore, the quantitative behavior of strength

of cardio-postural causality in relation to the vigor of orthostatic challenge remains to be generalized. A concept of near-infrared spectroscopy can be utilized in the future work to accurately measure the degree of blood pooling(167). Furthermore, it is pivotal to accurately measure translocation of blood volume as a consequence of different orthostatic challenge (head-up tilt, standing, LBNP) to validate the posture associated alteration in the physiological interplay to ascertain blood pressure.

6.2.3. Extraction of Pulse Transit Time using SCG-PPG combination to Estimate Blood Pressure

The physiological signals acquired in this research was acquired from typical laboratory equipment, therefore, to gain wide application, more portable and cheap alternatives need to be explored, especially for blood pressure and postural sway. Effect of posture should also be considered while developing a system for estimating blood pressure based on the concept of pulse transit time (PTT)(204). In the supine posture, blood pressure can be estimated by calculating the time difference between aortic-valve opening and arrival of blood in the external periphery. Seismocardiography (SCG), which is a recording of opening and closing of the heart valve can be a key towards annotating the proximal timing of a pulse wave. Using aortic-valve opening as a marker of the proximal timing of a pulse wave can address the limitation of the traditional used ECG signals R peak such purpose which may lead to erroneous result due to the inclusion of the isovolumetric contraction period(205). With the advent of sophisticated technology leading to the availability of lightweight accelerometers, significant elevation in the role of SCG towards monitoring cardiovascular functioning through heart rate variability(206), systolic time intervals(207–209), early detection of hemorrhage progression(110), and pulse transit time is observed of late(210–214). Figure 6.1 explains the extraction of pulse transit time utilizing

seismocardiography and photoplethysmography sensors to extract estimates of blood pressure.

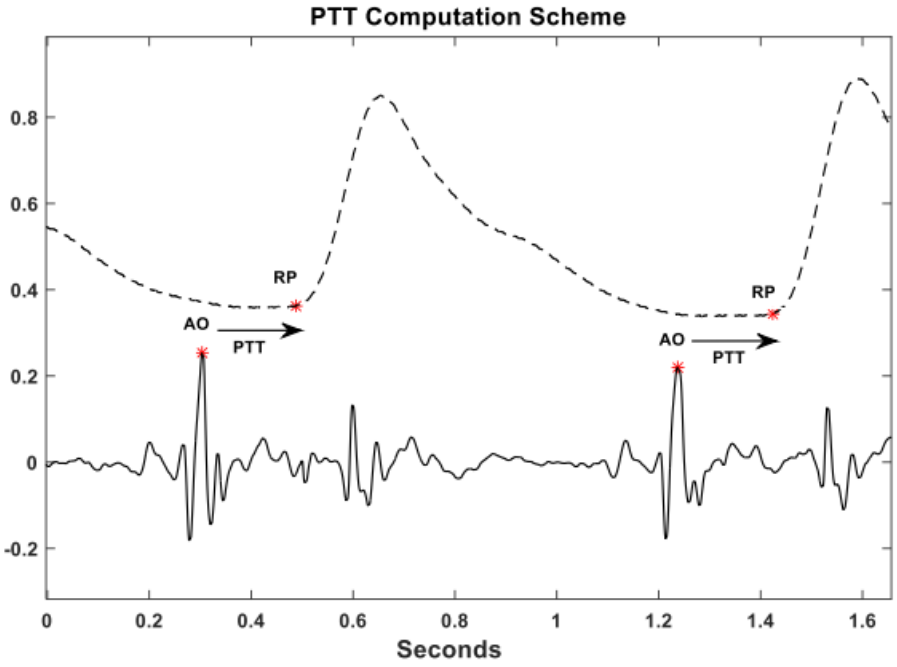

Figure 6.1. Extraction of PTT from a combination of SCH (solid) and PPG (dotted). The aortic-valve (AO) opening point in SCG, a marker of proximal timing and rise point in PPG, a marker of the distal timing of a pulse wave. The time difference between the two locations is pulse transit time (PTT) an estimate of blood pressure(210).

6.2.4. Extraction of Pulse Transit Time using BCG-PPG Combination to estimate Blood Pressure

Extracting estimates of blood pressure using BCG-PPG combination of great significance to move from that usage of traditional rather costly laboratory-based acquisition to cheap and portable system capable of acquiring representative signals of the cardio-postural control loop. To achieve such goals, in future, a weighing scale can be developed which can measure the postural sway using load cells placed on the appropriate scale location

along with measure the ballistic forces of heart (ballistocardiography) whose vibration can get transferred to the scale (Figure 6.2). Then I, J, K wave of the ballistocardiogram signal can be explored for timing the proximal pulse wave and PPG can be used for timing the distal pulse, PTT will be the result of the time difference between proximal and distal timing(215).The EMG signal can be acquired by placing EMG sensors on the surface of the scale (Figure 6.2).

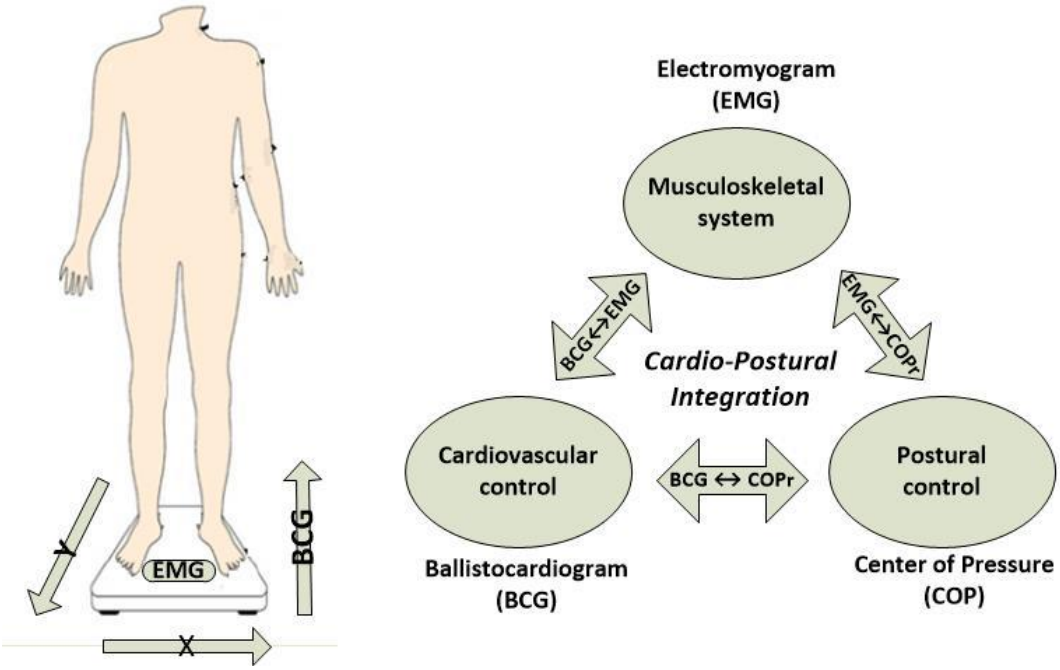

Figure 6.2. Development of weighing scale system to acquire representative signals of the cardio-postural system. EMG will be acquired by placing a signal on the surface of the developed weighing scale. Postural sway will be acquired by placing load cells on the four corners, and blood pressure will be estimated from PTT derived using a combination of BCG and PPG.

6.2.5. Extension of the Cardio-Postural Model to Centrifuge Study and the Effect of Gender on the design of System to Mitigate Effects of Spaceflight Deconditioning

This thesis laid focus on the study of cardiovascular variables (i.e. heart rate and blood pressure) in response to artificial gravity via short-arm human centrifuge. Additional mechanisms that account for blood pressure regulation such as skeletal muscle pump (cardio-postural blood pressure regulation) shall also be investigated and compared in the future(48,142,192). Furthermore, due to small sample size, the gender effect towards blood pressure regulation, and alteration in the dynamics of such behavior under artificial hypergravity remains to be understood. Female astronauts account for approximately 22% of total astronaut population(193), and studies have demonstrated significant gender difference in autonomic regulatory mechanisms leading to stable stance and in response to countermeasures designed to mitigate deleterious effect of spaceflight deconditioning(194–197). Therefore, a generalization of gender effect would further improve our understanding regarding the potential of the short-arm human centrifuge as a training tool towards evoking blood pressure regulatory controls analogous to standing.

6.2.6. Exploration of Multivariate Model to assess Connectivity between Physiological Systems under Orthostatic Challenge

In future, we aim to supplement the representative signals of a physiological system utilized in this research such as respiration, NIRS, and cerebral blood flow. Therefore, the bivariate model considered for investigating cause-and-effect relationship in this thesis may be insufficient to accurately quantify the strength of directional information flow among physiological systems under the respective physiological state. Therefore, in future, a multivariate model for studying cause-and-effect relationship shall be employed.

References

1. Rowell L. Human Cardiovascular Control. Oxford University Press; 1993.

2. Schiller AM, Howard JT, Convertino VA. The physiology of blood loss and shock: New insights from a human laboratory model of hemorrhage. Exp Biol Med. 2017;242(8):874–83.

3. Shaw BH, Claydon VE. The relationship between orthostatic hypotension and falling in older adults. 2014;3–13.

4. Kauvar DS, Lefering R, Wade CE. Impact of Hemorrhage on Trauma Outcome: An Overview of Epidemiology, Clinical Presentations, and Therapeutic Considerations. J Trauma Acute Care Surg. 2006;60(6):S3-11.

5. Terroso M, Rosa N, Torres Marques A, Simoes R. Physical consequences of falls in the elderly: A literature review from 1995 to 2010. Eur Rev Aging Phys Act. 2014;11(1):51–9.

6. Centers for Disease Control and Prevention. (Aug. 29, 2012) Web-based injury statistics query and reporting system (WISQARS). In U.S. Department of Health and Human Services, CDC, National Center for Injury Prevention and Control.

7. Burns ER, Stevens JA, Lee R. The costs of fatal and non-fatal falls among older adults. J Safety Res. 2016;58:99–103.

8. Rhee P, Joseph B, Pandit V, Aziz H, Vercruysse G, Kulvatunyou N, et al. Increasing Trauma Deaths in the United States. Ann Surg. 2014;0(0):1–9.

9. Evans JA, Van Wessem KJP, McDougall D, Lee KA, Lyons T, Balogh ZJ. Epidemiology of traumatic deaths: Comprehensive population-based assessment. World J Surg. 2010;34(1):158–63.

10. Hancock A, Weeks AD, Lavender DT. Is accurate and reliable blood loss estimation the “crucial step” in early detection of postpartum haemorrhage: an integrative review of the literature. BMC Pregnancy Childbirth. 2015;15:230.

11. Say L, Chou D, Gemmill A, Tunçalp Ö, Moller A-B, Daniels J, et al. Global Causes of Maternal Deaths: A WHO Systematic Analysis. Lancet Glob Heal. 2014;2(6):1–14.

12. Beekley AC, Sebesta JA, Blackbourne LH, Herbert GS, Kauvar DS, Baer DG, et al. Prehospital Tourniquet Use in Operation Iraqi Freedom : Effect on Hemorrhage Control and Outcomes. J Trauma Acute Care Surg. 2008;64(2):S28–37.

13. Dorlac WC, DeBakey ME, Holcomb JB, Pagan SP, Kwong KL, Dorlac GR, et al. Mortality from isolated civilian penetrating extremity injury. J Trauma Acute Care Surg. 2005;59(1):217–22.

14. Carroli G, Cuesta C, Abalos E, Gulmezoglu AM. Epidemiology of postpartum haemorrhage: a systematic review. Best Pract Res Clin Obstet Gynaecol. 2008;22(6):999–1012.

15. Dahlke JD, Mendez-Figueroa H, Maggio L, Hauspurg AK, Sperling JD, Chauhan SP, et al. Prevention and management of postpartum hemorrhage : a comparison of 4 national guidelines. Am J Obstet Gynecol. 2015;213(1):76-e1.

16. Tisherman SA, Schmicker RH, Brasel KJ, Bulger EM, Kerby JD, Minei JP, et al. Detailed Description of all Deaths in Both the Shock and Traumatic Brain Injury Hypertonic Saline Trials of the Resuscitation Outcomes Consortium. Ann Surg. 2016;261(3):586.

17. Haas B, Gomez D, Zagorski B, Stukel TA, Rubenfeld GD, Nathens AB. Survival of the fittest: The hidden cost of undertriage of major trauma. J Am Coll Surg. 2010;211(6):804–11.

18. Eastridge BJ, Mabry RL, Seguin P, Cantrell J, Tops T, Uribe P, et al. Death on the battlefield (2001Y2011): Implications for the future of combat casualty care. J Trauma Acute Care Surg. 2012;73(6):S431–7.

19. Pacagnella RC, Souza JP, Durocher J, Perel P, Blum J, Winikoff B, et al. A Systematic Review of the Relationship between Blood Loss and Clinical Signs. PLoS One. 2013;8(3):e57594.

20. Parks JK, Elliott AC, Gentilello LM, Shafi S. Systemic hypotension is a late marker of shock after trauma: a validation study of Advanced Trauma Life Support principles in a large national sample. Am J Surg. 2006;192(6):727–31.

21. Victorino GP, Battistella FD, Wisner DH. Does tachycardia correlate with hypotension after trauma? J Am Coll Surg. 2003;196(5):679–84.

22. Elstad M, Nådland IH, Toska K, Walløe L. Stroke volume decreases during mild dynamic and static exercise in supine humans. Acta Physiol. 2009;195(2):289–300.

23. Ryan KL, Rickards CA, Hinojosa-Laborde C, Cooke WH, Convertino VA. Sympathetic responses to central hypovolemia: New insights from microneurographic recordings. Front Physiol. 2012;3.

24. Johnson BD, van Helmond N, Curry TB, van Buskirk CM, Convertino V a, Joyner MJ. Reductions in central venous pressure by lower body negative pressure or blood loss elicit similar hemodynamic responses. J Appl Physiol. 2014;117(2):131–41.

25. Pottecher J, Chemla D, Xavier L, Liu N, Chazot T, Marescaux J, et al. The pulse pressure/heart rate ratio as a marker of stroke volume changes during hemorrhagic shock and resuscitation in anesthetized swine. J Trauma Acute Care Surg. 2013;74(6):1438–45.

26. Soller BR, Yang Y, Soyemi OO, Ryan KL, Rickards CA, Walz JM, et al. Noninvasively determined muscle oxygen saturation is an early indicator of central hypovolemia in humans. J Appl Physiol. 2008;104(2):475–81.

27. Verma AK, Xu D, Garg A, Cote AT, Goswami N, Blaber AP, et al. Non-linear Heart Rate and Blood Pressure Interaction in Response to Lower-Body Negative Pressure. Front Physiol. 2017;8.

28. Gerhardt RT, Berry JA, Blackbourne LH. Analysis of Life-Saving Interventions Performed by Out-of-Hospital Combat Medical Personnel. J Trauma Inj Infect Crit Care. 2011;71(supplement):S109–13.

29. Jimenez F, Sanchez G, Juarez JM. Multi-objective evolutionary algorithms for fuzzy

classification in survival prediction. Artif Intell Med. 2014;60(3):197–219.

30. Lim CP, Harrison RF, Kennedy RL. Application of autonomous neural network systems to medical pattern classification tasks. Artif Intell Med. 2015;11(3):215–39.

31. Becalick DC, Coats TJ. Comparison of artificial intelligence techniques with {UK TRISS} for estimating probability of survival after trauma. J Trauma Acute Care Surg. 2001;51(1):123–33.

32. Convertino VA, Moulton SL, Grudic GZ, Rickards CA, Hinojosa-Laborde C, Gerhardt RT, et al. Use of advanced machine-learning techniques for noninvasive monitoring of hemorrhage. J Trauma - Inj Infect Crit Care. 2011;71(1):25–32.

33. Bennis FC, Van Der Ster BJP, Van Lieshout JJ, Andriessen P, Delhaas T. A machine-learning based analysis for the recognition of progressive central hypovolemia. Physiol Meas. 2017;38(9):1791–801.

34. van der Ster BJP, Bennis FC, Delhaas T, Westerhof BE, Stok WJ, van Lieshout JJ. Support vector machine based monitoring of cardio-cerebrovascular reserve during simulated hemorrhage. Front Physiol. 2018;8(JAN).

35. Jorgensen L, T E, Jacobsen BK. Higher incidence of falls in long-term stroke survivors than in population controls: depressive symptoms predict falls after stroke. Stroke. 2002;33(2):542–7.

36. Heyer GL, Fischer A, Wilson J, MacDonald J, Cribbs S, Ravindran R, et al. Orthostatic intolerance and autonomic dysfunction in youth with persistent postconcussion symptoms: a head-upright tilt table study. Clin J Sport Med. 2016;26(1):40–5.

37. Senard JM, Raï S, Brefel C, Rascol O, Rascol A, Montastruc JL. Prevalence of orthostatic hypotension in Parkinson ’s disease. J Neurol Neurosurg Psychiatry. 1997;584–9.

38. Ricci F, Caterina R De, Fedorowski A. Orthostatic hypotension: epidemiology, prognosis, and treatment. J Am Coll Cardiol. 2015;66(7):848–60.

39. Ortman BJM, Velkoff VA, Hogan H. An Aging Nation : The Older Population in the

United States. United States Census Bur Econ Stat Adm US Dep Commer. 2014;

40. Elbaz A, Carcaillon L, Kab S, Moisan F. Epidemiology of Parkinson ' s disease. Rev Neurol (Paris). 2016;172(1):14–26.

41. Finucane C, O'Connell MDL, Donoghue O, Richardson K, Savva GM, Kenny RA. Impaired Orthostatic Blood Pressure Recovery Is Associated with Unexplained and Injurious Falls. J Am Geriatr Soc. 2017;65(3):474–82.

42. Shaw BH, Loughin TM, Robinovitch SN, Claydon VE. Cardiovascular responses to orthostasis and their association with falls in older adults. BMC Geriatr. 2015;15(1):174.

43. Amdani SOR, Allon GUT, Ernard PILOB, Lain HUB. Recurrence Quantification Analysis of Human Postural Fluctuations in Older Fallers and Non-fallers. Ann Biomed Eng. 2013;41(8):1713–25.

44. Fino PC, Mojdehi AR, Adjerid K, Habibi M, Lockhart TE, Ross SD. Comparing Postural Stability Entropy Analyses to Differentiate Fallers and Non-fallers. Ann Biomed Eng. 2016;44(5):1636–45.

45. Qiu H, Xiong S. Center-of-pressure based postural sway measures: Reliability and ability to distinguish between age, fear of falling and fall history. Int J Ind Ergon. 2015;47:28–35.

46. Garg A, Xu D, Blaber AP. Statistical validation of wavelet transform coherence method to assess the transfer of calf muscle activation to blood pressure during quiet standing. Biomed Eng Online. 2013;12:132.

47. Garg A, Xu D, Bruner M, Blaber A. Alteration in cardiovascular and postural control relationship in non-fainting elderly individuals. Conf Proc . Annu Int Conf IEEE Eng Med Biol Soc IEEE Eng Med Biol Soc Annu Conf. 2014;2014(March 2016):3521–4.

48. Garg A, Xu D, Laurin A, Blaber AP. Physiological interdependence of the cardiovascular and postural control systems under orthostatic stress. Am J Physiol Hear Circ Physiol. 2014;307(2):H259-64.

49. Singer J. Human Journey to Mars – The Next Steps. 2016; Available from: https://ntrs.nasa.gov/search.jsp?R=20160014578

50. Vernikos J, Walter N, Worms JC, Blanc S. THESEUS: The European research priorities for human exploration of space. npj Microgravity. 2016;2(1):16034.

51. Salotti JM, Heidmann R. Roadmap to a human Mars mission. Acta Astronaut. 2014;104(2):558–64.

52. Tanaka K, Nishimura N, Kawai Y. Adaptation to microgravity, deconditioning, and countermeasures. J Physiol Sci. 2016;271–81.

53. Goswami N. Falls and Fall-Prevention in Older Persons : Geriatrics Meets Spaceflight ! Front Physiol. 2017;8:603.

54. Cooke WH, Ames JE I V, Crossman AA, Cox JF, Kuusela TA, Tahvanainen KU, et al. Nine months in space: effects on human autonomic cardiovascular regulation. J Appl Physiol. 2000;89(3):1039–45.

55. Hargens AR, Richardson S. Cardiovascular adaptations, fluid shifts, and countermeasures related to space flight. Respir Physiol Neurobiol. 2009;169(SUPPL.):30–3.

56. Artiles AD. Exercise under Artificial Gravity - Experimental and Computational Approaches. PhD Thesis, Massachusetts Inst Technol. 2015;

57. Clément G, Pavy-Le Traon a. Centrifugation as a countermeasure during actual and simulated microgravity: a review. Eur J Appl Physiol. 2004;92(3):235–48.

58. Stenger MB, Evans JM, Knapp CF, Lee SMC, Phillips TR, Perez SA, et al. Artificial gravity training reduces bed rest-induced cardiovascular deconditioning. Eur J Appl Physiol. 2012;112(2):605–16.

59. Evans JM, Stenger MB, Moore FB, Hinghofer-Szalkay H, Rössler A, Patwardhan AR, et al. Centrifuge training increases presyncopal orthostatic tolerance in ambulatory men. Aviat Sp Environ Med. 2004;75(10):850–8.

60. Heesch CM. Reflexes That Control Cardiovascular Function. Adv Physiol Educ.

1999;277(6):S234.

61. Klabunde R. Cardiovascular Physiology Concepts. Lippincott Williams & Wilkins; 2011.

62. Rovere La MT, Pinna GD, Raczak G. Baroreflex Sensitivity : Measurement and Clinical Implications. Ann Noninvasive Electrocardiol. 2008;13(2):191–207.

63. Swenne CA. Baroreflex sensitivity: Mechanisms and measurement. Netherlands Hear J. 2013;21:58–60.

64. Parati G, Saul JP, Castiglioni P. Assessing arterial baroreflex control of heart rate: New perspectives. J Hypertens. 2004;22(7):1259–63.

65. Parati G, DiRienzo M, Mancia G. How to measure baroreflex sensitivity: From the cardiovascular laboratory to daily life. J Hypertens. 2000;18(1):7–19.

66. Malik M, Bigger J, Camm A, Kleiger R, Malliani A, Moss A, et al. Heart rate variability: Standards of measurement, physiological interpretation, and clinical use. Eur Heart J. 1996;17(44):354–81.

67. Tarvainen MP, Niskanen JP, Lipponen J, Ranta-aho PO, Karjalainen P. Kubios HRV - Heart rate variability analysis software. Comput Methods Programs Biomed. 2014;113(1):210–20.

68. Verma AK, Cabrera SD, Fazel-Rezai R. Continuous Balance Assessment of Autonomic Nervous System Using Time-Varying Analysis of Heart Rate Variability. J Med Device. 2016;10(2):20933.

69. Silvani A, Calandra-buonaura G, Johnson BD, Helmond N Van, Barletta G, Cecere AG, et al. Physiological Mechanisms Mediating the Coupling between Heart Period and Arterial Pressure in Response to Postural Changes in Humans. Front Physiol. 2017;8.

70. Porta A, Faes L. Wiener – Granger Causality in Network Physiology With Applications to Cardiovascular Control and Neuroscience. Proc IEEE. 2016;104(2):282–309.

71. Bressler SL, Seth AK. Wiener-Granger Causality: A well established methodology. Neuroimage. 2011;58(2):323–9.

72. Vicente R, Wibral M, Lindner M. Transfer entropy — a model-free measure of effective connectivity for the neurosciences. J Comput Neurosci. 2011;30(1):45–67.

73. Valenza G, Faes L, Citi L, Orini M, Barbieri R, Member S. Instantaneous Transfer Entropy for the Study of Cardio-Respiratory Dynamics. In: IEEE International Conference on Engineering in Medicine and Biology Society. 2015. p. 7885–8.

74. Krakovská A, Jakubík J, Budáčová H, Holecyová M. Causality studied in reconstructed state space . Examples of uni-directionally connected chaotic systems. arXiv Prepr arXiv151100505 2015 Nov 2. 2015;1–41.

75. Sugihara G, May R, Ye H, Hsieh CH, Deyle E, Fogarty M, et al. Detecting Causality in Complex Ecosystems. Science. 2012;338(6106):496–500.

76. Sugihara G, May R, Ye H, Hsieh C, Deyle E, Fogarty M. Supplementary Materials for Detecting Causality in Complex Ecosystems. 2012;

77. Schiecke K, Pester B, Feucht M, Leistritz L, Witte H. Convergent Cross Mapping: Basic concept, influence of estimation parameters and practical application. In: IEEE International Conference on Engineering in Medicine and Biology Society. 2015. p. 7418–21.

78. McCracken JM, Weigel RS. Convergent cross-mapping and pairwise asymmetric inference. Phys Rev E - Stat Nonlinear, Soft Matter Phys. 2014;90(6):1–7.

79. Schiecke K, Pester B, Piper D, Benninger F, Feucht M, Witte H. Nonlinear Directed Interactions between Heart Rate Variability and EEG Activity in Children with Temporal Lobe Epilepsy. IEEE Trans Biomed Eng. 2016;63(12):2497–504.

80. Mccracken JM. Exploratory Causal Analysis with Time Series Data. Morgan & Claypool; 2016.

81. Marwan N, Romano MC, Thiel M, Kurths J. Recurrence plots for the analysis of complex systems. Phys Rep. 2007;438(5):237–329.

82. Webber CL, Zbilut JP. Dynamical assessment of physiological systems and states using recurrence plot strategies. J Appl Physiol [Internet]. 1994;76(2):965–73. Available from: 175612

83. Marwan N, Wessel N, Meyerfeldt U, Schirdewan A, Kurths J. Recurrence-plot-based measures of complexity and their application to heart-rate-variability data. Phys Rev E. 2002;66(2):26702.

84. Shabani H, Mikaili M, Mohammad S, Noori R. Assessment of Recurrence Quantification Analysis (RQA) of EEG for Development of a Novel Drowsiness Detection System. Biomed Eng Lett. 2016;6(3):196–204.

85. Rolink J, Kutz M, Fonseca P, Long X, Misgeld B, Leonhardt S. Recurrence quantification analysis across sleep stages. Biomed Signal Process Control. 2015;20:107–16.

86. Wallot S, Roepstorff A, Mønster D. Multidimensional recurrence quantification analysis (MdRQA) for the analysis of multidimensional time-series: A software implementation in MATLAB and its application to group-level data in joint action. Front Psychol. 2016;7:1835.

87. Marwan N. Cross Recurrence Plot Toolbox for MATLAB®, Ver. 5.21 (R31.2), http://tocsy.pik-potsdam.de/CRPtoolbox/, accessed 2017-06-15.

88. Søreide K, Krüger AJ, Vårdal AL, Ellingsen CL, Søreide E, Lossius HM. Epidemiology and contemporary patterns of trauma deaths: Changing place, similar pace, older face. World J Surg. 2007;31(11):2092–103.

89. Alam HB. Trauma care : Finding a better way. PLoS Med. 2017;14(7):e1002350.

90. Hinojosa-Laborde C, Shade RE, Muniz GW, Bauer C, Goei K a, Pidcoke HF, et al. Validation of lower body negative pressure as an experimental model of hemorrhage. J Appl Physiol. 2014;116(4):406–15.

91. Brasel KJ, Guse C, Gentilello LM, Nirula R. Heart rate: is it truly a vital sign? J Trauma Acute Care Surg. 2007;62(4):812–7.

92. Cote AT, Phillips AA, Bredin SSD, Warburton DER. A questionable association of

stroke volume and arterial pulse pressure under gravitational stress. J Trauma Acute Care Surg. 2012;72(3):708–12.

93. Convertino VA, Wirt MD, Glenn JF, Lein BC. The Compensatory Reserve For Early and Accurate Prediction Of Hemodynamic Compromise: A Review of the Underlying Physiology. Shock. 2016;45(6):580–90.

94. Nadler R, Convertino VA, Gendler S, Lending G, Lipsky AM, Cardin S, et al. The value of noninvasive measurement of the compensatory reserve index in monitoring and triage of patients experiencing minimal blood loss. Shock. 2014;42(2):93–8.

95. Cote AT, Bredin SSD, Phillips AA, Warburton DER. Predictors of orthostatic intolerance in healthy young women. Clin Investig Med Médecine Clin Exp. 2012;35(2):E65-74.

96. Janak JC, Howard JT, Goei KA, Weber R, Muniz GW, Hinojosa-Laborde C, et al. Predictors of the Onset of Hemodynamic Decompensation During Progressive Central Hypovolemia: Comparison of the Peripheral Perfusion Index, Pulse Pressure Variability, and Compensatory Reserve Index. Shock. 2015;44(6):548–53.

97. Cooke WH, Ryan KL, Convertino VA. Lower body negative pressure as a model to study progression to acute hemorrhagic shock in humans. J Appl Physiol. 2004;96(4):1249–61.

98. Cooke WH, Rickards CA, Ryan KL, Kuusela TA, Convertino VA. Muscle sympathetic nerve activity during intense lower body negative pressure to presyncope in humans. J Physiol. 2009;587(20):4987–99.

99. Bighamian R, Hahn J-O. Relationship between Stroke Volume and Pulse Pressure during Blood Volume Perturbation: A Mathematical Analysis. Biomed Res Int. 2014;2014:1–10.

100. Teresa M, Rovere L, Pinna GD, Raczak G. Baroreflex Sensitivity : Measurement and Clinical Implications. 2008;

101. Zhong Y, Jan K, Ju KH, Chon KH. Quantifying cardiac sympathetic and parasympathetic nervous activities using principal dynamic modes analysis of heart rate variability. Am J Physiol Hear Circ Physiol. 2006;291(3):H1475–83.

102. Faes L, Nollo G, Porta A. Mechanisms of causal interaction between short-term RR interval and systolic arterial pressure oscillations during orthostatic challenge. 2013;(39):1657–67.

103. Porta A, Catai AM, Takahashi ACM, Magagnin V, Bassani T, Tobaldini E, et al. Causal relationships between heart period and systolic arterial pressure during graded head-up tilt. Am J Physiol Regul Integr Comp Physiol. 2011;300(2):R378–86.

104. Javorka M, Czippelova B, Turianikova Z, Lazarova Z, Tonhajzerova I, Faes L. Causal analysis of short-term cardiovascular variability: state-dependent contribution of feedback and feedforward mechanisms. Med Biol Eng Comput. 2017;55(2):179–90.

105. Javorka M, Czippelova B, Chladekova L, Turianikova Z, Visnovcova Z, Lazarova Z, et al. Causality of Heart Rate - Blood Pressure Interactions during Mental and Orthostatic Stress. In: Computing in Cardiology Conference (CinC). 2014. p. 769–72.

106. Porta A, Marchi A, Bari V, De Maria B, Esler M, Lambert E, et al. Assessing the strength of cardiac and sympathetic baroreflex controls via transfer entropy during orthostatic challenge. Philos Trans R Soc A. 2017;375:20160290.

107. Faes L, Nollo G, Porta A. Mechanisms of causal interaction between short-term RR interval and systolic arterial pressure oscillations during orthostatic challenge. J Appl Physiol. 2013;114(12):1657–67.

108. Faes L, Nollo G, Porta A. Information domain approach to the investigation of cardio-vascular, cardio-pulmonary, and vasculo-pulmonary causal couplings. Front Physiol. 2011;2.

109. Nollo G, Faes L, Porta A, Antolini R, Ravelli F. Exploring directionality in spontaneous heart period and systolic pressure variability interactions in humans:

implications in the evaluation of baroreflex gain. Am J Physiol Hear Circ Physiol. 2005;288(4):H1777-85.

110. Tavakolian K, Dumont GA, Houlton G, Blaber AP. Precordial vibrations provide noninvasive detection of early-stage hemorrhage. Shock. 2014;41(2):91–6.

111. Westphal G, Gallardo P, Almeida DP De, Rocha e Silva M, Poli-de-Figueiredo LF. Pulse Pressure Respiratory Variation as an Early Marker of Cardiac Output Fall in Experimental Hemorrhagic Shock. Artif Organs. 2007;31(4):284–9.

112. Convertino VA, Cooke WH, Holcomb JB. Arterial Pulse Pressure and Its Association With Reduced Stroke Volume During Progressive Central Hypovolemia. J Trauma Inj Infect Crit Care. 2006;61(3):629–34.

113. Scherhag A, Kaden JJ, Kentschke E, Sueselbeck T, Borggrefe M. Comparison of Impedance Cardiography and Thermodilution-Derived Measurements of Stroke Volume and Cardiac Output at Rest and During Exercise Testing. Cardiovasc Drugs Ther. 2005;19(2):141–7.

114. Olaussen A, Blackburn T, Mitra B, Fitzgerald M. Review article: Shock Index for prediction of critical bleeding post-trauma: A systematic review. Emerg Med Australas. 2014;26(3):223–8.

115. Montoya KF, Charry JD, Calle-Toro JS, Núñez LR, Poveda G. Shock index as a mortality predictor in patients with acute polytrauma. J Acute Dis. 2015;4(3):202–4.

116. Liu Y, Liu J-H, Fang ZA, Shan G-L, Xu J, Qi Z-W, et al. Modified shock index and mortality rate of emergency patients. World J Emerg Med. 2012;3(2):114.

117. Taneja I, Moran C, Medow MS, Glover JL, Montgomery LD, Stewart JM. Differential effects of lower body negative pressure and upright tilt on splanchnic blood volume. Am J Physiol Hear Circ Physiol. 2007;292(3):H1420-1426.

118. Dorantes-Mendez G, Ferrario M, Baselli G, Arbeille P, Shoemaker JK, Greaves DK, et al. Comparison of Baroreflex Sensitivity Gain during Mild Lower Body Negative Pressure in Presence and Absence of Long Duration Bed Rest. In: Computing in Cardiology. 2013. p. 763–6.

119. Goswami N, Loeppky JA, Hinghofer-Szalkay H. LBNP: Past protocols and technical considerations for experimental design. Aviat Sp Environ Med. 2008;79(5):459–71.

120. Kitano A, Shoemaker JK, Ichinose M, Wada H, Nishiyasu T. Comparison of cardiovascular responses between lower body negative pressure and head-up tilt. J Appl Physiol. 2005;98(6):2081–6.

121. Bronzwaer AGT, Verbree J, Stok WJ, Daemen MJAP, Buchem MA Van, Osch MJP Van, et al. The cerebrovascular response to lower-body negative pressure vs. head-up tilt. J Appl Physiol. 2017;122(4):877–83.

122. Hinghhofer-Szalkay HG, Vigas M, Sauseng-Fellegger G, Kuenig EM, Lichardus B, D. J. Head-up tilt and lower body suction: comparison of hormone responses in healthy men. Physiol Res. 1996;45:369–78.

123. Liu NT, Salinas J. Machine Learning for Predicting Outcomes in Trauma. Shock. 2017;48(5):504–10.

124. Błaszczyk JW, Orawiec R, Duda-Kłodowska D, Opala G. Assessment of postural instability in patients with Parkinson ' s disease. Exp Brain Res. 2007;183(1):107–14.

125. Kim SD, Allen NE, Canning CG, Fung VSC. Postural Instability in Patients with Parkinson ' s Disease. CNS Drugs. 2013;27(2):97–112.

126. Riemann BL, Guskiewicz KM. Effects of Mild Head Injury on Postural Stability as Measured Through Clinical Balance Testing. J Athl Train. 2000;35(1):19.

127. Eigenbrodt ML, Rose KM, Couper DJ, Arnett DK, Smith R, Jones D. Orthostatic Hypotension as a Risk Factor for Stroke : The Atherosclerosis Risk in Communities (ARIC) Study, 1987-1996. Stroke. 2000;31(10):2307–13.

128. Hallgren E, Migeotte P-F, Kornilova L, Delière Q, Fransen E, Glukhikh D, et al. Dysfunctional vestibular system causes a blood pressure drop in astronauts returning from space. Sci Rep. 2015;5:17627.

129. Olufsen MS, Ottesen JT, Tran HT, Ellwein LM, Lipsitz LA, Novak V. Blood pressure and blood flow variation during postural change from sitting to standing: model

development and validation. J Appl Physiol. 2005;99(4):1523–37.

130. Blaber AP, Landrock CK, Souvestre PA. Cardio-postural deconditioning: A model for post-flight orthostatic intolerance. Respir Physiol Neurobiol. 2009;169(SUPPL.):21–5.

131. Novak V, Hu K, Vyas M, Lipsitz LA. Cardiolocomotor coupling in young and elderly people. Journals Gerontol - Ser A Biol Sci Med Sci. 2007;62(1):86–92.

132. Verma AK, Garg A, Blaber A, Fazel-rezai R, Tavakolian K. Causal Cardio-Postural Interaction Under Orthostatic Stress. J Med Device. 2016;10(2):20932.

133. Verma AK, Garg A, Blaber A, Fazel-Rezai R, Tavakolian K. Causality Detection in Cardio-Postural Interaction under Orthostatic Stress Induced by Quiet Standing using Transfer Entropy. In: IEEE International Conference on Electro Information Technology (EIT). 2016. p. 633–7.

134. Verma AK, Garg A, Blaber A, Fazel-Rezai R, Tavakolian K. Analysis of Causal Cardio-Postural interaction under Orthostatic Stress using Convergent Cross Mapping. In: IEEE International Conference on Engineering in Medicine and Biology Society. 2016. p. 2319–22.

135. Verma AK, Garg A, Blaber A, Fazel-Rezai R TK. Causality in the Cardio-Postural Interactions during Quiet Stance. In: Computing in Cardiology Conference (CinC). 2015. p. 373–6.

136. Ding M, Chen Y, Bressler SL. 17 Granger causality: basic theory and application to neuroscience. Handbook of time series analysis: recent theoretical developments and applications. 2006;

137. Chen C, Member S, Maybhate A, Israel D, Thakor N V, Jia X. Assessing Thalamocortical Functional Connectivity With Granger Causality. IEEE Trans Neural Syst Rehabil Eng. 2013;21(5):725–33.

138. Porta A, Bassani T, Bari V, Pinna GD, Maestri R, Guzzetti S, et al. Accounting for Respiration is Necessary to Reliably Infer Granger Causality From Cardiovascular Variability Series. IEEE Trans Biomed Eng. 2012;59(3):832–41.

139. Porta A, Faes L. Assessing causality in brain dynamics and cardiovascular control. Philos Trans R Soc London A Math Phys Eng Sci. 2013;371:20120517.

140. Faes L, Marinazzo D, Jurysta F, Nollo G. Granger Causality Analysis of Sleep Brain-Heart Interactions. In: 8th Conference of the European Study Group on Cardiovascular Oscillations. 2014. p. 5–6.

141. Schreiber T. Measuring Information Transfer. Phys Rev Lett. 2000;85(2):461–4.

142. Xu D, Verma AK, Garg A, Bruner M, Fazel-rezai R, Blaber AP, et al. Significant role of the cardiopostural interaction in blood pressure regulation during standing. Am J Physiol Hear Circ Physiol. 2017;313(3):H568-77.

143. Ye H, Deyle ER, Gilarranz LJ, Sugihara G. Distinguishing time-delayed causal interactions using convergent cross mapping. Sci Rep. 2015;5.

144. Heskamp L, Meel -van den Abeelen AS, Lagro J, Claassen JA. Convergent cross mapping : a promising technique for cerebral autoregulation estimation. Int J Clin Neurosci Ment Heal. 2014;S20.

145. Halliwill JR. Mechanisms and clinical implications of post-exercise hypotension in humans. Exerc Sport Sci Rev. 2001;29(2):65–70.

146. Bruner M. The Effect of Exercise on the Cardio-Postural Relationship. MS Thesis Simon Fraser Univ. 2012;

147. Antonutto G, di Prampero PE. Cardiovascular deconditioning in microgravity: Some possible countermeasures. Eur J Appl Physiol. 2003;90(3–4):283–91.

148. Blaber AP, Zuj KA, Goswami N. Cerebrovascular autoregulation: Lessons learned from spaceflight research. Eur J Appl Physiol. 2013;113(8):1909–17.

149. Morita H, Abe C, Tanaka K. Long-term exposure to microgravity impairs vestibulo-cardiovascular reflex. Sci Rep. Nature Publishing Group; 2016;6:33405.

150. Otsuka K, Cornelissen G, Kubo Y, Hayashi M, Yamamoto N, Shibata K, et al. Intrinsic cardiovascular autonomic regulatory system of astronauts exposed long-term to microgravity in space: observational study. npj Microgravity. 2015;1:15018.

151. Harris LR, Jenkin M, Jenkin H, Zacher JE, Dyde RT. The effect of long-term exposure to microgravity on the perception of upright. npj Microgravity. 2017;3(1):3.

152. Lambertz D, Goubel F, Kaspranski R, Pérot C. Effects of long-term spaceflight on mechanical properties of muscles in humans. J Appl Physiol. 2003;94(2):490–8.

153. Hargens AR, Bhattacharya R, Schneider SM. Space physiology VI: Exercise, artificial gravity, and countermeasure development for prolonged space flight. Eur J Appl Physiol. 2013;113(9):2183–92.

154. Robertson D. The epidemic of orthostatic tachycardia and orthostatic intolerance. Am J Med Sci. 1999;317(2):75–7.

155. Lambert E, Lambert G. Sympathetic dysfunction in vasovagal syncope and the postural orthostatic tachycardia syndrome. Front Physiol. 2014;5:280.

156. Buckey JC, Lane LD, Levine BD, Watenpaugh DE, Wright SJ, Moore WE, et al. Orthostatic intolerance after spaceflight. J Appl Physiol. 1996;81(1):7–18.

157. Lee SMC, Feiveson AH, Stein S, Stenger MB, Platts SH. Orthostatic Intolerance After ISS and Space Shuttle Missions. Aerosp Med Hum Perform. 2015;86(12):54–67.

158. Williams D, Kuipers A, Mukai C, Thirsk R. Acclimation during space flight: effects on human physiology. Mil Med Res. 2016;180(13):1317–23.

159. Baisden DL, Beven GE, Campbell MR, Charles JB, Dervay JP, Foster E, et al. Human health and performance for long-duration spaceflight. Aviat Sp Environ Med. 2008;79(6):629–35.

160. Manzey D. Human missions to Mars: New psychological challenges and research issues. Acta Astronaut. 2004;55(3–9):781–90.

161. Clément GR, Charles JB, Paloski WH. Revisiting the needs for artificial gravity during deep space missions. Reach - Rev Hum Sp Explor. 2016;1:1–10.

162. Smith JJ, Porth CM, Erickson M. Hemodynamic Response to the Upright Posture. J Clin Pharmacol. 1994;34(5):375–86.

163. Olufsen MS, Tran HT, Ottesen JT. Modeling Cerebral Blood Flow Control During Posture Change From Sitting to Standing. Cardiovasc Eng. 2004;4(1):47–58.

164. LeBlanc A, Gogia P, Schneider V, Krebs J, Schonfeld E, Evans H. Calf muscle area and strength changes after five weeks of horizontal bed rest. Am J Sports Med. 1988;16(6):624–9.

165. Norsk P. Blood pressure regulation IV: Adaptive responses to weightlessness. Eur J Appl Physiol. 2014;114(3):481–97.

166. Jeong S-M, Hwang G-S, Kim S-O, Levine BD, Zhang R. Dynamic cerebral autoregulation after bed rest : effects of volume loading and exercise countermeasures. J Appl Physiol. 2013;116:24–31.

167. Blaber AP, Hinghofer-Szalkay H, Goswami N. Blood Volume Redistribution During Hypovolemia. Aviat Space Environ Med. 2013;84(1):59–64.

168. Stenger MB, Evans JM, Patwardhan AR, Moore FB, Hinghofer-Szalkay H, Rössler A, et al. Artificial gravity training improves orthostatic tolerance in ambulatory men and women. Acta Astronaut. 2007;60(4):267–72.

169. Frett T, Mayrhofer M, Schwandtner J, Anken R, Petrat G. An Innovative Short Arm Centrifuge for Future Studies on the Effects of Artificial Gravity on the Human Body. Microgravity Sci Technol. 2014;26(4):249–55.

170. Clément GR, Bukley AP, Paloski WH. Artificial gravity as a countermeasure for mitigating physiological deconditioning during long-duration space missions. Front Syst Neurosci. 2015;9:92.

171. Diaz A, Trigg C, Young LR. Combining ergometer exercise and artificial gravity in a compact-radius centrifuge. Acta Astronaut. 2015;113:80–8.

172. Zander V, Anken R, Pesquet T, Brungs S, Latsch J. Short Radius Centrifuges – A New Approach for Life Science Experiments Under Hyper-g Conditions for Applications in Space and Beyond. Recent Patents Sp Technol. 2013;3(1):74–81.

173. Bukley A, Lawrence D, Clément G. Generating artificial gravity onboard the Space Shuttle. Acta Astronaut. 2007;60(4):472–8.

174. Goswami N, Bruner M, Xu D, Bareille MP, Beck A, Hinghofer-Szalkay H, et al. Short-arm human centrifugation with 0.4g at eye and 0.75g at heart level provides similar cerebrovascular and cardiovascular responses to standing. Eur J Appl Physiol. 2015;115(7):1569–75.

175. Pan J, Tompkins WJ. A Real-Time QRS Detection Algorithm. IEEE Trans Biomed Eng. 1985;(3):230–6.

176. Bertinieri G, Di Rienzo M, Cavallazzi A, Ferrari A, Pedotti A, Mancia G. Evaluation monitoring of baroreceptor reflex by blood pressure in unanesthetized cats. Am J Physiol Hear Circ Physiol. 1988;254(2):H377–83.

177. Blaber AP, Yamamoto Y, Hughson RL. Methodology of spontaneous baroreflex assessed by surrogate data analysis. Am J Physiol Circ Physiol. 1995;4(268):H1682-7.

178. Silva AS, Ariza D, Dias DPM, Crestani CC, Martins-Pinge MC. Cardiovascular and autonomic alterations in rats with Parkinsonism induced by 6-OHDA and treated with L-DOPA. Life Sci. 2015;127:82–9.

179. Durand MT, Becari C, Tezini GC, Fazan R, Oliveira M, Guatimosim S, et al. Autonomic cardiocirculatory control in mice with reduced expression of the vesicular acetylcholine transporter. Am J Physiol Hear Circ Physiol. 2015;309(4):H655–62.

180. Kennel M, Brown R. Determining embedding dimension for phase-space reconstruction using geometrical construction. Phys Rev A. 1992;45(6).

181. White RJ, Averner M. Humans in space. Nature. 2001;409(6823):1115–8.

182. Takamatsu Y, Koike W, Takenouchi T, Sugama S, Wei J, Waragai M, et al. Protection against neurodegenerative disease on Earth and in space. npj Microgravity. 2016;2:16013.

183. Tzeng YC, Ainslie PN. Blood pressure regulation IX: Cerebral autoregulation under blood pressure challenges. Eur J Appl Physiol. 2014;114(3):545–59.

184. Mader TH, Gibson CR, Pass AF, Kramer LA, Lee AG, Fogarty J, et al. Optic disc

edema, globe flattening, choroidal folds, and hyperopic shifts observed in astronauts after long-duration space flight. Ophthalmology. 2011;118(10):2058–69.

185. Stewart JM, Medow MS, Montgomery LD, McLeod K. Decreased skeletal muscle pump activity in patients with postural tachycardia syndrome and low peripheral blood flow. Am J Physiol Heart Circ Physiol. 2004;286(3):H1216–22.

186. Artiles AD, Heldt T, Young LR. Effects of artificial gravity on the cardiovascular system: Computational approach. Acta Astronaut. 2016;126:395–410.

187. Iwasaki KI, Sasaki T, Hirayanagi K, Yajima K. Usefulness of daily+ 2Gz load as a countermeasure against physiological problems during weightlessness. Acta Astronaut. 2001;49(3):227–35.

188. Fontolliet T, Pichot V, Antonutto G, Bonjour J, Capelli C, Tam E, et al. Effects of gravitational acceleration on cardiovascular autonomic control in resting humans. Eur J Appl Physiol. 2015;115(7):1417–27.

189. Yanagida R, Ogawa Y, Ueda K, Aoki K, Iwasaki K ichi. Sustained mild hypergravity reduces spontaneous cardiac baroreflex sensitivity. Auton Neurosci Basic Clin. 2014;185:123–8.

190. Svacinova J, Javorka M, Novakova Z, Zavodina E, Czippelova B, Honzikova N. Development of causal interactions between systolic blood pressure and inter-beat intervals in adolescents. Physiol Res. 2015;64(6):821–9.

191. Miller JD, Pegelow DF, Jacques AJ, Dempsey JA. Skeletal muscle pump versus respiratory muscle pump: modulation of venous return from the locomotor limb in humans. J Physiol. 2005;563(Pt 3):925–43.

192. Verma AK, Garg A, Xu D, Bruner M, Fazel-Rezai R, Blaber AP, et al. Skeletal Muscle Pump Drives Control of Cardiovascular and Postural Systems. Sci Rep. 2017;7:45301.

193. Harm DL, Jennings RT, Meck J V, Powell MR, Putcha L, Sams CP, et al. Invited Review: Gender issues related to spaceflight: a NASA perspective. J Appl Physiol. 2001;91(5):2374–83.

194. Goswami N, Evans J, Schneider S, Von Der Wiesche M, Mulder E, Rössler A, et al. Effects of individualized centrifugation training on orthostatic tolerance in men and women. PLoS One. 2015;10(5):e0125780.

195. Arzeno NM, Stenger MB, Lee SMC, Ploutz-Snyder R, Platts SH. Sex differences in blood pressure control during 6° head-down tilt bed rest. Am J Physiol Heart Circ Physiol. 2013;304(8):H1114-23.

196. Hughson RL, Robertson AD, Arbeille P, Shoemaker JK, Rush JWE, Fraser KS, et al. Increased postflight carotid artery stiffness and inflight insulin resistance resulting from 6-mo spaceflight in male and female astronauts. Am J Physiol Heart Circ Physiol. 2016;310(5):H628-38.

197. Macaulay TR, Macias BR, Lee SM, Boda WL, Watenpaugh DE, Hargens AR. Treadmill exercise within lower-body negative pressure attenuates simulated spaceflight-induced reductions of balance abilities in men but not women. npj Microgravity. 2016;2:16022.

198. Esterov D, Greenwald BD. Autonomic dysfunction after mild traumatic brain injury. Brain Sci. 2017;7(8):1–8.

199. Dobson JL, Yarbrough MB, Perez J, Evans K, Buckley T. Sport-related concussion induces transient cardiovascular autonomic dysfunction. Am J Physiol - Regul Integr Comp Physiol. 2017;312(4):R575–84.

200. Rodriguez J, Blaber AP, Kneihsl M, Trozic I, Ruedl R, Green DA, et al. Poststroke alterations in heart rate variability during orthostatic challenge. Med (United States). 2017;96(14):4–8.

201. Ziemssen T, Reichmann H. Cardiovascular autonomic dysfunction in Parkinson's disease. J Neurol Sci. 2010;289(1):74–80.

202. Guskiewicz KM, Ross SE, Marshall SW. Postural Stability and Neuropsychological De cits After Concussion in Collegiate Athletes. J Athl Train. 2001;36(3):263–73.

203. Brown LA, Sleik RJ, Winder TR. Attentional demands for static postural control after stroke. Arch Phys Med Rehabil. 2002;83(12):1732–5.

204. Mukkamala R, Hahn J-O, Inan OT, Mestha LK, Kim C-S, Toreyin H, et al. Toward Ubiquitous Blood Pressure Monitoring via Pulse Transit Time: Theory and Practice. IEEE Trans Biomed Eng. 2015;62(8):1879–901.

205. Payne RA, Symeonides CN, Webb DJ, Maxwell SRJ. Pulse transit time measured from the ECG: an unreliable marker of beat-to-beat blood pressure. J Appl Physiol. 2006;100(1):136–41.

206. Laurin A, Blaber A, Tavakolian K. Seismocardiograms return Valid Heart Rate Variability Indices. In: Computing in Cardiology. 2013. p. 413–6.

207. Shafiq G, Tatinati S, Ang WT, Veluvolu KC. Automatic Identification of Systolic Time Intervals in Seismocardiogram. Sci Rep. 2016;6:37524.

208. Khosrow-Khavar F, Tavakolian K, Blaber A, Menon C. Automatic and Robust Delineation of the Fiducial Points of the Seismocardiogram Signal for Non-invasive Estimation of Cardiac Time Intervals. IEEE Trans Biomed Eng. 2016;64(8):1701–10.

209. Tavakolian K. Systolic Time Intervals and New Measurement Methods. Cardiovasc Eng Technol. 2016;7(2):118–25.

210. Verma AK, Fazel-Rezai R, Blaber A, Tavakolian K. Pulse Transit Time Extraction from Seismocardiogram and its Relationship with Pulse Pressure. In: Computing in Cardiology. 2015. p. 37–40.

211. Verma AK, Fazel-Rezai R, Zanetti J, Tavakolian K. Preliminary Results for Estimating Pulse Transit Time Using Seismocardiogram. J Mech Des. 2015;9(2):20916.

212. Verma AK, Zanetti J, Fazel-Rezai R, Tavakolian K. Pulse Transit Time Derivation using Xiphoidal and Carotid Seismocardiograms. In: Design of Medical Devices Conference. 2017. p. V001T01A010-V001T01A010.

213. Yang C, Tavassolian N. Pulse Transit Time Measurement Using Seismocardiogram, Photoplethysmogram, and Acoustic Recordings: Evaluation and Comparison. IEEE J Biomed Heal Informatics. 2017;

214. Di Rienzo M, Vaini E, Lombardi P. Use of seismocardiogram for the beat-to-beat assessment of the Pulse Transit Time: A pilot study. Proc Annu Int Conf IEEE Eng Med Biol Soc EMBS. 2015;7184–7.

215. Kim CS, Carek AM, Mukkamala R, Inan OT, Hahn JO. Ballistocardiogram as proximal timing reference for pulse transit time measurement: Potential for cuffless blood pressure monitoring. IEEE Trans Biomed Eng. 2015;62(11):2657–64.